Host range and environmental transmission of CWD

by

Elizabeth Triscott

A thesis submitted in partial fulfilment of the requirements for the degree of

Doctor of Philosophy

Department of Biological Sciences
University of Alberta

Abstract

The geographic range of chronic wasting disease, a fatal prion disease of cervids, is expanding throughout North America and northern Europe. The ecological effects of this highly infectious disease are unclear, as the host range and routes of transmission of CWD are not fully characterized. I infected Syrian Golden hamsters with a number of experimental and hunter harvested CWD isolates in order to compare their host range. There was variability in the ability of specific isolates to infect the hamsters, indicative of CWD strain diversity in free-ranging cervids. Differences were correlated with cervid species, geographical location and the presence of polymorphisms in the prion protein gene. Another important aspect to understand CWD ecology is understanding how infectivity interacts with the environment, and developing methods detecting environmental CWD. To this end, I developed a method of detecting plant-adhered prions. Using this assay, I described how prion-plant interactions differed depending on the species of vegetation. These data suggest that importance of plant consumption of CWD transmission will be dependent on climatic and geographic factors. Contaminated vegetation may not only transmit CWD to naïve deer, but also result in interspecies transmission, putting native species and livestock at risk of contracting prion disease. My technique of detecting vegetation-adhered prions can be developed into a method of monitoring environmental contamination. This thesis expands our knowledge of CWD epidemiology, demonstrating the complexity of prion transmission and the diversity of this fatal neurodegenerative disease.

Preface

The research project, of which this thesis is a apart, received research ethics approval from the University of Alberta Research Ethics Board and were conducted in accordance with the Canadian Council on Animal Care Guidelines and Policies with approval from the Health Sciences Animal Care and Use Committee of the University of Alberta, Animal Use Protocol 914. This project was conceived and performed with the input of Dr Debbie McKenzie and Dr. Judd Aiken.

A version of Chapter 2 was published as Herbst A, Duque Velásquez C., Triscott E., Aiken JM., and McKenzie D. (2017). Primary passages of the experimental CWD inocula into hamsters and mice were performed by Drs. Herbst and Duque Velasquez. My contribution to the Herbst et al manuscript was analysis of the hamster samples and assistance in manuscript preparation. Histology was performed by Hristina Gapeshina and Dr Nathalie Daude of the CPPFD histology core. I designed and performed all the second passage work described in this chapter.

Data from a single CWD isolate in Chapter 3 has been included in a manuscript currently submitted to a peer-reviewed journal as: Hannaoui S, Triscott E, Duque Velásquez C., Chang S.C., Arifin M.I., Zemlyankina I., Tang X., Bollinger T., Wille H., McKenzie D., Gilch S. (2020). Additionally, a version of Chapter 3 is intended for publication. Primary passage of the CWD inocula into hamster and mice were performed by Dr. Allen Herbst and Dr. Camilo Duque Velásquez. Genotyping of the deer isolates was performed by Chiye Kim. Histology was performed by Hristina Gapeshina and Dr. Nathalie Daude of the CPPFD histology core. I contributed to the experimental design, data collection, and data analysis of all other work.

A version of Chapter 4 is intended for publication. I contributed to the experimental design, data collection, and data analysis.

Acknowledgements

My deepest thanks to my supervisor, Dr. Debbie McKenzie, and committee members Dr. Judd Aiken, and Dr. Janice Cooke for their mentoring and guidance.

I would like to acknowledge our collaborators, especially those who shared samples used in this work, including Dr. Sabine Gilch (University of Calgary), Dr. Margo Pybus (AEP), Dr. Trent Bollinger (University of Saskatchewan), and the CFIA.

I would also like to acknowledge my funding agencies: NSERC, Genome Canada, Genome Alberta, and APRI for supporting these projects, as well as the CPPFD, especially the histology core and the animal technicians.

I would like to thank the members of the Aiken/McKenzie lab, especially Dr. Duque Velasquez, for their contributions to this work and for their support and comradery. As well, a big thank you to Dr. Alicia Otero Garcia and Danielle Gushue for their input and writing assistance.

Finally, my deepest thanks to my family and friends for their unwavering support and encouragement.

Table of Contents

List of Tables

List of Figures

List of Abbreviations

AB	Alberta
AEP	Alberta Environment and Parks
BSE	Bovine spongiform encephalopathy
CNS	Central nervous system
CPPFD	Centre for prions and protein folding disorders
CWD	Chronic wasting disease
Dpi	Days post-infection
DY	Drowsy
ECL	Enhanced chemiluminescence
EDTA	Ethylenediaminetetraacetic acid
GALT	Gut-associated lymphoid tissue
GndHCl	Guanidine hydrochloride
GFAP	Glial fibrillary acidic protein
GPI	Glycosylphosphatidylinositol
GSS	Gerstmann-Straussler-Scheinker disease
H&E	Hematoxylin and eosin staining
hCWD	Hamster-adapted chronic wasting disease
hElk	Hamster adapted elk CWD
HRP	Horseradish peroxidase
HY	Hyper
IC	Intracranial inoculation
iCJD	Iatrogenic Creutzfeldt-Jakob disease
IHC	Immunohistochemistry
LD_{50}	Median lethal dose
LD_{50}/g	Median lethal dose per gram
MBM	Meat and bone meal
MD	Mule deer
MOPS	3-(N-morpholino)propanesulfonic acid
Mpi	Months post-infection

MW	Molecular weight
N	Number of animals in experimental group
NaPTA	Sodium phosphotungstic acid
ND	Not done
NEB	New England Biolabs
PIRIBS	Parallel in-register intermolecular beta-sheet model
PK	Proteinase K
PMCA	Protein misfolding cyclic amplification
PNGase f	N-glycosidase F
PrP	Prion protein
PrP^{C}	Cellular prion protein
PrP^{d}	Deposited PrP
PrP^{res}	Proteinase K resistant prion protein
PrP^{Sc}	Pathological prion protein
PVDF	Polyvinylidene difluoride
RAMALT	Rectoanal mucosa-associated lymphoid tissue
recPrP	Recombinant prion protein
RIPA buffer	Radioimmunoprecipitation assay buffer
RPLN	Retropharyngeal lymph node
RT-QuIC	Real-time quaking-induced conversion
sCJD	Sporadic Creutzfeldt-Jakob disease
SDS	Sodium dodecyl sulfate
SK	Saskatchewan
StDev	Standard deviation
TBS-T	Tris-buffered saline with 1% Tween 20
tg33	Transgenic mice expressing wildtype white-tailed deer PrP
TME	Transmissible mink encephalopathy
vCJD	Variant Creutzfeldt-Jakob disease
WMU	Wildlife management unit
Wt/wt	Wildtype homozygous
WTD	White-tailed deer

1 Prion Diseases: Strains and Environmental Transmission

1.1 Introduction

Zoonotic diseases of wildlife pose a growing risk to human health as well as to domesticated livestock and other animals. Prion diseases are fatal neurodegenerative diseases caused by the misfolding of the prion protein and can occur either via infection or sporadically. Chronic wasting disease (CWD) is a transmissible prion disease of cervids that is enzootic in North America and is present in Korea and northern Europe. Given its geographic range, which continues to expand, its increasing prevalence, and the diversity of hosts and PrP genotypes, it is critical to gain a greater understanding of this disease as well as develop methods of disease surveillance. This will aid in assessing the risk this infectious, fatal disease poses to human and animal health, as well as its impact on global ecosystems.

1.2 The cellular prion protein (PrP^C)

The cellular prion protein, PrP^C, is a GPI-anchored surface protein found in most vertebrates. It is expressed at high levels in the central nervous system (CNS) and at lower levels in peripheral tissues. PrP^C is composed of two domains, an unstructured N-terminus, and an ordered C-terminus, connected by a hydrophobic region. The N terminal domain contains 5-6 octapeptide repeats that interact with metal cations, especially copper [1–3], while the C terminal domain consists of three α helices and two β sheets [4–7]. The C terminal domain also contains two glycosylation sites at residues 181 and 197 (human numbering) as well as a disulphide bond between residues 179 and 214 [8]. The PrP protein is highly conserved with a high degree of homology between birds, reptiles, amphibians, and mammals, and with similar structural domains in fish [9].

Despite its ubiquity in mammals, the function of PrP is not well understood. Goats naturally lacking PrP, as well as transgenic PrP-knockout cattle, do not display overt dysfunction, although the goats do develop a subclinical demyelinating neuropathy [10–12]. As well, PrP knockout mouse models present with subtle phenotypes that may be the result of genetic

confounding instead of PrP ablation [13–15]. PrP has a large interactome which suggests a role in a number of cellular processes, including synaptic maintenance and transmission, memory, circadian rhythm stabilization, and neuronal plasticity [16–23]. PrP may also have a role in neuroprotection and in ion metabolism due to the cation binding domains in its unstructured N-terminus [21,24–29].

1.3 The pathologic prion protein (PrP^{Sc})

1.3.1 PrP^{Sc} structure and mechanisms of misfolding

In prion disease, PrP^{C} misfolds into a disease-associated amyloidogenic isoform, PrP^{Sc}, where a 'seed' of PrP^{Sc} guides normal PrP^{C} to adopt an identical misfolded conformation, forming amyloid fibrils [30–32]. Unlike PrP^{C}, PrP^{Sc} is predominantly composed of β sheets and is resistant to physical and chemical denaturation [33–37]. Currently there are no high-resolution structural models of PrP^{Sc} due to its low solubility and propensity for aggregation, however, there is a growing consensus that PrP^{Sc} forms a four-rung β solenoid structure, where individual subunits stack into fibrils that form the PrP^{Sc} amyloid and plaques characteristic of prion disease [38–40]. These amyloid fibrils are thought to be formed and held together in part due to steric zippers, where the amino acid side chains of two different β-sheets interdigitate (Figure 1-1A) [41]. An alternative model, called the parallel in-register intermolecular beta-sheet model (PIRIBS), posits that PrP^{Sc} amyloid is composed of a single filament where each monomer forms a single layer stacked in parallel [42].

PrP^{Sc} accumulates in the CNS producing neuropathological changes which lead to neurological signs and, ultimately, death. Clinical signs of prion disease vary, but commonly include locomotor and behavioural signs. Neuropathological changes, including vacuolation, gliosis, and neuronal loss, are common features of prion diseases. Although it is unclear how PrP^{Sc} accumulation and deposition are associated with disease, several mechanisms of

neurotoxicity have been proposed including proteasomal dysfunction, oxidative stress, and synaptic dysfunction [43,44,53,45–52].

1.3.2 Prion diseases

Prion diseases can be categorized into three major groups based on the source of the initial PrP^{Sc} seed. Inherited or familial prion diseases, such as Gerstmann-Straussler-Scheinker disease (GSS) and fatal familial insomnia, are due heritable dominant genetic mutations in the prion protein gene (*Prnp*) that increase the propensity of PrP to misfold. In sporadic prion disease, which includes the most common human prion disease, sporadic Creutzfeldt-Jakob disease (sCJD), PrP^{C} misfolds without any overt cause. The third category of prion diseases are transmissible or infectious prion diseases, which transmit between animals or humans, often due to shedding of infectivity in biofluids or the consumption of infectious tissues [54–58]. Chronic wasting disease (CWD) of cervids and scrapie of sheep and goats represent the most contagious prion diseases. Prion transmission can also occur due to medical procedures that involve prion contaminated tools or tissues (iatrogenic prion disease).

1.3.3 Prion pathogenesis

While iatrogenic prion transmission has occurred due to medical procedures involving the CNS, such as corneal transplants, dura mater grafts, and the use of cadaver-derived growth hormone [59–61], many prion outbreaks have been traced to the consumption of prion-contaminated tissue. Kuru, a transmissible human prion disease, was linked to the practise of funerary cannibalism in the peoples of the Fore language group of Papua New Guinea [62]. Kuru was most prevalent in women and children who were most likely to consume the brain of the deceased [63]. The kuru epidemic ended with the cessation of these practises in the 1950s, although isolated cases in elderly individuals, likely due to a prolonged incubation period, occurred as recently as 2003 [64]. Another human prion epidemic, variant Creutzfeldt Jakob Disease (vCJD), occurred due to the consumption of beef from cattle infected with

bovine spongiform encephalopathy (BSE). The emergence of BSE in cattle corresponded to the elimination of a solvent-extraction step in British meat and bone meal (MBM) production in the 1980's [65]. MBM is produced by rendering tissues, including parts of the CNS, and is used to supplement cattle feed. The change in MBM processing allowed prion infectivity, either scrapie or a sporadic prion disease of cattle [66–68], to persist in the cattle feed. This allowed infected material to cycle through and adapt to bovine populations, as prion-infected cattle were processed into MBM. In the 1990s, a novel human prion disease, vCJD, was identified and linked to the consumption of these BSE-infected cattle [55,69–71]. vCJD can be differentiated from sCJD due to the younger age of onset (26 vs. 65 years), short clinical duration (4.5 vs. 14 months), and distinct clinical signs (sensory and psychiatric symptoms common at onset of vCJD, rare in sCJD) [72–74]. Both the BSE and vCJD epidemics ended following a MBM feed ban in 1987, although, as in kuru, isolated cases of vCJD still occur occasionally due to prolonged incubation periods [75].

In oral infection, infectivity must withstand the digestive process and be transported to the CNS. Consumed prions first accumulate in the lymphoid tissue of the digestive tract prior to neuroinvasion [76–78]. They cross the intestinal lumen through M cells, specialized cells that facilitate immune sampling of the gut contents [79–82]. It is believed that immune cells, especially follicular dendritic cells, frequently located near M cells in the Peyer's patches, phagocytose prions but are unable to degrade them, allowing infectivity to spread to other immune cells and to organs like the spleen. Eventually, PrP^{Sc} will interact with the nerves of the gut-associated lymphoid tissue (GALT), and retrotransmission of PrP^{Sc} will occur through these peripheral neurons too the CNS, resulting in neuroinvasion [76,77,82–86]. Peripheral prion infection, notably iatrogenic CJD, may also occur through blood transfusions and the use of cadaver-derived medical products, likely through a similar mechanism (i.e.: interaction with immune cells and organs leading to retrotransmission and neuroinvasion) [60,87–89].

1.4 Prion Strains

The different prion agents that can infect a host species, causing stable, distinctive disease phenotypes within a defined host, are called strains. These strains are characterized by their distinct incubation periods, neuropathology, and clinical phenotypes [90–93]. Strains are defined within a single host through bioassay, and their characteristics remain stable when passaged multiple times under standard conditions [94,95]. Although structural studies currently lack the resolution to compare the PrP^{Sc} structures of different strains, differences in a number of biochemical features, such as protease resistance and stability in detergents, suggest that they are conformationally distinct [96–101]. The immunoblot migration and glycosylation patterns of protease-digested strains can also differ (Figure 1-2), due to differences in the protease cleavage sites caused by these structural differences [100] or to different proportions of di-, mono-, and unglycosylated forms of PrP [96,97]. Different protease cleavage sites can also lead to the exposure of different antibody epitopes, resulting in the differential detection of some strains using antibodies [102–104]. Animals with the same PrP sequence can propagate different strains [94,95]. Interestingly, the β-sheets in the PrP of some species can form multiple steric zipper conformations (Figure 1-1B), which would vary in misfolded conformation and stability, perhaps explaining how strains, with different misfolded conformations, could exist [41].

1.5 Prion techniques used their use in strain characterization

1.5.1 In vivo techniques

Animals can be experimentally infected via a number of different routes, the most common in prion research being intracerebral inoculation, i.e., direct injection into the CNS. Peripheral routes of infection (oral or intraperitoneal) are less common as some strains do not appear to replicate in the periphery or invade the CNS [105,106]. Peripheral transmission, when successful, results in significantly longer incubation periods compared to intracerebral infections [105,107,108]. A number of rodent models are commonly used in prion studies,

including voles, hamsters, and transgenic mice. These mice are modified so that their murine *Prnp* gene is ablated and the *Prnp* gene of other animals, such as cervids, humans, and livestock, is inserted and expressed. This allows researchers to investigate prion diseases that would otherwise be difficult to study. Rodents are comparatively easy to manipulate and maintain, and the incubation period of prion diseases can be shortened by using mice expressing PrP at levels above those found in wild-type animals, although this can affect experimental results [30,109].

The clinical signs of animals experimentally infected with prions can vary depending on strain. The length of time it takes for clinical signs to emerge, called the incubation period, can differ, as can the length of the clinical period, although this is affected by the initial levels of infectivity [90,95,100,110]. A number of histopathological techniques are used to differentiate prion strains. PrP amyloid, in the form of deposited PrP (PrP^{d}), can be detected in tissue immunohistochemistry using antibodies against PrP, and by using Congo Red staining [111–113]. In the brain, prion disease-associated gliosis is detected using antibodies against glial fibrillary acid protein (GFAP), a marker of neuroinflammation, while hematoxylin and eosin staining allows visualization of vacuolation (Figure 1-2A) [91,93,114,115]. Some histopathological features are associated with particular prion strains, such as florid kuru plaques [62], but other features, such as neuroinflammation, are non-specific markers of neurological pathologies [116].

1.5.2 Biochemical techniques

Disease-associated PrP can be differentiated from normal PrP by a variety of biochemical methods. Incubation in chaotropic agents and proteinase K digestion of tissue homogenates (usually brain) allows researchers to differentiate between PrP^{C} and PrP^{Sc}. Unlike PrP^{C}, PrP^{Sc} is resistant to protease digestion, leaving a protease-resistant core called PrP^{res} [117], although PK-resistance varies between strains [99,100]. When analyzed by immunoblot,

PrP^{res} generally displays a distinctive pattern, composed of three bands representing di-, mono- and non-glycosylated PrP (Figure 1-2B). PrP^{res} banding patterns can vary depending on the antibody used and the type of prion disease [103,118–120]. For instance, GSS lacks the classical three-band signature and displays a diagnostic single 7 kDa PrP^{res} band [121]. PrP^{Sc} can also be differentiated from PrP^{C} using chaotropic agents, which will denature normal PrP^{C} at lower concentrations while PrP^{Sc} will retain its misfolded structure. Similar to protease resistance, prion strains can be differentiated by their stability in this chaotropic agent [98,122].

1.5.3 Protein misfolding cyclic amplification (PMCA) and real-time quaking-induced conversion (RT-QuIC)

A number of amplification methods have been developed to detect low levels of PrP^{Sc}. Protein misfolding cyclic amplification (PMCA) uses a series of sonication and incubation steps to convert PrP^{C} to PrP^{Sc} and appears to mimic the natural templated misfolding of prions, preserving the strain characteristics [123]. In PMCA, a sample containing (or thought to contain) prions seeds the PMCA reaction substrate (brain homogenate from uninfected animals) and induces it to misfold [124]. After PMCA, the amplified PrP^{Sc} is digested with PK and visualized by western blot using anti-PrP antibodies [125].

Real-time quaking-induced conversion also amplifies low levels of PrP^{Sc}. Like PMCA, RT-QuIC reactions are seeded by a sample containing PrP^{Sc}, which will induce PrP substrate to misfold. However, in RT-QuIC, the substrate is usually recombinant PrP (recPrP). As well, RT-QuIC utilizes intermittent shaking and monitors the formation of amyloid during the reaction using the dye thioflavin T, which fluoresces when bound to amyloid [126]. Both methods allow for the comparison of strain conversion efficiency, the rate at which a seed misfolds the PrP substrate. Similar to interspecies transmission, conversion efficiency is

dependent on both the prion seed and type of PrP substrate, so PMCA and RT-QuIC have been used to model interspecies transmission in lieu of bioassay [127–129].

1.6 Scrapie, CWD, and hamster prions

1.6.1 Scrapie

Scrapie, a prion disease of sheep and goats, was first documented in Britain in 1732 and has become endemic in many areas, spreading through livestock import [130,131]. Classical scrapie most commonly affects sheep between the ages of 2 and 5 years with a clinical course of 1-6 months. The clinical signs begin with behavioural changes, progressing to head pressing, tremors, ataxia, and pruritus, where the animal scrapes against objects leading to bald spots, gives scrapie its name [132]. Three PrP amino acid variants make sheep more resistant to scrapie, an alanine (A) at residue 136, and arginines (R) at residues 154 and 171, which led to the selective breeding of 'ARR' sheep [133–137]. Although ARR sheep were resistant to classical scrapie, they could still develop a different prion disease, called Nor98 or atypical scrapie, which occurred at an older age and does not include the characteristic pruritus of classical scrapie [132,138]. Classical scrapie spreads via horizontal transmission with relatively high levels of infectivity found in placenta and birthing materials [139–141]. Nor98 is thought to be sporadic, although low levels of infectivity are present in a range of peripheral tissues [142].

1.6.2 HY and DY

Two prion strains in hamsters, HY and DY, are frequently used to study the prion strain phenomenon. For this reason, I will now discuss the origin of these two strains as well as their distinct biochemical and pathophysiological characteristics. A TME isolate originated from a ranch near Hayward, Wisconsin in 1963 was intracranially inoculated into Syrian Golden hamsters. These animals demonstrated signs of prion disease, notably hyperesthesia and progressive ataxia after around 18 months [143]. In subsequent passages, the hamsters

became notably lethargic after 19 weeks and lacked the ataxic movement noted in the earlier passages [144]. A second isolate of TME, this time originating from a mink ranch in Stetsonville, Wisconsin in 1985, was also passaged into Syrian Golden hamsters. Similar to the initial TME experiment, these hamsters displayed clinical signs such as hyperaesthesia, tremors, and ataxia after an incubation period of 15-16 months. Upon further passages, two distinct clinical syndromes were observed. The first, HY, preserved the hyperaesthesia and ataxia observed in the earlier passages, with the second (DY) displayed the lethargy present in the later passages of the Hayward TME transmission experiments [95]. HY and DY were further passaged in hamsters until the strains stabilized, resulting in two distinct, stable incubation periods (HY: 65±1 dpi; DY: 168±2 dpi). Although earlier passage lines seemed to be composed of a mixture of strains [95], DY can be isolated from a mixture by passaging the mixed isolate at a high dilution (10^{-4}), continuing to passage the same isolate at a low dilution (10^{-1}) will result in the selection of the HY agent [145].

These two strains could also be distinguished by a number of pathological characteristics, including the location and severity of both spongiform degeneration and PrP^{d}, and the level of infectivity in the brain using endpoint titration (HY: $10^{9.5}$ LD_{50}/g; DY: $10^{7.4}$ LD_{50}/g) [99,100]. In addition to the clinical and pathological differences, HY and DY can be differentiated based on their PrP^{res} migration pattern on immunoblot [99] (Figure 1-2B). DY has a lower migration pattern, with its unglycosylated band at 19 kDa, compared to HY's 21 kDa unglycosylated band. DY is also less resistant to PK digestion than HY and displays different epitopes [99,100]. These biochemical differences are explained by the different misfolded conformations of these two strains, since slight differences in the infectious prion structure could alter the protease cleavage sites, preserving different antibody epitopes and causing the shift in migration pattern [100].

HY and DY have also been used to demonstrate important strain phenomena, such as strain competition [145,146], a phenomenon previously identified in mouse scrapie [147,148]. In strain competition, two co-infected prion strains interfere with the conversion activity of each other, likely due to competition for PrP^C or cofactors necessary for prion conversion, leading to extended incubation periods [149]. The disease phenotype exhibited by hamsters coinfected with HY and DY depended on the strain ratios used. HY reliably outcompeted DY until the HY:DY ratio was 10^{-7}:10^{-2}, when a mixture of phenotypes is observed. Upon second passage, however, the incubation period shortens and only the HY strain phenotype is observed [145]. Strain competition can also occur when one prion is inoculated months after the other or when the two strains are inoculated peripherally [105,146]. *In vitro*, multiple rounds of PMCA using different ratios of HY and DY as seeds resulted in competition similar to *in vivo* experiments, with small amounts of HY eventually out-competing DY and dominating the reaction after several rounds of PMCA [149].

1.6.3 Chronic Wasting Disease

Chronic wasting disease (CWD) is an infectious prion disease of cervids, including mule deer (*Odocoileus hemionus*), white-tailed deer (*Odocoileus virginianus*), moose (*Alces alces*), elk (*Cervus elaphus nelsoni*), and reindeer (*Rangifer tarandus*). CWD was first documented in captive mule deer in Colorado in the 1960's, and later in free-ranging white-tailed deer, but not identified as a prion disease until decades later [150,151]. It affects both free-ranging and captive animals and has spread to 26 American states and three Canadian provinces, as well as northern Europe and South Korea [152–156]. While some of this expansion is due to the movement of free-ranging animals, spread has been facilitated by the transfer of cervids between game farms and zoos [152,153,155,157]. CWD has an incubation period of ~ 2 years but can be longer in cervids with specific *prnp* polymorphisms [158]. Clinical signs of CWD begin with behavioural changes and progress over several months, to ataxia, low posture,

polyuria, polydipsia, wasting, and, ultimately, death [150]. Infected free-ranging deer are likely to be removed from the landscape during the early stages of clinical disease, as they are at a greater risk of predation, hunting, and road collisions [159–162]. CWD has a high degree of peripheral distribution, with PrP^{Sc} present in many tissues, especially lymphoid tissues, early in the disease process, although this can be affected by cervid species and genotype [163–166]. CWD prions are shed in the urine, saliva, and feces of infected animals, even during the preclinical stage of disease [167–172].

1.7 Host range and the transmission barrier

1.7.1 Transmission barrier and host range of prion diseases

In addition to infecting hosts with the same PrP sequence (homologous transmission), prions can be transmitted between hosts of different species and PrP alleles (heterologous transmission). The ease with which a specific prion can infect novel hosts is called the transmission barrier, and the range of animal species infected by a prion agent is called its host range. The transmission barrier is thought to be due to a mismatch between the infectious seeding template and the PrP sequence of the new host [30,95,98]. When a novel host can replicate a specific prion agent, the first infection, or passage, can have an extended incubation period which may exceed the life expectancy of the new host. Serial transmission in the new host can result in agent adaptation, resulting in reduction and eventual stabilization of the incubation period [90,95,173]. This new agent may exhibit novel neuropathology and clinical signs, and once the prion has adapted to the new host it may lose its ability to infect the original host [99,174].

According to the steric zipper model, transmission barriers may be due to amino acid mismatches between PrP molecules that result in steric hindrance, preventing the formation of a stable steric zipper, and thus the formation of new PrP^{Sc} (Figure 1-1C) [175]. This mismatch is due to differences in the size and charge of specific amino acid side chains.

Several amino acid residues have been demonstrated to influence host range in experiments using transgenic mice. Many of these residues were located in the β2-α2 loop of PrP and had bulky side groups, which could clash in mismatching PrP sequences and interfere with the formation of a steric zipper [175,176]. On the other hand, if these bulky side groups can properly interdigitate their mass would stabilize the resulting PrP^{Sc}, lowering the energy necessary to misfold PrP^{C} and increasing the probability of cross-species seeding [177].

A number of PrP variants can play a role in prion disease susceptibility. The importance of residues 136, 154, and 171 in classical scrapie transmission has already been mentioned. In humans, vCJD occurred primarily in M129 homozygous individuals, while subclinical infections and a recent clinical case have occurred in MV129 heterozygous individuals [75,178]. Similarly, M129 or V129 homozygous individuals were overrepresented in young kuru patients, while prolonged incubation periods were associated with MV129 heterozygosity [178–180]. Interestingly, a novel PrP variant (V127) that appears to confer prion resistance has been observed in the area affected by kuru, and is thought to have evolved as a result of selection pressures caused by the prion epidemic [181]. It has been proposed that the V129 variant in humans emerged in a similar way, due to past prion epidemics in human evolutionary history, providing an explanation for the different prevalence of V129 in different human populations [179].

1.7.2 CWD Prnp polymorphisms that affect transmission

Genetic studies of free-ranging cervids revealed a number of cervid *Prnp* polymorphisms that were underrepresented in CWD positive deer, including H95 and S96 in white tailed deer, D20, N138, and F225 in mule deer, and L132 in elk [182–189]. Oral transmission of wildtype white-tailed deer CWD to white-tailed deer expressing at least one H95 or S96 *Prnp* allele demonstrated that these polymorphisms extend the incubation period and disease progression but do not prevent infection [190]. Similarly, the mule deer F225, reindeer or caribou

N138, and elk L132 alleles extend the incubation period of the disease, but do not confer resistance [166,190–192]. Not only do these *Prnp* alleles delay the progression of the disease, they also limit peripheral PrP^{Sc} deposition [164,166,193]. This has the potential to alter CWD transmission characteristics, as a prolonged preclinical phase may result in infectivity being shed into the environment for a longer period of time [194,195], impacting transmission and environmental contamination. In addition, these PrP variants may lead to the emergence of new strains with altered prion properties (Section 1.6).

The impact of these PrP variants on the ecology and spread of CWD is unclear. There is an assumption that PrP variants that delay the onset of CWD will delay the emergence of CWD in an area and prevent cervid population declines [159,160,196,197]. One study in north-central Illinois demonstrated that a higher frequency of CWD-protective alleles resulted in delays in the county reporting CWD positives than in counties where deer had lower frequencies of these protective alleles [188]. In another study, there was a moderate increase in the elk L132 allele in some CWD-enzootic areas [195], suggesting that pressure exerted by CWD selected for these alleles. When white-tailed deer populations, in Wyoming, were followed for over 7 years, monitoring CWD prevalence, pregnancy, and mortality [160], it was found that mortality was four times higher in CWD positive than CWD negative deer, leading to a prediction of a 10.4% yearly population decline. A similar study in mule deer, from 2010-2014, predicted an annual population decline of as much as 21%, although when the F225 variant was included in the model, the decline was 1% annually, with a 10% increase of F225 frequency each year. These studies noted CWD positive animals were more likely to succumb to predation and harvesting, further complicating CWD modelling, as predator dynamics and wildlife management can have a large effect on the future viability of cervid populations [161,198–205].

1.8 Prion Strains and transmission

1.8.1 Models of prion strains

Although prion strains differ in their conformations, the mechanisms of strain emergence and propagation are not clear. Strains can exist as mixtures, as in some cases of sporadic human prion disease [206–208] and natural scrapie [209–211], however, it is thought that strains can be purified by passaging isolates at a high dilution [90,145]. Once a strain is biologically cloned it will retain its strain properties upon serial dilution, although the incubation period will increase as titre decreases [90,147,212]. An alternate hypothesis, conformational selection model, posits that strains are composed of a 'cloud' of misfolded conformations, called quasi-species, which co-exist in the host [213,214]. According to this model, transmission to a new host occurs if some of the quasi-species are also kinetically possible in the novel host ('conformational selection'). The quasi-species structures that the original strain and the novel host have in common will then form a new strain cloud [215]. A third model of interspecies transmission, the deformed templating model, proposes that the PrP^{Sc} seed will attempt to misfold heterotypic PrP^{C}, but, due to the novel molecular environment and PrP sequence, the new PrP^{Sc} will not be identical to the seed. During this first passage, a number of slightly different PrP^{Sc} conformations may be produced and the "best" conformation will outcompete the others, resulting in a new strain distinct from the original isolate in its pathological and biochemical characteristics [216]. Unlike the conformational selection model, the deformed templating supports the existence of pure strains while explaining how new strains may be generated.

1.8.2 CWD strains

A number of CWD strains have been characterized (Table 1-1). Many of these strains were isolated from cervids expressing non-wild type PrP and were characterized by comparison with another CWD strain (ex.: CWD from a cervid with a *Prnp* polymorphism compared to

CWD from a wildtype cervid). The first CWD strains identified, CWD1 and CWD2, were identified by their clinical and histological characteristics in a specific line of cervidized mice, tg1536$^{+/-}$ [217]. CWD isolates from elk and deer were transmitted into the tg1536$^{+/-}$ mice and different incubation periods and distinct neuropathologies were observed. Shorter incubation periods (225±18 dpi), and higher levels of vacuolation in the hippocampus and paraterminal body, as well as symmetrical PrP^{d} staining, denoted the CWD1 strain. CWD2 was characterized by a longer incubation period (301±35 dpi) and asymmetrical PrP^{d} deposition. Many deer isolates produced both CWD1 and CWD2 pathologies upon first passage in the cervidized mice, while elk samples produced either a CWD1 or CWD2 pattern. However, the strain characteristics did not remain stable on second passage, resulting in a mixture of neuropathologies in the inoculated mice. Another CWD strain was described in Norwegian moose. The neuropathology and immunoblot migration pattern were distinct from both CWD-infected Norwegian reindeer and North American moose.

Other CWD strains were identified in cervids expressing *Prnp* polymorphisms, suggesting a mechanism for emergence of novel prion strains. The H95 and S96 alleles in white-tailed deer extend the incubation period of CWD [218]. When CWD from a wt/wt white-tailed deer (homozygous for glutamine at codon 95 and glycine at codon 96) was experimentally passaged into deer expressing the H95 allele, a new strain called H95^{+} emerged. Unlike the CWD from the wild-type deer (Wisc-1), H95^{+} can successfully infect cervidized mice expressing cervid S96-PrP [219], previously believed to be refractory to CWD [220]. Wisc-1 and H95^{+} have different biochemical and neuropathological properties, and their host range in wild-type rodents differ [164,219,221]. Another polymorphism of white-tailed deer, G116, also appears to be associated with the emergence of novel strain properties [222]. In elk, animals homozygous for the L132 *Prnp* polymorphism had prolonged CWD incubation periods, along with differences in neuropathology and PrP^{Sc} biochemistry compared to wild-

type elk [193]. CWD from these L132 homozygous elk was characterized in transgenic mice expressing elk M132 PrP, and demonstrated different strain characteristics, including a longer incubation period, a lower immunoblot migration pattern, and distinct neuropathology than the M132 homozygous elk agent [223]. It is unclear whether strains that emerge in cervid with *Prnp* polymorphisms, like the ones mentioned above, will spread in cervid populations and add to the diversity of CWD, especially since some of these variants limit peripheral PrP^{d} and shedding [164,166,224].

1.8.3 Host range of CWD

CWD transmits naturally to mule deer, white-tailed deer, elk, moose, red deer (*Cervus elaphus*), sika deer (*Cervus nippon*), and reindeer (*Rangifer tarandus*) [150,153,154,225–227]. In addition, caribou (*Rangifer tarandus caribou*), Reeve's muntjac deer (*Muntiacus reevesi*), and fallow deer (*Dama dama*) have been experimentally infected [192,228,229]. Many of these cervids are used for food or hunted recreationally by humans, and their geographical distribution often overlaps with agricultural areas. Until the diversity of CWD strains is characterized, we cannot quantify the risk CWD poses to humans and animals health.

A number of studies have attempted experimental transmission of CWD to human disease models. Experiments in transgenic mice expressing human PrP have failed to demonstrate transmission in mice expressing the M129 and V129 PrP variants [230], and in mice overexpressing human PrP [231–233]. These experiments tested CWD isolates from white-tailed deer, mule deer, and elk [232–234]. CWD has also been transmitted to non-human primates. Whereas squirrel monkeys are susceptible to CWD [235], macaques appear to be resistant, although one unpublished study suggests they may accumulate PrP^{Sc} [236–238]. A number of *in vitro* studies have demonstrated that CWD can convert human PrP, albeit at low

levels [127,239–242]. These studies used PMCA and RT-QuIC with human PrP substrate from a number of sources, including recombinant PrP [127,242], cell culture-derived PrP [234,243], and human PrP from transgenic mouse models [240,241]. As in the humanized mouse bioassays, these experiments used a variety of CWD isolates, including elk, mule deer, reindeer, and white-tailed deer, and one studied demonstrated that elk prion polymorphisms affected the susceptibility of human PrP to misfolding [241].

Cervids and livestock often coexist in agricultural areas. Not only is this an economic concern, as demonstrated with the BSE outbreak in cattle, the adaption of prions to new species can change host range [91,94,244], potentially increasing the risk of human transmission. As well, transmission of CWD to native species would have important ecological consequences. Cattle, sheep, mink, and raccoons are susceptible to CWD (Table 1-2), although these species are only susceptible after intracerebral challenge, which is unlikely to occur naturally [245–251]. Pigs orally infected with CWD accumulate PrP^{Sc} by six months post infection (at market weight) but do not become clinical (euthanized at 73 mpi) [245]. Domestic cats also accumulate infectivity after oral challenge with CWD, although the initial interspecies transmission did not result in clinical disease upon first passage, but did upon second passage [252]. CWD can also be transmitted to several North American vole and mouse species, along with ferrets [244,253–255], but again most of these *in vivo* infection experiments occurred via intracerebral inoculation.

1.9 CWD Transmission

1.9.1 Vertical and horizontal transmission of CWD

Understanding how an infectious disease is transmitted is central to predicting how it will impact a population, as well as identifying potential interventions. Three CWD transmission routes have been investigated: vertical transmission, direct horizontal transmission, and indirect horizontal transmission. In vertical transmission, the infectious disease is transmitted

between the mother and offspring prior to parturition, while in horizontal transmission a disease spreads between individuals, either through social contact (direct transmission) or through contaminated fomites (indirect transmission). CWD positive deer and elk have been found to be pregnant at a rate similar to uninfected cervids [159,160]. However, experimental evidence indicates that, although CWD positive elk and Muntjac dams can carry young to term, there is an increase in stillbirths and spontaneous abortions during the later stages of maternal disease [228,256]. Furthermore, PrP^{Sc} has been detected by PMCA in birthing tissues of CWD positive elk [228,256], indicating that *in utero* transmission may occur, although avoiding contamination in these studies is difficult.

The primary mode of CWD transmission is likely horizontal, either due to direct contact between cervids or indirect transmission through the environment. However, it is unclear which mode of transmission predominates. CWD prevalence is associated with landscape factors that increase deer densities, such as habitat fragmentation [257–265], which is in accord with both direct and indirect transmission models of CWD. Increased deer densities result in a greater likelihood of direct contact between naïve and infected cervids but would also concentrate shed infectivity into a small area, increasing the likelihood of transmission. It is likely that direct and indirect transmission occur concurrently, with the initial introduction of CWD occurring through direct contact and indirect transmission arising once the environment becomes sufficiently contaminated [196].

Deer densities may also explain why mule deer have a higher prevalence of CWD than white-tailed deer when these two populations coexist [197,266,267]. Mule deer form larger herds than white-tailed deer, especially during winter, resulting in a greater chance of transmission between mule deer compared to less gregarious white-tailed deer [266,268]. Male deer, travelling alone or in small bachelor groups, are thought to spread CWD between groups of

does since males have been tracked travelling large distances [262,269,270]. Once CWD has been introduced to an area, it transmits readily within closely related females of the matrilocal herds [270–274]. Landscape features that restrict deer movement, such as large rivers and highways, act as barriers to both CWD transmission and gene flow [262,263,275]. CWD prevalence in free-ranging males is generally higher than females [264,266,273,276,277]. There has been speculation that this is due to increased contact with other herds, differences in social behaviour, or even increased food intake, which could lead to a greater interaction with shed infectivity [205,262,273].

1.9.2 Pathogenesis of CWD: Peripheral deposition and shedding of CWD prions

CWD can be shed by infected cervids prior to the onset of clinical signs. PrP^{res} has been detected in the follicular germinal centres of the Peyer's patches and retropharyngeal lymph nodes (RPLNs) as early as 42 days after oral exposure, although this was relatively rare (8/119 RPLN samples; 1/190 Peyer's patches samples) [76]. Mule deer orally exposed to CWD had PrP^{Sc} deposition in their rectoanal mucosa-associated lymphoid tissue (RAMALT) and tonsil tissue as early as 90 dpi, in the Peyer's patches and vagus nerve at 190 dpi, then the GALT and spinal cord at 272 dpi, and finally the brain at 482 dpi [166]. Seeding activity in saliva is detectable as early as three months after exposure to CWD, and infectivity in urine is detectable at 6 months post-infection [278]. Infectivity can be detected in mule deer feces, by bioassay, 9-10 months post-exposure [170] and in elk feces, by RT-QuIC, as early as 2 weeks post-exposure [194]. CWD positive cervids with *Prnp* polymorphisms begin shedding prions at a similar time as wildtype cervids, although there is a high degree of variability in pre-clinical samples [278–280]. This is concerning, since the preclinical phase is longer in these animals, thus the total amount of infectivity shed into the environment may be greater in these deer than in wildtype cervids [194,195]

There is variability in the levels of infectivity in different biofluids. Henderson et al. [127,278] estimated infectivity by comparing the RT-QuIC seeding activity of biofluids to the seeding activity of brain homogenate dilutions that had been used to estimate infectious dose in cervidized mice. They found one LD_{50} of infectivity in 10-20 mL of urine and 1-10 mL of saliva. This is similar to another study using deer bioassay, which found that 16.5 mL of saliva was sufficient to cause infection in deer, which is equivalent to 300 ng of infectious brain as determined by comparisons performed in RT-QuIC. In this study, this amount of infectivity was sufficient to cause disease, although the cumulative dose spread over three days resulted in a 100% attack rate (3/3 deer), while a single dose resulted in transmission to only 25% of the deer (1/4 deer) [281]. When infectivity of faeces was calculated using endpoint dilution in mice expressing elk PrP, Tamguney et al. (2009) found faeces were highly infectious (around 10^6 LD_{50}/g wet feces) [170]. Low levels of infectivity have also been detected in antler velvet by transgenic mouse bioassay [282]. Experimental oral transmission of CWD to cervids through blood (225 mL intravenously) and saliva (50 mL orally) have been demonstrated. When cervids were exposed to urine and feces (85 mL urine and 112.5 g feces) transmission did not occur [168], however, contaminated fomites such as feed buckets and bedding, or even paddocks where CWD-infected animals were kept is sufficient to transmit CWD naturally to cervids [168,192,283].

1.10 Where in the environment is CWD?

1.10.1 Soils and CWD

Scrapie research demonstrates that shed prions can contaminate the environment, forming reservoirs of infectivity and complicating disease control and eradication. Pastures formerly housing scrapie positive flocks remain infectious for over 15 years [284,285]. Pen furniture, such as water troughs and fence posts, can contribute much of this infectivity [286]. Replacement of contaminated pasture furniture with clean furniture reduces indirect

transmission (from 20/23 to 1/12 positive sheep after 11 months of exposure) [286]. CWD, like scrapie, can transmit through the environment, with 1/9 deer infected after one year of exposure to a paddock that had housed CWD positive animals two years prior [283]. Deer exposed to contaminated water, feed buckets, and bedding also became CWD positive after a year of exposure [168]. Serial PMCA experiments have also demonstrated how infectivity may be present in the areas around mineral licks, suggesting such areas could become hotspots for transmission, not just for cervids but for livestock [287].

Most studies on the environmental transmission of CWD have focused on prion interactions with soils, especially soil mineralogy. Compared to the complexity of the organic content of soils, soil mineralogy is relatively easy to standardize and, unlike most aerial vegetation, remains constant throughout the year, forming an ideal location for the formation of a reservoir of infectivity. The persistence of prions in soils likely plays a role in environmental transmission of CWD, similar to anthrax (*Bacillus anthracis*) transmission [288,289]. The composition of soils is highly variable, depending on the specific geology and climatic conditions of an area. Prions can tightly adsorb to some soil minerals, (i.e., montmorillonite), or interact weakly with others (i.e. quartz-type minerals) [290,291]. Mineral-associated prions not only remain infectious, but the binding to montmorillonite clays enhances both infectivity and resistance to degradation by rumen contents [190,290,292]. The link between soil composition and CWD prevalence is complex, likely due to the multiplicity of factors that impact CWD prevalence in these areas. One study found that CWD prevalence was correlated with clay content below 18% and pH over 6.6, speculating that these conditions would facilitate the release of infectivity from soil minerals [293], while another found that odds of CWD infection increased 8.9% for every 1% increase in clay content. Other studies, however, found CWD prevalence and soil clay content were unrelated [260,263,265,294,295]. One reason for these inconsistencies may be the length of time CWD

has been present in the study area, as it would take time to establish a reservoir of infectivity. As well, *in vitro* studies suggest that other soil components may complicate the interaction between soil and prions. Manganese oxides reduce infectivity in soils [296], and organic soil compounds such as humic acid, can reduce both infectivity and detection of prions [297–299]. Multiple freeze-thaw cycles decrease the PMCA seeding activity of soil-bound prions [300], as do serine proteases produced by some lichens [301].

1.10.2 Vegetation and CWD

Prions shed into the environment in saliva, feces, or urine may interact with a number of natural surfaces that compose the cervid habitat. The interactions cervids have with these contaminated materials will determine the routes of environmental CWD transmission. Precipitation and seasonal changes may affect the interactions of prions with environmental materials. Prions can adhere to plants and can be transmitted to a new host through both consumption and physical contact [302]. Interestingly, plants may absorb infectivity from contaminated soils, which was demonstrated by testing the PMCA seeding ability of barley plants grown in soil heavily contaminated with the hamster prion 263K [302]. This is not as remarkable as it might first appear, as the passive uptake of bacteria and viruses by a number of food crops has been well characterized [303]. It is, however, possible that the barley plants were contaminated when infectivity was first applied to the soil, rather than absorbed during the experiment. In a separate study, controlled to minimize inadvertent surface contamination, Rasmussen et al. (2014) did not find prion uptake by wheat plants, although their detection method was less sensitive [304]. In this experiment, wheat plants were grown in an agarose growth medium prior to the immersion of the cleaned plant roots into new, prion contaminated media. After exposure, the roots, leaves, and stem of the plants were separated and handled to limit potential cross contamination [304]. Detection was performed

using antigen-capture enzyme assays, which lack the prion amplification step of the Pritzkow study (2015).

It is more likely that infectious biofluids will directly contaminate the aerial surfaces of vegetation. Prions readily adhere to surfaces, although this may be affected by the prion strain and the composition of the surface [302,305], and the adherence can be increased by drying [306]. However, the surfaces of vegetation are highly variable [307–311]. Many plant surfaces are covered with a waxy layer called cuticle, which affects how plants interact with water [312–315]. Greater water repellency, associated with high surface roughness, is associated with a lower level of contamination by small particles [315]. Surface roughness depends on the developmental stage [316] and can be altered by fungal colonization [317]. Variation in plant surface structure may also play a role in the indirect transmission of CWD through plants.

1.11 Project overview

Without a clear understanding of the epidemiology of CWD, our ability to model the spread of this disease and predict its effects is limited. This thesis has two main objectives. The first (Chapters 2-3) is to explore the diversity of North American CWD strains using Syrian Golden hamsters as a research model of host range. Differences in interspecies transmission could indicate different strains. The second objective (Chapter 4) is to detect CWD adhered to plant surfaces and to characterize the interaction between prions and vegetation. This work will increase our understanding of environmental prion interactions, aiding our efforts to understand, detect, and prevent the spread of CWD.

Table 1-1. Strains of CWD

Strain name	Host species	Host genotype	Compared to	Rodent model	Bioassay and histology evidence	Biochemical evidence	Note	Citation
CWD1	Various	-	CWD2	Tg(CerPrP)1536$^{+/-}$ express wildtype cervid PrP	Shorter incubation period, symmetrical PrP deposition, more vacuolation in hippocampus and paraterminal body	identical PrP^{res} migration patterns and biochemical properties	Strain switching/instability present	[217]
CWD2	various	-	CWD1		Longer incubation period, asymmetrical PrP deposition			
Wisc-1	WTD	Wt/wt	H95^{+}	wt-PrP^{C} TgDeer (tg33) S96-PrP^{C} Tgdeer (tg60) hamsters C57Bl6	Shorter incubation in wt-PrP^{C} TgDeer, no transmission in S96-PrP^{C} TgDeer, transmission to hamsters but not wild type mice IHC/histology differences	high MW migration pattern lower stability in GdnHCl		[219,221,318]
H95^{+}	WTD	H95	Wisc-1		Longer incubation in wt-PrP^{C} TgDeer, transmission in S96-PrP^{C} TgDeer, transmission to wildtype mice but not hamsters IHC/histology differences	low MW migration pattern and antibody epitope greater stability in GdnHCl		
A116G	WTD	G116	wt WTD (A116)	tg(CerPrP132M)1536$^{+/+}$ overexpress wt deer PrP	shorter incubation period in wt cervidized mice	Reduced RT-QuIC seeding capacity, less stable in GdnHCl than wt	From free-ranging Alberta deer; Computer simulations demonstrate differences in stability and compactness	[222]
Elk L132	Elk	L132	M132	M132 TgElk	Longer incubation period higher vacuolation in white matter tracts, PrP^{d} differences	lower PrP^{res} migration more stable in GdnHCl		[193,223]
Norway moose	moose	Wt (K109, M209)	reindeer CWD (similar to 'North American CWD')	none	IHC differences, no IHC positive peripheral tissue,	lower PrP^{res} migration and antibody epitopes	Found in older moose (>13 years old), proposed to be sporadic prion disease, different from Canadian moose CWD	[319]

Table 1-2. Host range of CWD in livestock, domestic animals, and North American wildlife

Exposed species	Inoculum	Method	First passage clinical?	WB or IHC positive	Note	Citation
Cattle	MD pool	IC	4/13 (23-59 mpi)	5/13	No periphery PrP^d	[247]
	WTD pool	IC	11/14 (18-26 mpi)	12/14	Periphery PrP^d	[248]
	Elk pool	IC	2/14 (16-17 mpi)	2/14	No periphery PrP^d	[249]
Suffolk Sheep	MD pool	IC	1 (36 months)	2/8	Clinical sheep only lamb heterozygous at codon 126 (AV), most of other animals ARQ,	[246]
Pigs	WTD pool	IC	No	0/8 (6 mpi) 0/10 (aged)	5/6 positive by RT-QuIC 6/7 positive by RT-QuIC	[245]
		Oral	no	0/10 (6 mpi) 2/10 (aged)	5/6 positive by RT-QuIC 4/6 positive by RT-QuIC	
Domestic Cats	MD isolate	IC	2/5 (40-42 mpi)	2/5		[252]
		Oral	0/5	0/5		
Raccoon	WTD pool	IC	No	1/4		[251]
	Elk pool 1	IC	1 /4 (23 mpi)	1/4		
	Elk pool 2	IC	No	0/4	Inoculum from an elk inoculated with MD CWD	
Ferrets	MD isolate	IC	2/2 (9.6-9.7 mpi)	ND		[254]
	MD pool	IC	3/3 (14.8-20.25 mpi)	ND		
	MD isolate	IC	0	6/8		[244]
Voles	WTD isolates	IC	18/18 meadow 9/10 red-backed	18/18 meadow 9/10 red-backed	Rodents inoculated with either wt or heterozygous S96 deer; not all rodents tested by WB/IHC	[253]
Mice			19/20 deer mice 13/17 white-footed	17/17 deer mice 7/11 white-footed		
Mink	Elk isolate	IC	2/8 (31-33 mpi)	8/8		[250]
		oral	0/22	0/22		

IC: inoculated intracranially; MD: mule deer, WTD: white-tailed deer; WB: Western blot; IHC: immunohistochemistry

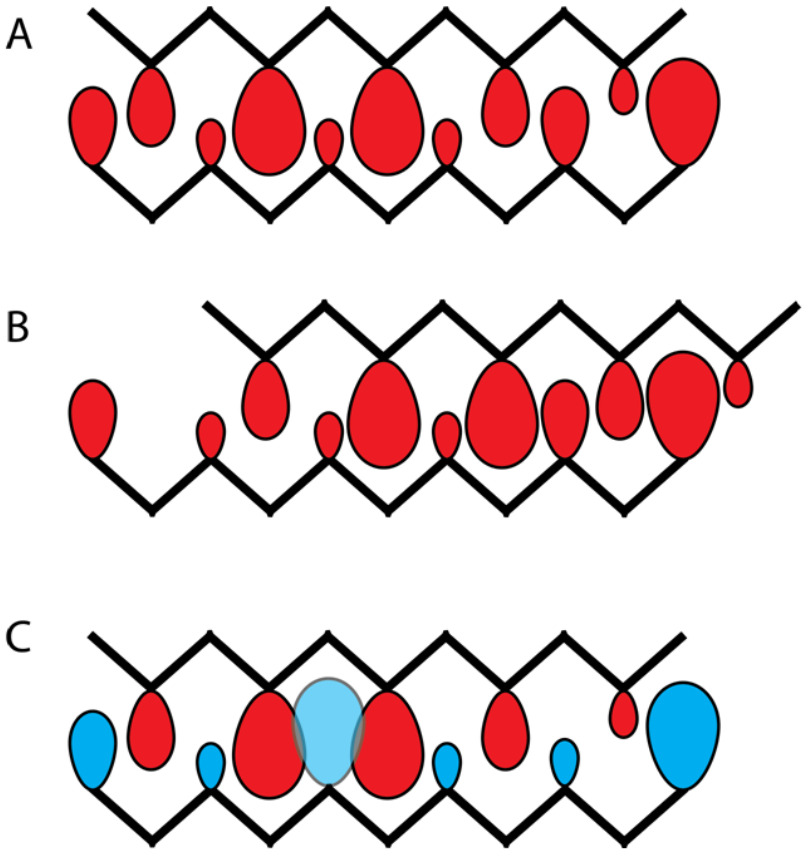

Figure 1-1. Simplified space-filling representation of a steric zipper. A. Amino acid side chains interdigitate to form a steric zipper. B. The same protein sequence may form multiple steric zippers. C. Residue differences in heterotypic transmission may lead to steric hindrance (blue), preventing the formation of a steric zipper.

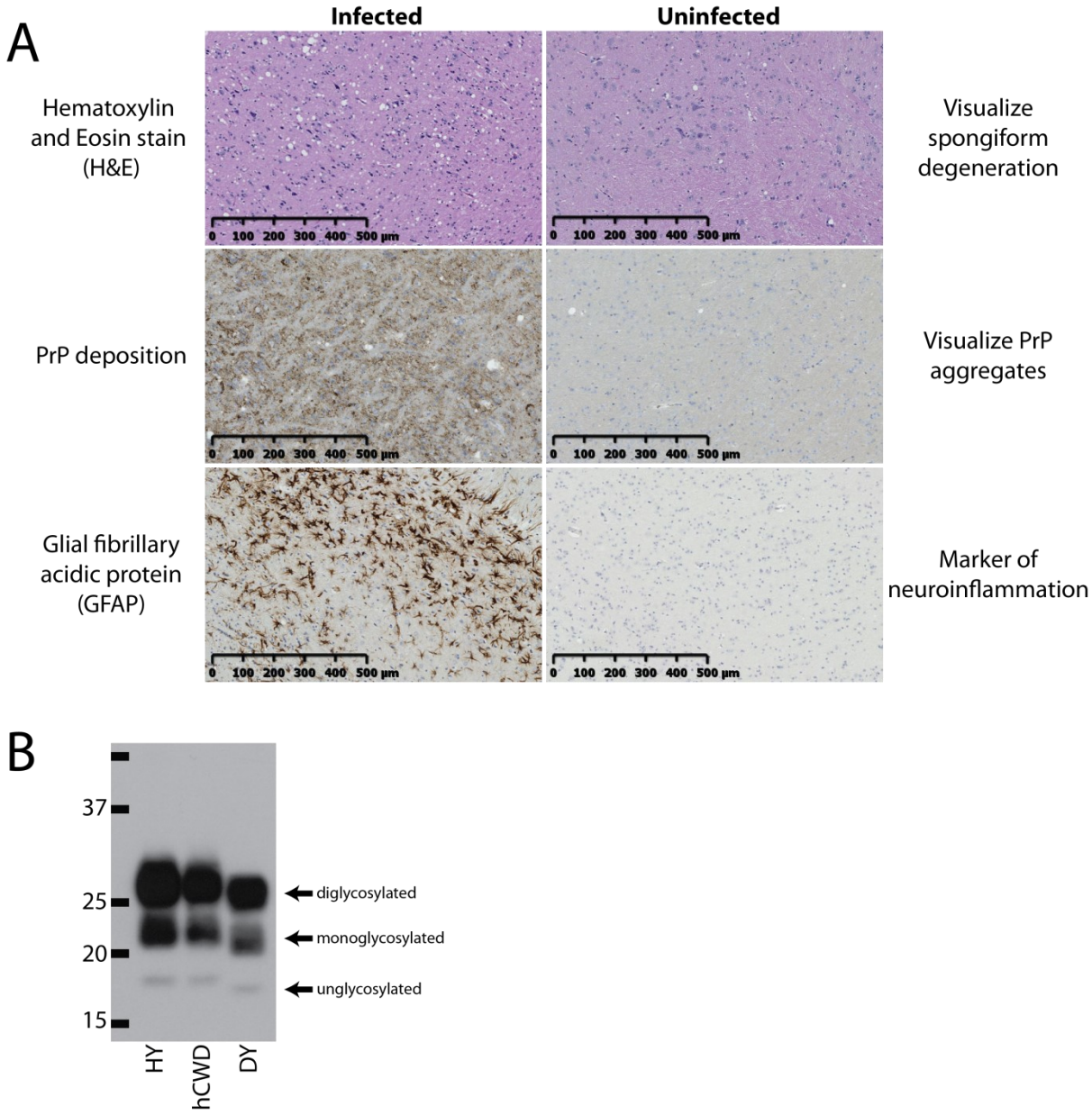

Figure 1-2. Techniques used to differentiate prion strains. **A**. Different histological stains used in prion disease. **B**. Example of migration differences between two strains. The first lane contains the protein ladder demonstrating molecular weight in kilodaltons (kDa).

2 Effect of white-tailed deer genotype on the interspecies transmission of CWD

Part of this work was published in the Journal of Emerging Infectious Diseases and is reproduced here with additional data

Herbst A, Duque Velásquez C, Triscott E, Aiken JM, and McKenzie D.

Chronic Wasting Disease Prion Strain Emergence and Host Range Expansion. Emerging Infectious Diseases 23(9): 1598-1600.

2.1 Abstract

Chronic wasting disease (CWD) is an infectious neurological disease affecting cervids whose geographic range is expanding. The transmission barrier of a prion disease is due to the compatibility between the invading prion and the host PrP and is dependent on the strain properties of the invading prion. Infection of deer expressing the H95 PrP variant with the Wisc-1 CWD strain led to the emergence of $H95^{+}$, a distinct prion strain. To determine if the two strains had different host ranges, we inoculated CWD from white-tailed deer expressing four different genotypes into mice and hamsters. Wisc-1, present in deer expressing at least one wildtype allele, was able to infect hamsters, but not mice. Conversely, mice were susceptible to CWD from deer expressing the H95 PrP variant (strain $H95^{+}$), with low levels of transmission to hamsters. In addition, two PrP^{res} migration patterns were present in hamsters infected with these CWD inocula, perhaps emerging from the amplification of minor PrP^{Sc} isoforms generated during the heterotypic transmission between cerivds of different genotypes or during the interspecies transmission between the cervids and hamsters. The altered host range of $H95^{+}$ compared to Wisc-1, and the amplification of two distinct PrP^{res} migration patterns in hamsters, demonstrates the importance of strain characterization in understanding transmission barriers.

2.2 Introduction

Chronic wasting disease (CWD) is an infectious neurological prion disease affecting cervids in North America, South Korea, and Scandinavia [150,152–154]. CWD, like all prion diseases, is caused by the templated misfolding of the prion protein (PrP), a widely conserved protein found throughout the body, but especially in the central nervous system of all mammals and most vertebrates. Distinct prion diseases, called strains, can be stably propagated under standard passaging conditions, that is, in animals of the same species or transgenic line [94,95]. Strains vary both in their pathophysiology, including clinical signs and histopathology as well as their biochemical properties [90–93]. Strains can also be

differentiated by their host range, or the ability of a strain to transmit to a new host with a dissimilar PrP^C sequence (heterotypic transmission). These transmission differences are likely due to the ability, or in the case of a complete transmission barrier, inability, of the strain to act as a template to the PrP^C of the novel host [98,99,320]. Even when heterotypic transmission is successful, reduced replication fidelity due to a mismatch between PrP^{Sc} and PrP^C can lead to strain mutation or novel strain emergence [92,93,95,147,216,219,222,251].

Given the epizootic nature of CWD, understanding the species barriers between cervids and livestock or humans is of utmost importance for veterinary and human health. Unlike PrP^C, PrP^{Sc} is composed of fibrils of stacked β-sheets, likely forming a four-rung β-solenoid structure [33–40]. β-sheets are formed by hydrogen bonding between amino acid backbones, leaving the amino acid side chains free to interact. It is thought that these side chains interdigitate, forming what is called a steric zipper, and that this stabilizes the prion fibril, aiding in conversion of PrP^C to PrP^{Sc} [41]. It has been posited that these side chain interactions are key to understanding host range. During heterotypic conversion there is a mismatch in these amino acid side chains. If the mismatched side chains are still able to interdigitate, conversion of the PrP^C will occur and the prion strain will transmit. However, PrP^C conversion will be hampered if there is a mismatch where steric hindrance or charge prevents the meshing of the amino acid side chains, resulting in a transmission barrier [175]. A number of amino acid residues may impact steric zipper formation, especially bulky or charged residues located in the β2-α2 loop of PrP^C. These include residues 169, and 174 in the β2-α2 loop and several asparagine and glutamine residues in other locations [176,177,321].

A number of PrP polymorphisms affect CWD prevalence [182–189], including H95, S96, and A116 in white-tailed deer (wildtype is Q95, G96, and G116), F225 in mule deer (wildtype is S225). These polymorphisms are not located in the β2-α2 loop and cannot be

explained through asparagine substitutions, nor result in a complete transmission barrier. Understanding how these common polymorphisms affect the strain characteristics of CWD, especially host range, is important to understanding the future risks of this disease. A number of PrP polymorphism located in the N-terminal are important in modulating the transmission some prion diseases, including codons 129 [75,178] and 127 [181] and codon 108, in conjunction with codon 189, in mice (PrP^a: L108/T189, PrP^b: F108/V189) [322], as well as residues 108 and 111 in transgenic mice [323]. There are also GSS-linked polymorphisms in this area of PrP, including P102 and P105 (wildtype: L102 and L105) [324,325]. The two human codon 129 variants do not differ in PrP^C conformation or stability, although codon 129 appears to play a role in steric zipper formation which could prevent the initial nucleation step of PrP^{Sc} aggregation [326]. Human codon 127 also appears to be part of the same steric zipper sequence and modulates the conversion of PrP^C, but not gross PrP^C structure or stability [327,328]. Similarly, murine codons 108 and 189 also appear to affect the nucleation step of prion misfolding [329]. GSS-linked substitutions of leucine for proline at codons 105 and 102 accelerate *in vitro* PrP conversion, perhaps by altering the arrangement of surrounding cationic residues and interaction with potential cofactors [330]. In deer, the difference between polar glutamine to the positively charged histidine at codon 95, or between non-polar glycine to polar serine at codon 96 may similarly alter residue interactions, likewise modulating the transmission barrier of CWD.

Deer expressing the H95 and S96 PrP alleles had extended incubation periods when orally dosed with CWD [190] compared to wildtype deer (Q95 and G96) and have altered peripheral PrP deposition patterns [164]. Further examination of these polymorphisms through heterotypic and homotypic bioassay in transgenic mice expressing cervid PrP and through biochemical studies demonstrated that a new strain, $H95^+$, emerged through the passaging CWD through deer expressing the H95 polymorphism (wt/H95 or H95/S96), while

deer expressing one or more wild-type alleles (wt/wt, wt/H95, wt/S96) propagate the strain Wisc-1 [219]. Wisc-1 prions are less stable in GdnHCl than $H95^{+}$ prions, while the PrP^{Sc} from heterozygous deer contained greater conformational heterogeneity than the homozygous PrP^{Sc}, which is reduced upon serial passage [318]. This demonstrates how heterotypic prion transmission can lead to an expansion of PrP^{Sc} conformation heterogeneity, which may alter host range. In this study, the host range of CWD from deer expressing different PrP alleles is compared using wild type mice and hamsters, demonstrating how the heterotypic transmission of CWD can cause the expansion of CWD host range.

2.3 Methods

This study was carried out in accordance with the guidelines of the Canadian Council on Animal Care and approved by the Animal Care and Use Committee: Health Sciences at the University of Alberta.

2.3.1 Rodent Infections

Four brain homogenates were prepared from clinical, experimentally infected white-tailed deer (*Odocoileus virginianus*) of defined genotypes [218]. Weanling C57Bl/6 and FVB mice were intracerebrally inoculated with 30 µL of a 1% deer homogenate, wt/wt (homozygous Q95, G96), wt/H95 (heterozygous wildtype and H95, G96), wt/S96 (heterozygous wildtype and Q95, S96), and H95/S96 (heterozygous H95, G96 and Q95, S96). Weanling Syrian Golden hamsters (*Mesocricetus auratus*), purchased from Envigo, were intracerebrally inoculated with 50 µl of 10% cervid brain homogenates. Animals were monitored for the onset of clinical signs and euthanized when clinical disease was established. The experimental endpoints for animals not displaying clinical signs were 708 dpi for mice and 659 dpi for hamsters. Brains were removed, cut in half sagittally, with half used for making brain homogenates and the other half fixed in formalin. To make the brain homogenates, the samples were homogenized to 10% (wt/vol) in HyClone Ultrapure water (FisherScience). For

the second hamster passage, 50 µL of 10% first passage hamster homogenates were inoculated (intracranially, i.c.) into weanling hamsters. Hamsters were monitored for onset of clinical disease and euthanized when clinical disease established. The wt/wt CWD isolate had previously been passaged three times in hamsters until the incubation period stabilized. This inocula is referred to as hamster-adapted CWD (hCWD). The incubation periods and standard deviation were calculated using Microsoft Excel.

Unlike the first hamster passage samples, hCWD should be fully adapted to its new host and is unlikely to be heterologous. Second passage hamsters were weighed at 38 and 46 weeks post infection by individually transferring them into a cage on top of a tared scale. These time points coincided with noticeable differences in mass at 38 weeks without evidence of clinical signs and overt disease in wt/wt and hCWD inoculated hamsters at 46 weeks. The hamster weights at each week were compared by one-way ANOVAs, using Tukey's HSD test for post hoc analysis at the $p<0.05$ level. The statistical analysis of transmission experiments was performed with GraphPad Prism (version 5.04) software.

2.3.2 Immunoblotting and the detection of PrP^{res}

PrP^{res} was detected following proteinase K digestion and immunoblotting as described in Appendix I. In brief, 10µL of brain homogenate was digested for 45 minutes with 50 µg/µL (final concentration) proteinase K. Immunoblots were performed as described in Appendix 4. Immunoblots were probed using 3F4 (a kind gift from Richard Rubenstein, SUNY-Downstate) for hamsters or SAF83 (Cayman Chemical, Michigan) for mice at a dilution of 1:10 000.

2.3.3 Histopathological analysis

The formalin fixed sagittal sections were embedded and sectioned as in Appendix 8. Serial sections were processed for lesion profiling and immunohistochemistry (Appendix 8). Sample embedding, sectioning, and staining were performed by Hristina Gapeshina in the

CPPFD histology core. Slides were scanned using a NanoZoomer 2.0RS (Hamamatsu Photonics) and analyzed using NanoZoomer digital pathology software (Hamamatsu Photonics). Lesion profiling was performed as previously described [114]. In brief, for each brain, three trained individuals, including myself, evaluated 10 different regions on a scale of 0-4 based on severity of the spongiosis (Figure 1). Identification of brain structures was performed using a hamster brain atlas [331]. The average of the three graders' scores were calculated. The lesions profile itself presents the average score of each brain section, composed of at least 3 different hamster brains scored as above, using GraphPad Prism (version 5.04) software.

2.4 Results

2.4.1 First passage rodent transmission

Hamsters and mice were intracerebrally inoculated with 4 different CWD brain homogenates from white-tailed deer expressing different PrP alleles, wt/wt, wt/H96, wt/S96, and H95/S96. Five hamsters showed signs of clinical disease, three inoculated with the wt/wt CWD isolate and one each from the wt/H95 and the wt/S96 homogenates (Table 2-1). However, the majority of the animals were PrP^{res} positive by immunoblot, suggesting they were subclinically infected. Transmission with the H95/S96 isolate was inefficient, with no animals presenting with clinical disease and only one of eight hamsters accumulating detectable levels of PrP^{res}. Clinical signs of CWD in hamsters were initially subtle, progressing into lethargy and ataxia. In contrast to the hamster results, all C57Bl/6 mice inoculated with the H95/S96 isolate presented with clinical prion disease with an average incubation period of 575±47 dpi, while five of the 7 mice inoculated with the wt/H95 inocula developed clinical disease with an average incubation period of 692±9 dpi, the other two mice accumulated PrP^{res}. The other two inocula (wt/wt and wt/S96) did not result in infection. Transmission was similar in the FVB mice, with clinical signs present in 3 of 8 mice from both the wt/H95 and H95/S96 transmissions (474±136 dpi and 551±143 dpi, respectively),

and none in FVB mice inoculated with wt/wt and wt/S96. Clinical signs in both C57Bl/6 and FVB mice included ataxia, lethargy, tail rigidity, and dermatitis.

2.4.2 Hamster-adapted CWD

Prior to the commencement of these experiments, the wt/wt CWD white-tailed deer inocula was adapted to hamsters by passaging it three times until the incubation period stabilized at 371 dpi (Table 2-2). This hamster-adapted CWD was used as a positive control in these experiments. Clinical signs in third-passage hamster-adapted CWD (hCWD) began with the onset of mild ataxia, which progressed into severe ataxia, lethargy, tremors, and dystonic movement such as retrocollis. Clinical signs progressed over a period of two months. PrP^{res} migration patterns were similar between inocula, but signal strength varied (Figure 2.2).

2.4.3 Histopathological analysis

Lesion profiling and immunohistochemistry was performed on sagittal brain sections from 3-4 hamsters from each inocula and from hCWD. PrP deposition (PrP^{d}) was present in all brains infected with wt/wt, wt/H95, wt/S96, and hCWD inocula (Table 2-1). PrP deposition was not present in any of the hamsters inoculated with H95/S96 inocula. The single PrP^{res} positive H95/S96 hamster was not analyzed as the brain was not properly sectioned during necropsy.

In all PrP^{d} positive samples, staining was diffuse and most evident in the hindbrain, superior and inferior colliculus, and thalamus (Figure 2-3). Unsurprisingly, staining was most intense in the hCWD-inoculated hamsters. PrP^{d} staining intensity varied between individual hamsters, being most pronounced in animals infected with wt/wt isolate, and least pronounced in wt/H95 isolate-inoculated hamsters. Interestingly, vacuolation was present in all animals, including those negative for both PrP^{d} and PrP^{res} (Figure 2-4). Vacuolation was most prominent in the inferior and superior colliculus and evident in the thalamus and hindbrain of all samples. Similar lesion profiles were observed in all samples, although the

hCWD samples had a higher magnitude of vacuolation in every brain region except the cerebellum and the pons (Figure 2-5). There was no difference between PrP^{d} positive and negative lesion profiles from first passage hamsters.

2.4.4 Second passage hamster transmission

We performed second hamster passages of the four inocula. One sample from each genotype was used to inoculate a second passage of hamsters. Each inocula had not been previously screened for PrP^{res}. The wt/wt second passage inoculum was from a hamster (hamster 8000C) that was strongly positive by immunoblot. The wt/S96 second passage inoculum (hamster 8005C) was faintly positive by immunoblot. Both the wt/H95 and H95/S96 second passage inocula (hamsters 8007C and 8009C, respectively) were negative by immunoblot. We also inoculated hamsters with a western blot positive sample from fourth passage hCWD (from hamster 8110A). A second hamster passage was also performed using the blot-positive first passage sample from H95/S96 (hamster 8010A). Hamsters were euthanized upon the appearance of clinical symptoms or at 502dpi. Clinical signs were similar to those observed in the first passage and in hCWD, with the addition of dystonic movement, specifically retrocollis, and tremors. The clinical course, from the observation of first clinical signs to terminal stage, was approximately two months. Wt/wt animals presented with clinical disease at 368-377 dpi (372.5±5.2 dpi) (Table 2-3). Two of the wt/S96 animals were clinical at 418 and 433 dpi. None of the wt/H95 animals or H95/S96 animals were clinical at 502dpi. When screened by immunoblot, PrP^{res} was present in the wt/wt, wt/H95, and wt/S96 isolates, but not in the H96/S96 isolate. The PrP^{res} of the wt/H95 second passage samples have a slightly lower molecular weight than the other samples, 20kDa compared to the 21kDa molecular weight of the other samples (Figure 2-6). All hamsters inoculated with the single H95/S96 positive sample were clinical (368±19.3 dpi) at a similar incubation period and with similar clinical symptoms and migration pattern as the second passage of wt/wt inocula (Table 2-3).

To compare these second hamster passages to hamster-adapted CWD, we inoculated hamsters with fourth passage hCWD (hamster 8110A). All hamsters inoculated with hCWD were euthanized with clinical signs between 328 and 368dpi (348±23.1 dpi) (Table 2-3).

A month prior to the onset of clinical signs I noticed that hamsters inoculated with the hCWD, wt/wt, and wt/96 first passage inocula (which later became clinical) were heavier than hamsters inoculated with the wt/H95 or H95/S96 first passage inocula. By comparing the hamster weights I determined that hamsters inoculated with the hCWD (week 38: 242.8±27.6 g ; week 46: 185±37.6 g) and wt/wt (week 38: 225±7.7 g ; week 46: 158.8±18.4 g) inocula were heavier than the wt/H95 (week 38: 164.7±9.5 g; week 46: 166.3±13.5 g) and H95/S96 (week 38: 165.5±21.4 g; week 46: 157.3±25.6 g) inoculated hamsters at week 38 ($F(4, 13)=9.08$, $p=0.00099$), but not at week 46 ($F(4, 13)=2.61$, $p=0.084$) when the wt/wt and hCWD inoculated hamsters were displaying clinical signs (Figure 2-7). Hamsters inoculated with wt/S96 were not significantly different from the other inocula groups at either time point.

2.5 Discussion

Prion polymorphisms in a similar location as the H95 and S96 substitutions have played a role in the host range and incubation periods of prion disease, including residues 127 and 129 in humans and residue 108, along with 138, in mice [75,178,181,322,323]. Previous work in my lab demonstrated how the transmission of CWD into deer expressing the H95 polymorphism led to the emergence of a novel CWD strain, $H95^{+}$ [219]. Wisc-1, from deer expressing at least one wildtype allele, transmitted to hamsters but not to either of our wild-type mouse models. Conversely, $H95^{+}$ transmitted to both mouse models but poorly in hamsters (Table 2-1). This demonstrates how a PrP polymorphism can alter the strain properties, such as host range, of CWD. The mechanism by which the glutamine to histidine substitution alters PrP^{Sc} conformation is unclear, although substitutions in similar areas

appear to affect the initial nucleation step of amyloid formation [326,329]. The histidine substitution may change the cervid PrP^{Sc} in such a way to hamper the conversion of hamster PrP, while promoting murine PrP^{Sc} formation.

2.5.1 Wisc-1 CWD in hamsters

The histopathological, clinical, and biochemical similarities in the hamsters infected with the wt/wt, wt/S96, and H95/S96 inocula suggest that the hamster transmission of these isolates was due to the same strain, namely Wisc-1. The different incubation periods of the second hamster passage of the inocula containing Wisc-1 (wt/S96 and wt/wt) were likely due to the different titres in the first passage sample, and not strain-related transmission differences. The first passage wt/S96 sample used for the second passage had a fainter signal by immunoblot than the wt/wt sample with a corresponding delay in the onset of clinical signs (Table 2-3). Only one hamster inoculated with the H95/S96 inocula showed signs of prion infection. The first passage PrP^{res}, as well the second passage incubation period and clinical signs, was very similar to the other Wisc-1 samples, suggesting that transmission might have been due to the presence of a small amount of Wisc-1 rather than transmission of $H95^{+}$ or some other minor PrP^{Sc} conformation that emerged as a result of the H95 polymorphism.

A month before the onset of neurological signs in wt/wt and hCWD-infected hamsters I observed an increase in hamster mass. To confirm this, I weighed the hamsters at week 38, prior to the onset of clinical signs, and week 46, when some hamsters were overtly clinical. Hamsters inoculated with Wisc-1 (wt/wt or hCWD) were significantly heavier than the H95/S96 or wt/H95 inoculated hamsters, which did not develop clinical signs. This difference disappeared as the disease progressed (Figure 2-7). Preclinical weight gain is also a feature of the hamster prion diseases 139H and WST [332,333]. The similarity to WST is especially interesting, as WST also originated from CWD and shares a similar incubation period and disease course as our hamster-passaged Wisc-1. However, care should be taken in comparing

WST and hCWD, as WST emerged after passaging CWD through mice overexpressing hamster PrP [332]. The expression levels of PrP^{C} plays a role in which strains will emerge during transmission into a new host [109], which may have altered how CWD adapted to the hamsters.

2.5.2 Novel molecular shift in hamsters infected with wt/H95

The wt/H95 inocula samples had a lower molecular weight in the second passage compared to the other samples (Figure 2-6). While this shift may be due to the H95 allele, a corresponding shift was not observed in the H95/S96 samples, which instead appeared identical to the hamster-passaged Wisc-1 samples (Figure 2-6). It's possible that the low molecular weight hamster PrP^{Sc} originated not from $H95^{+}$ itself, since it was not evident in the hamster-passaged H95/S96 inoculum, but instead due to some other novel PrP^{Sc} conformation that emerged during the heterotypic transmission of CWD [318]. If this is the case, this new structure may have became discernible in the second passage wt/H95 samples due to the low titre of the infecting inocula, given that the first passage hamster sample used to infect the second wt/H95 passage was PrP^{res} negative. Thus, the wt/H95 bioassays may have functioned as a high dilution passage, allowing the emergence of a minor PrP^{Sc} structure [145]. This low migration pattern was associated with a prolonged incubation period (Table 2-3), although this might be a result of the low titre of the inocula instead of a feature of this distinct structural conformation.

2.5.3 Histopathology

Lesion profile analysis was not useful for discerning strain differences in very old hamsters (i.e., the majority of the first passages). Lesions were present in both PrP^{d} positive and PrP^{d} negative brains (Figure 2-5B), suggesting these lesions are idiopathic rather than disease-related. Gerhauser (2013) also observed idiopathic spongiosis in hamsters at two years of age [334]. PrP^{d} deposition in the brains of hamsters from the first passage were similar, if less

intense, to the PrP^d of hCWD samples (Figure 2-5), consistent with the adaptation of Wisc-1 to hamsters. Vacuolation was also more intense in the hamster-adapted Wisc-1. As these animals were clinical at 1 year post-inoculation when, based on the Gerhauser study, idiopathic vacuolation was minimal, it is likely these lesions are due to prion infection. It is interesting that both idiopathic and prion-related spongiosis occur in the same brain regions, perhaps due to these areas being at increased vulnerability to stress [335,336].

2.5.4 Relation to previously published literature

Previous studies of CWD host range have also demonstrated inconsistency in the transmissibility of CWD to hamsters (Table 2-4). Some CWD inocula do not transmit to hamsters at all, while another inoculum not only transmitted to hamsters, but had an incubation period under 100 days [244,255]. Like my hamster experiments, these studies demonstrate how diverse CWD is using the lens of host range; however, due to differences in experimental methods, it is difficult to directly compare the results of these studies. I previously mentioned the similarities between hamster-passaged Wisc-1 and WST; however, unlike in my study, the primary passage of CWD that was used in the characterization of WST was performed in transgenic mice overexpressing hamster PrP [332]. This is problematic, as the expression level of PrP can drive the evolution of strains [109]. Thus, WST and CHY, another strain generated from that initial transgenic passage, may not realistically reflect the host range of CWD. In another study, Raymond et al (2007) inoculated hamsters with CWD from three different cervid species [255]. This study found differences in the hamster infectivity of these inocula, from a lack of transmission from the white-tailed deer inocula, to transmission to 86% of hamsters from the mule deer inocula. They also observed differences in incubation period between the hamster-passaged elk and mule deer isolates (427±53 dpi vs. 85±0 dpi). It should also be noted that the inocula used in these experiments were made using pools of brain homogenate from cervids containing a

variety of genotypes, some of which were not fully characterized [239]. Similar to what I observed in the wt/H95 inocula, this may have allowed minor PrP^{Sc} conformations to transmit to the hamsters and become more prominent (Figure 2-6).

2.5.5 Conclusions

The host range of $H95^{+}$ was shown to be quite different compared to that of its parent strain, Wisc-1, highlighting the importance of strain characterization when defining transmission barriers. Previous CWD transmission studies in hamsters have also demonstrated the variability of the CWD host range [244,255,332]. These results demonstrate how PrP polymorphisms such as H95 can increase the diversity of CWD showing the dynamic nature of this disease, but also how a series of heterotypic transmission may result in the propagation of previously generated minor PrP^{Sc} species. The heterogeneity of CWD hamster infectivity raises concern about the CWD transmission potential to other, more relevant, species, such as livestock and humans. Although a number of studies in transgenic mice have demonstrated that the zoonotic risk of CWD is low [230,234], a greater understanding of CWD strains is necessary to predict the consequences of this panzootic.

2.6 Tables and Figures

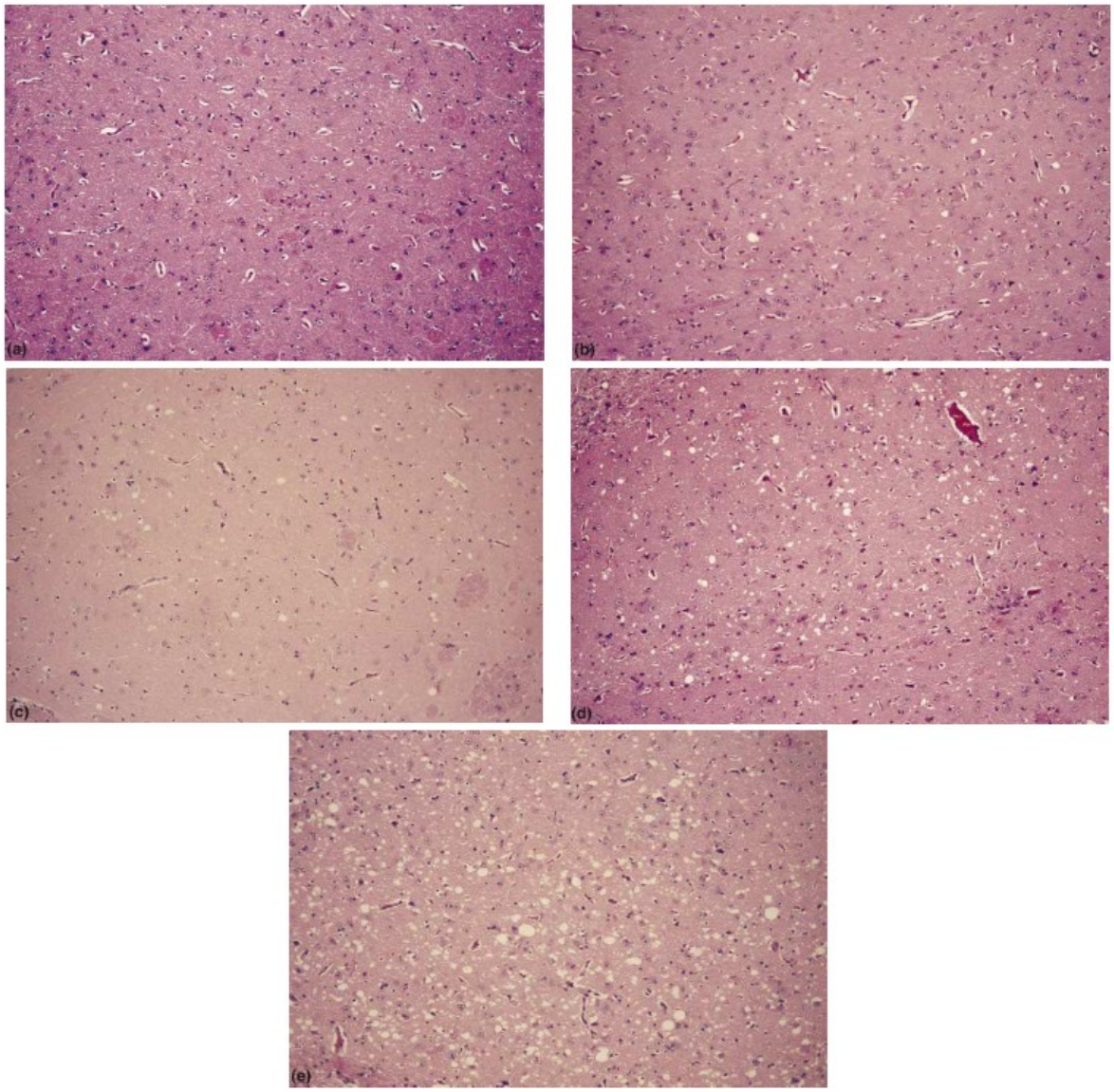

Figure 2-1. Scoring scale used to visually assess the lesion density in sagittal brain sections. Sections are scored on a scale of 0-4, as shown here. Score 0 (a) has no lesions, with the degree of vacuolation increasing in score 1 (b), 2 (c), 3 (d), until the entire field is filled with coalescing vacuoles (score 4, e). Taken from Ligios et al. 2002 [337].

Table 2-1. Primary transmission of CWD isolates from experimentally infected deer of different PrP genotypes (wt/wt, wt/S96, wt/H95, H95/S96) to hamsters and wildtype mice.

Animal model	Inocula	N	Clinical	PrP^{res} +	Incubation Period (dpi)	IHC+
Hamster	Wt/wt	8	3	8	652, 653, 653	3/3
	Wt/S96	8	1	6	634	3/3
	Wt/H95	8	1	7	652	3/4
	H95/S96	8	0	1	-	0/3
C57Bl/6 (*Prnp*$^{a/a}$)	Wt/wt	6	0	0	-	ND
	Wt/S96	6	0	0	-	ND
	Wt/H95	7	5	7	669, 671, 706, 706, 706	ND
	H95/S96	7	7	7	306, 593, 593, 593, 673, 675	ND
FVB (*Prnp*$^{a/a}$)	Wt/wt	5	0	0	-	ND
	Wt/S96	6	0	0	-	ND
	Wt/H95	8	3	8	363, 432, 626	ND
	H95/S96	8	3		432, 512, 710	ND

* Experiment was ended at 708 dpi for mice and 659 dpi for hamsters. Adapted from Herbst et al. 2017. ND: not done

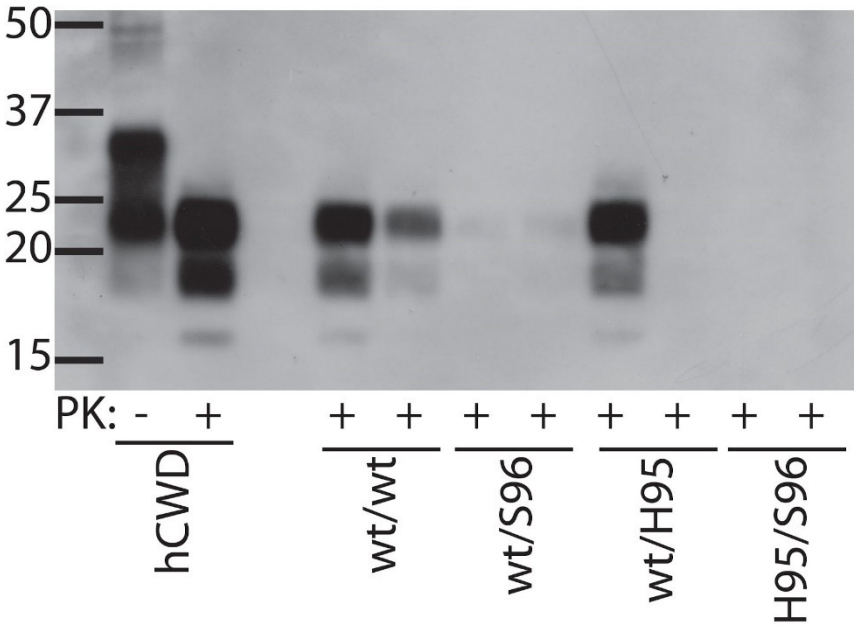

Figure 2-2. Variable PrP^{res} signal intensity following the first passage of deer inocula into hamsters. Proteinase K (PK) digested hamster brain homogenate (+ is digested, - is undigested) was digested in 50 µg/mL of PK and incubated for 45 minutes at 37°C. The origin of the isolate inoculated into the hamsters is shown below the immunoblot; either the genotype of the deer from which the sample originated (wt/wt, wt/S96, wt/H95, or H95/S96), or serial passaged, hamster-adapted CWD (hCWD). The first lane contains the protein ladder demonstrating molecular weight in kilodaltons (kDa). Primary antibody: 3F4.

Table 2-2. Creation of hamster-adapted CWD (hCWD) by adapting CWD from wildtype white-tailed deer to hamsters through serial passaging.

	Incubation period (dpi)	Note
Second passage	344±5.6	Euthanized upon the onset of early clinical signs
Third passage	371±18	
Fourth passage	371±24	

Table 2-3. Second passage of CWD isolates to hamsters, with a description of the first passage sample used for the second passage inoculation. The initial cervid isolate is either the genotype of the deer from which the sample originated (wt/wt, wt/S96, wt/H95, or H95/S96), or hamster-adapted CWD (hCWD).

Initial cervid isolate	Inocula	First passage PrP^{res} description	N	Clinical	Incubation Period (dpi)	PrP^{res}+
Wt/wt	8000C	Strong blot positive	4	4	373±5.2	4
Wt/S96	8005C	weak blot positive	3	2*	426±10.6	3
Wt/H95	8007C	blot negative	3	0	-	3
H95/S96	8009C	blot negative	4	0	-	0
	8010A	blot positive	8	8	368±19.3	8
hCWD	8110A	strong blot positive	4	4	348±23**	4

*The single non-clinical hamster was euthanized at 368dpi due to intercurrent disease; **Half of hamsters euthanized upon the onset of clinical signs. IC: euthanized due to intercurrent disease

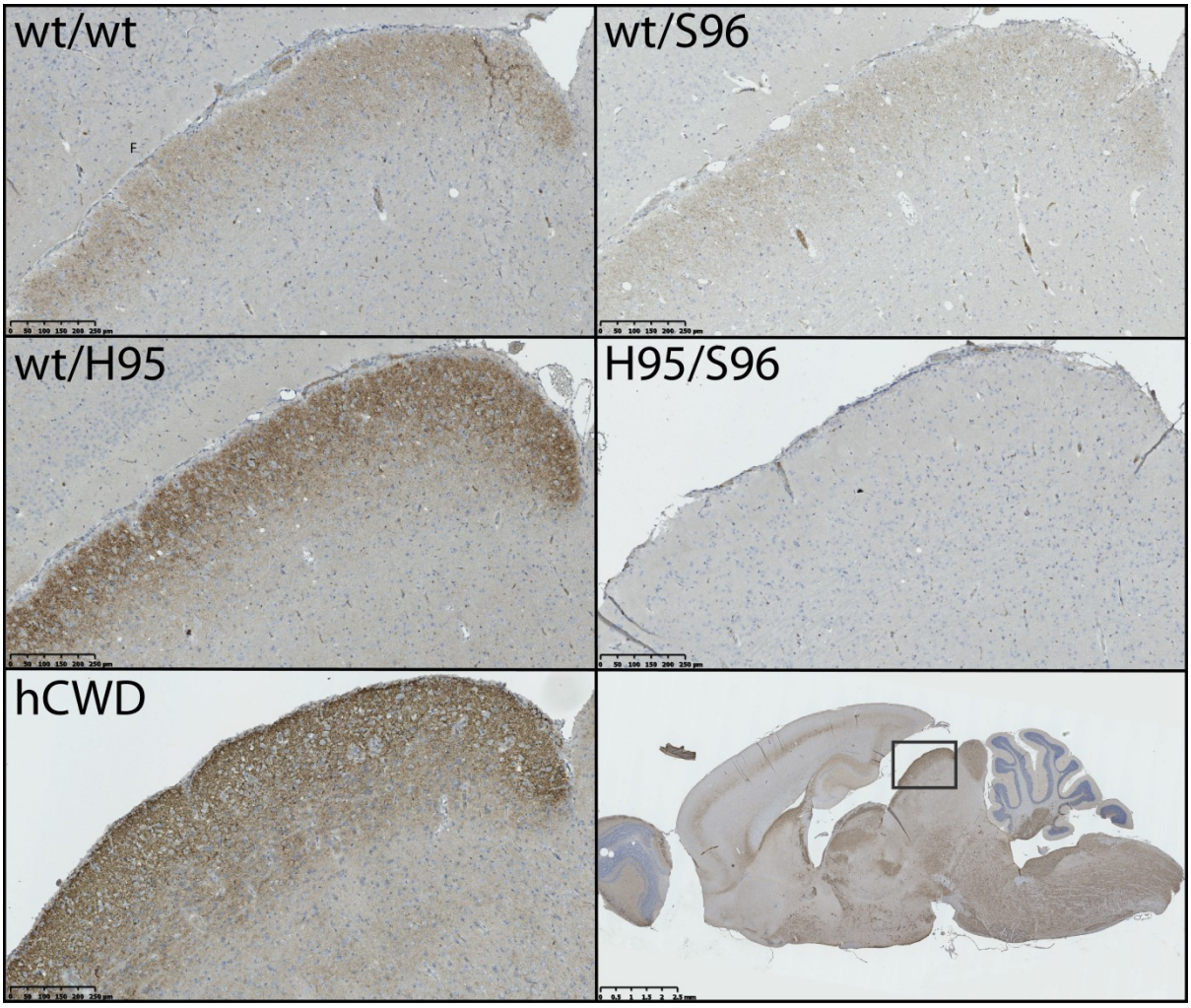

Figure 2-3. Variable signal intensity of PrP deposition the inferior superior colliculus of the first passage hamsters inoculated with different CWD isolates. The indicated area is the inferior colliculus. The label indicates the origin of the sample used to inoculate the hamsters, either a white-tailed deer with a certain PrP genotype (wt/wt, wt/S96, wt/H95, or H95/S96), or hamster-adapted CWD (hCWD). Primary antibody 3F4.

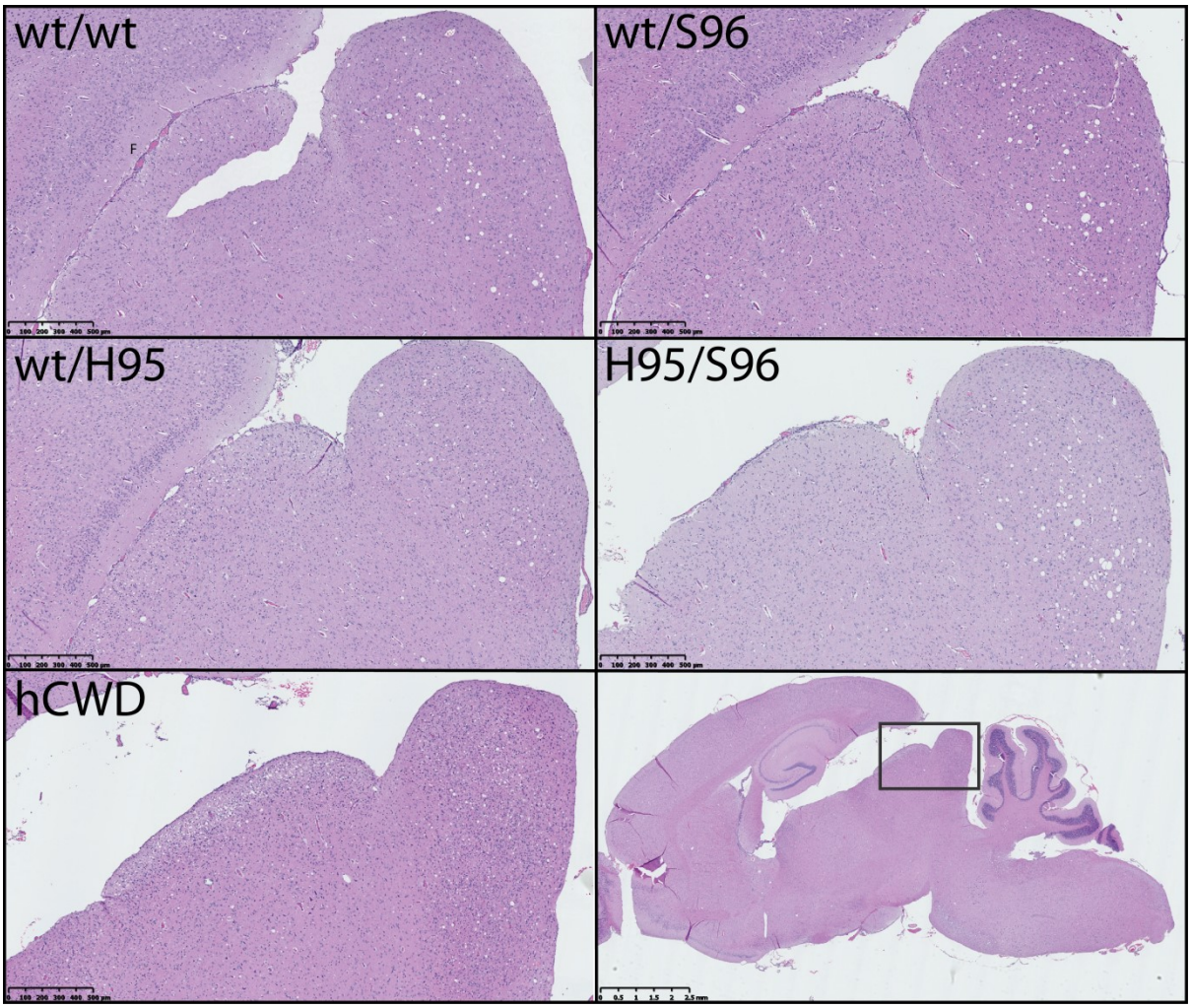

Figure 2-4. Vacuolation in the inferior and superior colliculus of the first passage hamsters inoculated with different CWD isolates. The indicated area is the inferior and superior colliculus. The label indicates the origin of the sample used to inoculate the hamsters, either a white-tailed deer with a certain PrP genotype (wt/wt, wt/S96, wt/H95, or H95/S96), or hamster-adapted CWD (hCWD). Primary antibody 3F4.

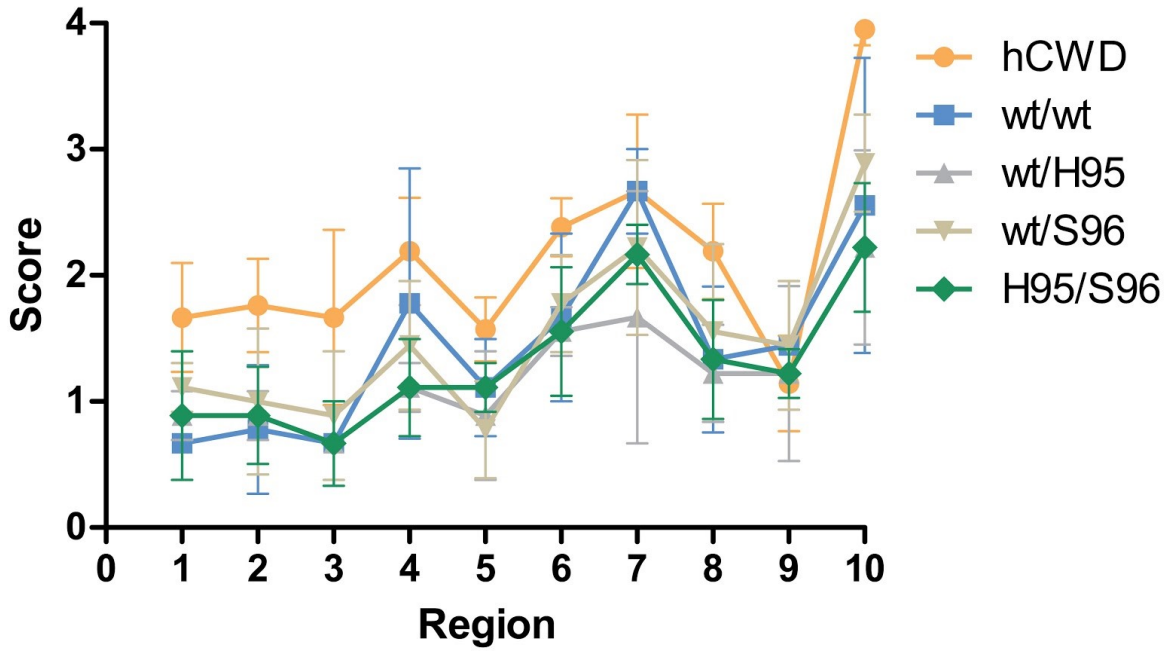

Figure 2-5. Similar lesion profiles from hamsters following the first passage of deer inocula. Areas scored included the corpus callosum (1), central nuclei (2), hippocampus (3), thalamus (4), hypothalamus (5), midbrain (6), pons (7), medulla (8), cerebellum (9), and inferior and superior colliculus (10). The label indicates the origin of the sample used to inoculate the hamsters, either a white-tailed deer with a certain PrP genotype (wt/wt, wt/S96, wt/H95, or H95/S96), or hamster-adapted CWD (hCWD).

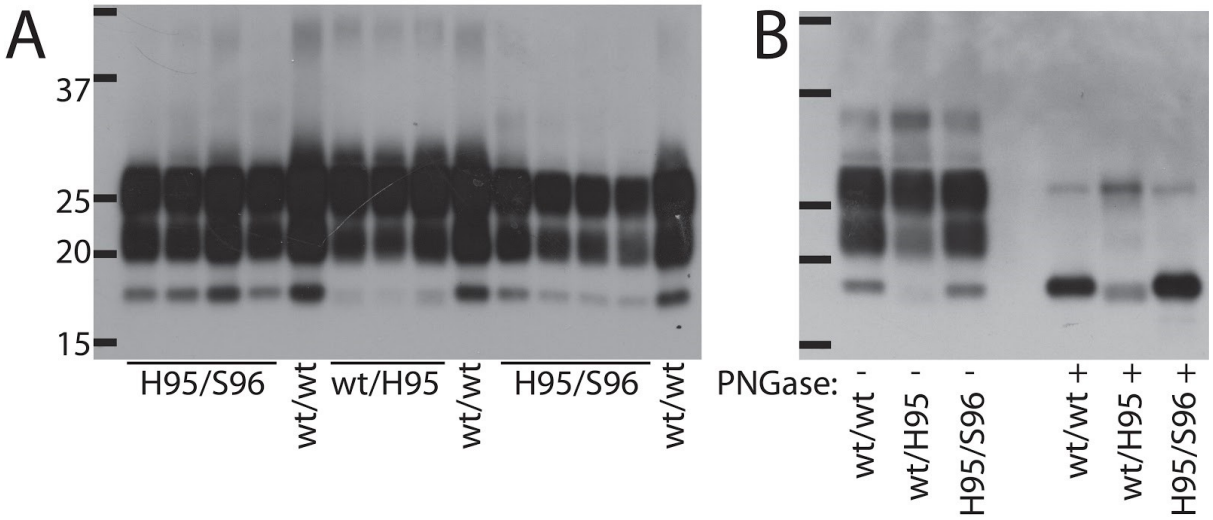

Figure 2-6. PrP^{res} from the brains of hamsters following the second passage of CWD to hamsters. **A.** Samples were digested for 45 minutes in 50 µg/mL proteinase K at 37ºC. **B.** Proteinase K digested samples compared to PNGase f digested samples. The first lane contains the protein ladder demonstrating molecular weight in kilodaltons (kDa). The genotype of the deer the CWD isolate originated in (wt/wt, wt/S96, wt/H95, or H95/S96) is shown below the immunoblot. Primary antibody: 3F4 1:10000.

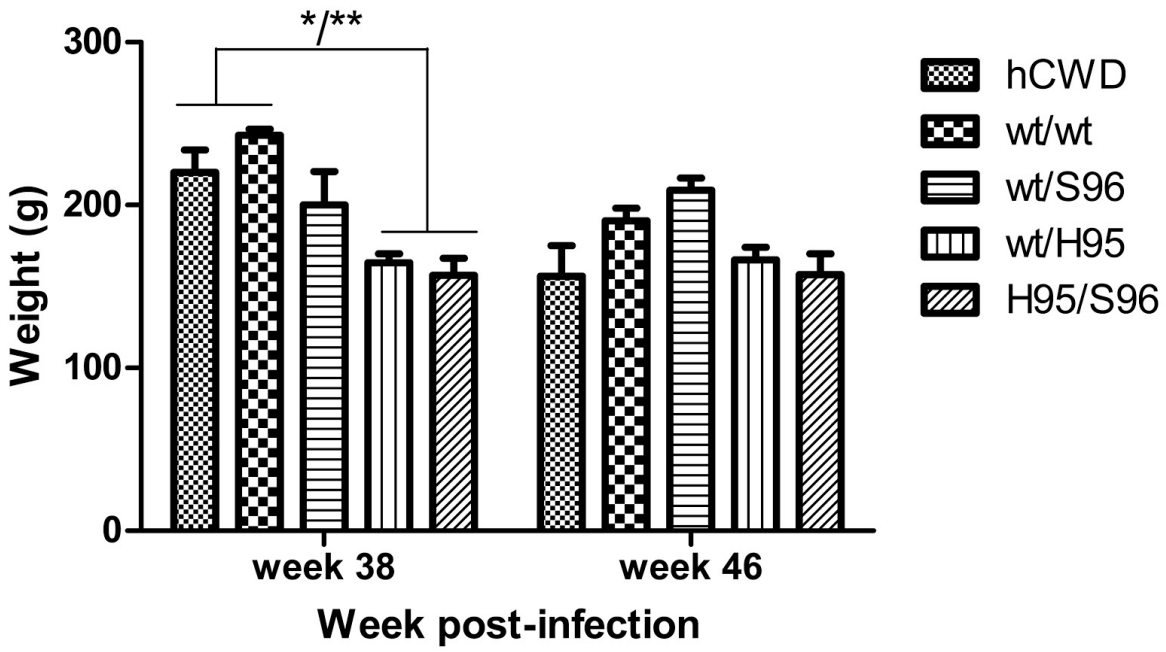

Figure 2-7. There was a significant difference in weights of hamsters inoculated with different inocula at week 38, but not at week 46. Wt/wt and hCWD hamsters were heavier than both wt/H95 and H95/S96 hamsters at week 38 (wt/wt vs. both wt/H95 and H95/S96 $p<0.01$; hCWD vs. both wt/H95 and H95/S96 $p<0.05$), but not at week 46 ($p>0.05$). The label indicates the origin of the CWD sample, either a white-tailed deer with a certain PrP genotype (wt/wt, wt/S96, wt/H95, or H95/S96), or hamster-adapted CWD (hCWD).

Table 2-4. Summary of prior CWD isolate transmission into Syrian Golden hamsters.

Inoculum	% Transmission	2nd passage incubation period	Note	Citation
Elk pool	28.6	427±53	Inocula contained heterologous genotypes	[255]
MD pool	85.7	85±0		
WTD pool	0	NA		
MD isolate*	0**	NA		[244]
WTD isolate*	ND***	379±3	WST strain	[332]
		479±6	CHY strain	[338]

*Isolate genotype not reported; **no clinical signs at 1 year; ***Primary passage performed in transgenic mice overexpressing hamster PrP

3 Heterogeneity of hamster transmissibility of free-ranging CWD isolates

Data in this chapter has been included in two manuscripts, one currently submitted to a peer-reviewed journal as: Samia Hannaoui, Elizabeth Triscott, Camilo Duque Velásquez, Sheng Chun Chang, Maria Immaculata Arifin, Irina Zemlyankina, Xinli Tang, Trent Bollinger, Holger Wille, Debbie McKenzie, Sabine Gilch (2020). Cervid polymorphism at codon 116 of the *Prnp* gene generates new and distinct chronic wasting disease strains.

The other manuscript is currently in preparation (Triscott E, Duque Vélasquez C, Herbst A, Aiken JM, McKenzie D).

3.1 Abstract

The geographical area affected by Chronic Wasting Disease (CWD), an infectious prion disease of farmed and free-ranging cervids, is expanding throughout North America, Scandinavia, and Korea. A given prion disease can be represented by strains, which differ in a number of characteristics, including host range. To assess the diversity of CWD strains currently present in free-ranging Canadian cervids, I characterized the host range, and thus strain variability, of 23 hunter-harvested CWD isolates by comparing their transmissibility into Syrian Golden hamsters. In addition, thirteen of the isolates were also inoculated into transgenic cervidized mice to assess the relative levels of infectivity present in each sample. I was able to separate 13 of the isolates, which contained similar infectious titres according to the mouse transmission data, into three categories of their hamster transmission properties: low (0-15%) hamster transmission (3 isolates, all from a similar geographic location), high (83-100%) hamster transmission (3 isolates, all from WTD), while the others (7 isolates, primarily MD) transmitted to 50-67% of the hamsters. Immunoblot analysis of the hamster PrP^{res} from these transmission assays identified two different migration patterns: 'A' (21 kDa) and 'B' (20kDa). Upon the second passage of these samples, a double unglycosylated band was observed, which was associated with an extended incubation period, both features of a strain mixture. These data indicate that, while these isolates appear similar in their native host, they vary in their transmission properties, suggesting the presence of multiple, coexisting CWD conformers, raising concerns for interspecies CWD transmission.

3.2 Introduction

Chronic wasting disease, an infectious prion disease of cervids, exists throughout North America, South Korea, and Scandinavia. Several cervid species have been naturally infected with CWD, including mule deer, white tailed deer, elk, reindeer, moose, red deer, and sika

deer. Several CWD strains, which differ in their pathological and biochemical characteristics, have been identified in deer and elk, including CWD1, CWD2, A116G, Wisc-1, and $H95^{+}$ [217,219,339]. In addition, CWD from Norwegian moose has a number of unique characteristics and is theorized to be a novel, spontaneous prion disease [154,319]. In addition to affecting the pathophysiology and epidemiology, strains may vary in their interspecies transmissibility, or host range. Therefore, characterizing the strains of CWD by examining host range is important in understanding the ramifications of CWD not only in the cervid populations, but also to predict the likelihood of interspecies transmission to other wildlife, livestock, and humans.

The existence of prion strains hindered the acceptance of the protein-only hypothesis [90,340] as it was difficult to explain how multiple distinct, stable disease phenotypes could arise from the misfolding of identical proteins. It was later theorized that PrP misfolds into specific PrP^{Sc} conformations during prion disease, and differences in these misfolded conformations could give rise to different strains [100], reconciling strains and the protein-only hypothesis. Structural studies, to date, lack the resolution to directly compare the PrP^{Sc} structures of different strains, however, indirect evidence supports these structural differences. Different PrP^{Sc} conformations may also vary in their immunoblot migration and glycosylation patterns, likely because differences in conformation can alter protease cleavage sites [100], and strains may selectively incorporate mono-, di-, or unglycosylated PrP [96,97]. As well, alterations in protease cleavage sites means different antibody epitopes are preserved and exposed, allowing some strains to be differentiated by the binding of certain antibodies [99,103,219]. Differences in β-sheet stability may also alter the stability of prion strains in detergents or guanidine [98,101] and change their resistance to protease digestion [99]. Biochemical differentiation of strains is usually secondary to the observation of distinct clinical and histological differences, including length of incubation periods, clinical signs, the

location and severity of vacuolation and PrP^{d} in the central nervous system, and host range [94,95,341]. How, exactly, differences in PrP^{Sc} conformation lead to such pathological variation is unclear.

Interspecies transmission has been central to the study of prion epizootics. A number of BSE isolates from the same outbreak had identical histopathology and host range [55], implying that this epizootic was caused by a single strain. This is in contrast to scrapie, which appears much more heterogeneous [209–211]. Furthermore, similarities in neuropathology between bovine spongiform encephalopathy (BSE), variant Creutzfeldt-Jakob's Disease (vCJD), and feline spongiform encephalopathy (FSE) allowed researchers to link these novel human and feline diseases to the consumption of prion-contaminated beef [55,342,343]. In contrast, experimental transmission of scrapie isolates to various laboratory rodents has given rise to a number of distinct strains, such as 263K in hamsters, and RML and ME7 in mice [173,174,340]. It should be noted that the cross-species stability of BSE is not typical of prion strains, as transmission to a new host can alter strain properties [91,94]. In this study, we analysed the interspecies transmission characteristics from a number of CWD isolates, predominantly Canadian CWD isolates, to Syrian Golden hamsters. By comparing the transmission of CWD into the hamsters, and the characteristics of the hamster passaged CWD, we will discuss the similarity of CWD to other prion epizootics, yielding a greater understanding of how CWD strains exist in free-ranging cervids.

3.3 Methods

This study was carried out in accordance with the guidelines of the Canadian Council on Animal Care and approved by the Animal Care and Use Committee at the University of Alberta.

3.3.1 CWD isolates

Eleven hunter-harvested CWD samples were obtained from the Saskatchewan CWD tissue bank via Dr. Trent Bollinger (University of Saskatchewan) (Table 3-1). These brain samples were obtained from deer harvested between 2006 and 2011, in 3 major CWD foci in Saskatchewan (Lloydminster, Swift Current, and Nipawin). Ten of the eleven samples were male. Five were from mule deer (MD) and six were from white-tailed deer (WTD). A pooled sample of clinically infected M132 homozygous elk (CWD2 strain) was received from Dr. Catherine Graham (CFIA Lethbridge). A CWD positive, hunter-harvested WTD expressing the A116 PrP variant (A116G) was provided by Dr. Samia Hannoui (University of Calgary) [222]. An additional 10 CWD-positive hunter-harvested samples were obtained, via Dr. Margo Pybus, the Alberta Environment and Parks (AEP) 2016 Surveillance program, with 8 of the 10 isolates from males and only one WTD isolate, the rest being MD. Alberta and Saskatchewan isolates were genotyped by Ms. Chiye Kim (Table 3-1).

3.3.2 Rodent transmissions

Seventeen of the CWD isolates were homogenized to 20% (w/vol) in HyClone Ultrapure water (FisherScience). As these samples were obtained from hunter-harvested animals, they were pasteurized by incubating at 70ºC for 20 minutes to remove any bacterial contamination. Each isolate was intracerebrally inoculated at either 1 or 2% (w/vol) into weanling transgenic mice expressing wildtype WTD deer PrP (tg33) and observed for the onset of clinical signs, including kyphosis, ataxia, and tail rigidity. Weanling Syrian Golden hamsters (*Mesocricetus auratus*), purchased from Envigo, were intracerebrally inoculated with 50 µl of 1% pasteurized cervid brain homogenates, and then monitored for onset of clinical signs. Animals were euthanized either when clinical disease was established, or at a predetermined time point (Table 3-2). Brains were removed and divided sagittally; one half

was used to generate a homogenate, the other half fixed in formalin for histochemistry. Brains were homogenized to 10% (w/vol) in HyClone Ultrapure water (FisherScience) using an Omniprep tissue homogenizer. Second passage was performed by intracerebrally inoculating 50 µL of 10% first passage hamster homogenates into weanling hamsters as above and euthanized upon establishment of clinical disease. The incubation periods and standard deviation were calculated using Microsoft Excel.

3.3.3 Digestion reactions and immunoblotting procedure

PrP^{res} was detected following proteinase K digestion as described in Appendices 2. In brief, brain homogenate (10 µL when screening brain homogenate and 100 µg to compare PrP^{res} migration) was digested for 45 minutes with 50 µg/µL (final concentration) proteinase K. PNGase f digestion was performed using NEB's deglycosylation kit (#P074S) following the manufacturer's recommended protocol and described in detail in Appendix 3. The immunoblotting procedure can be found in Appendix 4. Immunoblots were probed with 3F4 (a kind gift from Richard Rubenstein, SUNY-Downstate), SAF83 (Cayman Chemical, Michigan), or Bar224 (Cayman Chemical, Michigan) at a dilution of 1:10 000.

3.3.4 Histopathological analysis

Brain samples were formalin fixed, embedded in paraffin, and sectioned sagittally. Sections were processed for immunohistochemistry as described in Appendix 8. Sample embedding, sectioning, and staining were performed by Hristina Gapeshina in the CPPFD histology core. Slides were scanned using a NanoZoomer 2.0RS (Hamamatsu Photonics) and analyzed using NanoZoomer digital pathology software (Hamamatsu Photonics).

3.4 Results

3.4.1 Homologous transmission into cervidized mice

Transgenic mice expressing wildtype white-tailed deer PrP (tg33) were inoculated with 17 inocula (Table 3-1). Sixteen of the isolates resulted in clinical disease with incubation periods ranging from 285 to 417 dpi, while the seventeenth did not result in clinical disease in mice at 500 dpi. Clinical signs included ataxia, kyphosis, and rigid tail. Isolates with incubation periods in tg33 mice of 370 dpi or longer did not transmit into hamsters (95148, 99012, 74148, and 95083) (Table 3-3).

3.4.2 First hamster passage

In total, 181 hamsters were inoculated with 23 different CWD isolates (Table 3-1). Three isolates (A116G, 70023, and 73931) resulted in clinical disease in hamsters (552-764 dpi) (Table 3-2). Clinical signs included ataxia progressing to lethargy. An additional 7 isolates caused the subclinical accumulation of PrP^{res}. Interspecies transmissibility can be affected by the initial titre of the isolate. Four isolates (98148, 99012, 74148, and 95083) that did not transmit into hamsters also had a prolonged incubation period in tg33 mice, suggesting these isolates had a low infectious titre (Table 3-3). The 19 isolates with sufficient infectivity to transmit to hamsters (according to the tg33 bioassays) can be grouped into three categories. High transmissibility samples (A116G, 70023, and 75020) caused PrP^{res} accumulation in over 80% of hamsters. Low transmissibility samples (70023, 74754, and 74488) caused PrP^{res} accumulation to less than 15% of hamsters. The medium transmissibility samples (95047, 74299, 73931, Elk, 74030, and 74128) caused PrP^{res} accumulation in 50-67% of hamsters (Table 3-3).

3.4.3 PrP^{res} migration patterns in hamsters.

I also noticed that two distinct PrP^{res} migration patterns were present in the hamster samples, a Wisc-1-like pattern, 'A', with the unglycosylated band around 21 kDa and a second, slightly lower migration pattern, 'B', at 20 kDa (Figure 3-1). Some hamster-passaged isolates, such as the elk pool and 70023, displayed a single pattern, while other inoculum resulted in a mixture of migration patterns (Table 3-2). Some hamsters inoculated with Saskatchewan isolates displayed neurological signs, including head tilt, tremors, and ataxia, between 538 and 726 dpi (Table 3-5). However, when screened by immunoblot, some of these animals had migration patterns that did not appear to correspond to PrP^{res} (Supplemental Figure 3-4). I later determined that the neurological signs were not prion-related, and the atypical migration pattern was due to crossreativity of the secondary antibody (Supplemental Figure 3-5).

3.4.4 Histology

Half of each brain from clinically affected hamsters, as well as 3 animals per box at the end of the experiment, were analyzed for PrP^{d} deposition. The PrP^{d} in the positive samples was diffuse, primarily affecting the colliculus, hindbrain, hypothalamus, and thalamus, similar to what was reported in Chapter 2, Figure 2-2. PrP^{d} deposition was present in both clinical and subclinical samples. There was considerable variation in staining intensities between samples (Figure 3-2).

3.4.5 Serial passage of isolates with different PrP^{res} migration patterns

To further characterize the differences between PrP^{res} with the 'B' and 'A' migration patterns, I inoculated a second cohort of hamsters with 'A' migration-pattern (75020-A, hamster 8218B) and Elk (hElk; hamster 8234B), and 'B' migration-patterns (75020-B, hamster

8220C) and 70023 (70023-B, hamster 8231B). Clinical signs were similar to those observed in hamster-passaged Wisc-1 (Chapter 2), including ataxia, dystonia (specifically retrocollis), and hyperactivity, progressing to weight loss and lethargy. Clinical onset was subtle, and the clinical course lasted about 2 months after the onset of ataxia. Many of these clinical animals appeared scruffy and heavier two months prior to onset of ataxia. Hamsters infected with 75020-A had incubation periods of 382±10 dpi. The hElk-infected animals had incubation periods of 526±8 dpi, while the 75020-B and 70023-B hamsters had incubation periods of 464±3 dpi and 490±25 dpi, respectively (Table 3-4).

Immunoblot analysis showed that the 75020-A samples replicated the 21 kDa PrP^{res} migration pattern observed in the first passage (Figure 3-3, Table 3-4). However, the hElk, 70023-B, and 74020-B second passage samples had a double unglycosylated band instead of a single 20 kDa band. This double band was not found in the second passage of the experimentally passaged wt/wt Wisconsin CWD isolates (Figure 3-3), and appears to consist of both the Wisc-1 like 21 kDa 'A' band as well as the 20 kDa 'B' band from first passage Saskatchewan samples.

3.5 Discussion

The CWD isolates used in this study demonstrated considerable variability in their host range. The CWD transmission characteristics fell into three categories, which correlated with cervid species and geographical origin of the isolates (Table 3-3). The three highly transmissible isolates, transmitting to over 80% of the hamsters, were all from white-tailed deer, while the three low-transmitting isolates (transmitting to <15% of hamsters) originated from the same geographic area (Table 3-3). These transmission differences were not due to infectious titre, as the incubation periods of these isolates in cervidized mice was similar. While differences may be expected between CWD isolates originating from dissimilar cervid

PrP sequences [219,222,344] and between CWD pools originating in different species [247–249,251,255], I also observed transmission differences between cervids of the same species and with identical PrP sequences (Table 3-3). This suggests an unexpected level of diversity in CWD.

3.5.1 Geographical variance and its relation to scrapie

A correlation between host range and geographical location was also previously observed in scrapie isolates [209,210]. In these studies a variety of sheep and goat scrapie isolates were passaged into a panel of rodent models, demonstrating host range variability not only between animals of different PrP sequence or geographical origins, but even between animals of the same PrP sequence and flock [209]. As well, the emergence of different migration patterns in some isolates were also noted after interspecies transmission to novel hosts [210,211], similar to the two migration patterns I observed in hamsters (Figure 3-1). CWD and scrapie share a number of similarities. They transmit throughout diverse populations, which can differ in the type and prevalence of PrP polymorphisms, as well as breed or species [134–137,182]. These factors have the potential to foster and maintain heterogeneous prion populations, since different PrP polymorphism can lead to the diversification of PrP^{Sc} conformations and the emergence of novel strains [219,223,345], and there is emerging evidence that peripheral prion replication can foster PrP^{Sc} conformations with different properties [210,211]. Thus, CWD from different locations, in which cervid species composition and PrP allele prevalence vary, may also differ in prion strain features. Another factor that may contribute to geographical variation is the source of the original CWD agent in an area. While the American CWD epizootic originated primarily in deer [150,151], the first CWD cases in Saskatchewan and South Korea were likely spill over from infected elk to game farms [152,153,155], which may affect how CWD strains evolved in these locations.

3.5.2 Migration patterns

In addition to variations in hamster transmissibility, I also observed biochemical differences in the resulting hamster-passaged isolates, namely differences in electrophoretic migration due to differences in PK cleavage [100]. Two migration patterns were observed in the PrP^{res} positive hamsters (Figure 3-1), a higher molecular weight pattern at 21 kDa similar to hamster-passaged Wisc-1 isolate in Chapter 2 and second pattern with a lower molecular weight, similar to the 20 kDa pattern found in the wt/H95 second passage samples in Chapter 2. Pattern A was stable upon second passage with an incubation period similar to hamster-passaged Wisc-1, while second passage of 'B' resulted in a double unglycosylated band with an extended incubation period, suggesting a mixture of conformers. Surprisingly, the hamster-passaged elk isolate resulted 'A' pattern upon first passage but was similar to 'B' in second passage (double unglycosylated banding pattern and an extended incubation period) (Figure 3-3).

In Chapter 2 we hypothesized that the PrP^{Sc} conformer that resulted in the lower molecular weight pattern in hamsters emerged either in the wt/H95 deer or during the interspecies transmission to hamsters, however, since 'B' was present in many of our hamster-passaged wildtype cervid isolates, it seems unlikely that the conformation that resulted in 'B' emerged during the heterotypic transmission of CWD from a wt/wt deer to a wt/H95 deer. As well, although possible, it seems unlikely that 'B' emerged during the experimental transmission into hamsters, which would require the conformer to emerge multiple times independently in some, but not all, inocula groups. Another explanation is that this PrP^{Sc} conformer was present in the initial wildtype CWD isolates, even forming a minor part of Wisc-1. This was similar to a study of scrapie transmission to different ovidized mouse models, where different PrP^{res} isoforms in the transgenic mice were linked to heterogeneity in the original scrapie

isolates [211]. However, future work should focus on examining the original CWD isolates for strain differences in order to substantiate the presence of different PrP^{Sc} conformers.

3.5.3 Speculation on natural prion mixtures

The presence of conformer mixtures in the hunter-harvested isolates, similar to what has been proposed in natural scrapie [174,209–211,343], may explain the diversity in transmission of CWD to hamsters [244,255,332,338], as well as the findings by Angers et al. (2010), where CWD1 and CWD2 could not be clearly differentiated [217]. However, these studies do not explain how these prion conformers can coexist in a single clinical host, since coinfected prion strains are commonly believed to interfere with each other, likely due to competition for PrP^{C} or other molecular resources [149]. This results in extended incubation periods and lowered rates of propagation [145,147]. However, Eckland (2018) recently proposed that strain competition may only occur in high conversion efficiency strains, like HY, as coinfection of hamsters with two strains with low conversion efficiency, such as DY and 139A, does not result in elongated incubation periods, perhaps because there is less competition for cellular resources [333]. As well, evidence of strain mixtures has also been found in cases of sporadic human prion disease [206–208].

Like the VRQ alleles in scrapie, cervid PrP polymorphisms can alter the strain characteristics of CWD [191,219,339,344], so different populations with different allele prevalence may not only alter the spread of CWD [188] but also change the composition of CWD cycling through an area. Furthermore, CWD and scrapie are also the only known prion diseases where peripheral PrP deposition and shedding are important routes of transmission [56,169,170,224,278,279,346,347]. Perhaps peripheral prion replication aids in creating and maintaining the heterogeneity of these diseases, since differences in PrP expression can influence strain evolution and there is growing evidence that different scrapie strains can be propagated by the CNS and lymphoid tissue [109,211,348]. Constant cycling between

different populations and PrP^C concentrations, due to both heterozygosity and peripheral replication, may create stable mixtures of conformers or substrains, whose existence only become apparent through serial passaging and interspecies transmission (Figure 3-4).

3.5.4 Model shortcomings

While hamsters were useful in finding host range differences, there are several drawbacks in developing hamster models of prion strains. I previously demonstrated how the lesion profiles of two-year-old hamsters (both negative and positive for PrP^{Sc}) are indistinguishable (Chapter 2). Furthermore, ten hamsters (aged 538-726 dpi) were scored as clinically positive but did not accumulate PrP^{Sc}, developed neurological signs (Supplemental Table 3-5). The idiopathic vacuolation and spontaneous neurological signs are in accordance with Gershauser et al. (2013), who found an increase in idiopathic vacuolation in hamsters over the age of one year and the spontaneous occurrence of neurological signs in 10% of hamsters [334]. When screened by immunoblot, I observed cross reactivity with the secondary antibody in some of the aged hamsters (Supplemental Figure 3-5). Parameters that are typically modified to decrease nonspecific signal in prion blots (PK concentration, digestion time, and brain homogenate volume), increased the signal strength of these nonspecific bands (Supplemental Figure 3-6). Therefore, caution should be taken when attempting to resolve such signals.

3.5.5 Conclusion

By comparing the host range of a number of CWD isolates, I demonstrated the variability present in free-ranging CWD isolates. While some of this variability was associated with cervid species, host range differences were also present in CWD isolates originating from wildtype cervids of the sample species (Table 3-3). The results of this study were similar to previous experiments performed on scrapie isolates, suggesting how strain variability may be fostered in these diseases. Cycling of prions through disparate cervid or sheep populations with different PrP allele prevalence may generate and later maintain

location-dependent conformer mixtures. The importance of peripheral spread and the shedding of infectivity, important for both scrapie and CWD transmissibility, may also contribute to conformer diversity in these diseases. These results complicate our ability to understand the potential impacts of this disease on livestock and human health. Although a number of studies have demonstrated low risk of transmission to humans [234,349,350] and low levels of transmissibility to most livestock [239,245–247,249], it is unlikely these experiments tested the full spectrum of CWD strains, especially as the geographical range of CWD expands and new cervid populations are threatened by this implacable disease.

3.6 Tables and Figures

Table 3-1. Description of the CWD positive hunter-harvested isolates used to infect hamsters.

Isolate	Species	Sex	WMU	Year	Province	Genotype	Obtained from	Tg33 incubation period (dpi)
57836	MD	M	728	2016	AB	wt	AEP	ND
70023	WTD	M	49	2010	SK	wt	Bollinger	311±27
70045	WTD	M	24	2011	SK	wt	Bollinger	297±26
73931	WTD	M	50	2009	SK	wt	Bollinger	324±28
74128	MD	M	13	2008	SK	wt	Bollinger	360±30
74148	MD	F	47	2008	SK	wt	Bollinger	417±34
74200	WTD	M	24	2008	SK	wt	Bollinger	ND*
74299	MD	M	13	2008	SK	wt	Bollinger	302±20
74303	MD	M	13	2008	SK	wt	Bollinger	347±17
74448	MD	M	13	2008	SK	wt	Bollinger	344±30
74686	WTD	M	236	2016	AB	wt	AEP	ND
74754	MD	M	13	2009	SK	wt	Bollinger	342±19
75020	WTD	M	50	2009	SK	wt	Bollinger	338±23
95024	MD	M	728	2016	AB	wt	AEP	ND
95046	MD	F	728	2016	AB	wt	AEP	ND
95047	MD	M	728	2016	AB	wt	AEP	285±23
95075	MD	M	728	2016	AB	wt	AEP	ND
95083	MD	F	728	2016	AB	20G/wt	AEP	>500
95098	MD	M	728	2016	AB	wt	AEP	ND
98148	MD	M	234	2016	AB	wt	AEP	370±49
99012	MD	M	162	2016	AB	wt	AEP	371±33
A116G	WTD	-	-	-	SK	A116/wt	[222]	300±23
Elk	Elk	-	-	-	-	wt	Graham	327±34

*ND=Not done. WMU: wildlife management unit. Year: year of harvest. Tg33 IP: incubation period in cervidized mice expressing wt deer PrP.

Table 3-2. Primary passage of CWD isolates to hamsters with a description of the PrP^{res} migration patterns present in the first passage hamster samples.

Inocula	Experimental endpoint (dpi)	N	Number of Clinical Animals	Incubation Period (dpi)	PrP^{res}+*	Migration pattern**
57836	575	6	0	-	0	-
70023	726	8	3	552, 709, 712	8	B
70045	727	7	0	-	1	A
73931	778	9	1	764	6	B
74128	771	8	0	-	4	both
74148	726	9	0	-	0	-
74200	726	7	0	-	0	-
74299	728	8	0	-	4	B
74303	727	9	0	-	5	B
74448	726	9	0	-	0	-
74686	575	8	0	-	0	-
74754	726	6	0	-	0	-
75020	726	9	0	-	9	both
95024	575	8	0	-	0	-
95046	575	8	0	-	0	-
95047	575	6	0	-	3	A
95075	575	6	0	-	0	-
95083	575	8	0	-	0	-
95098	575	8	0	-	0	-
98148	575	6	0	-	0	-
99012	575	8	0	-	0	-
A116G	683	12	1	638	10	both
Elk	726	8	2	674, 719	4	A

*PrP^{res} positive by immunoblot, **A migration at 21 kDa, B migrates at 20 kDa

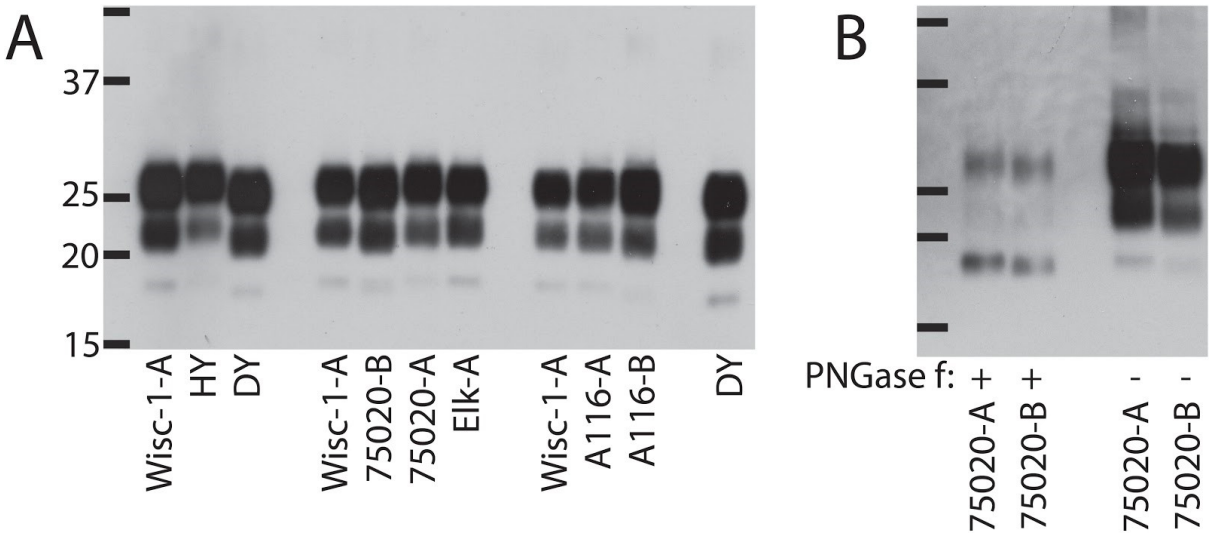

Figure 3-1. Two different PrP^{res} migration patterns, A and B, identified in the first hamster passage of CWD isolates. **A**. Samples were digested in 50µg/mL proteinase K. **B**. Proteinase K digested samples compared to PNGase digested samples. The first lane contains the protein ladder demonstrating molecular weight in kilodaltons (kDa). The origin of the isolate inoculated into the hamsters is shown below the immunoblot, along with the migration pattern associated with the hamster sample (i.e., samples labelled Wisc-1-A were inoculated with Wisc-1 and has migration pattern A). HY and DY are characterized hamster prion strains. Primary antibody: 3F4 1:10000.

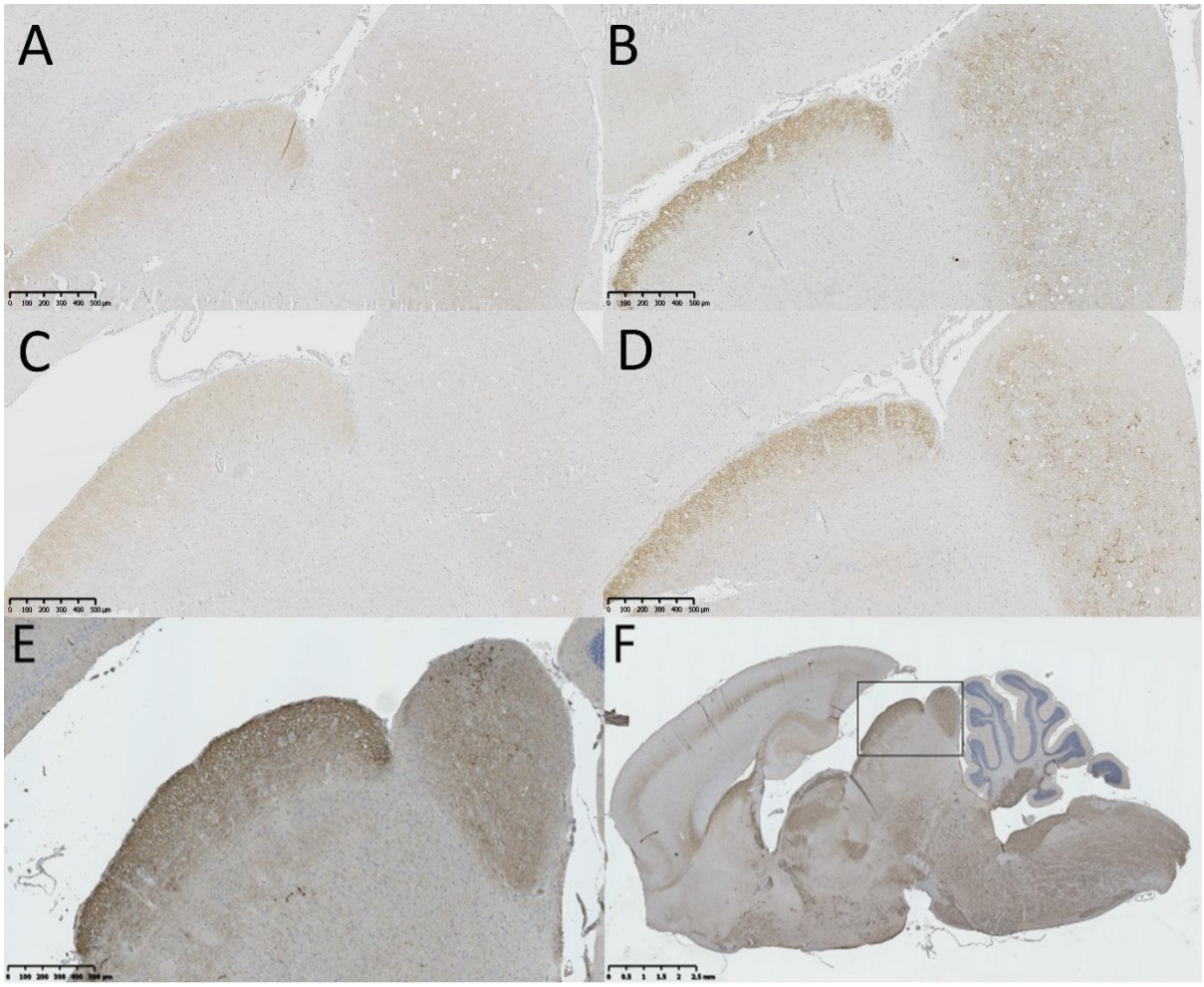

Figure 3-2. Variable PrP^d signal intensity in the inferior and superior colliculus of first passage hamsters. (A: inoculated with isolate 75020; B: inoculated with elk isolate; C and D: inoculated with isolate 70023) compared to fourth passage hCWD (E). F: PrP deposition the entire brain section of hCWD-infected hamsters, E is a close up of panel F. The indicated area is the inferior and superior colliculus. Primary antibody: 3F4.

Table 3-3. Comparison of the primary transmission characteristics of CWD isolates to hamsters and cervidized mice, demonstrating correlations between transmission and species or geographic origin.

Inocula	Species	Location	Cull	N	PrP^{res}+	% Transmit	MW	Tg33 incubation
95047	MD	Lloydminster	575	6	3	50%	A	285±23
70045	WTD	Swift Current	727	7	1	14%	A	297±26
A116G	WTD	--	683	12	10	83%	both	300±23
Wisc-1*	WTD	--	659	8	8	100%	A	300±19
74299	MD	Swift Current	728	8	4	50%	B	302±20
70023	WTD	Nipawin	726	8	8	100%	B	311±27
73931	WTD	Nipawin	778	9	6	67%	B	324±28
Elk	Elk	--	726	8	4	50%	B	327±34
75020	WTD	Nipawin	726	9	9	100%	both	338±23
74754	MD	Swift Current	726	6	0	0%	-	342±19
74488	MD	Swift Current	726	9	0	0%	-	344±30
74303	MD	Swift Current	727	9	5	56%	B	347±17
74128	MD	Swift Current	771	8	4	50%	both	360±30
98148	MD	Lloydminster	575	6	0	0%		370±49
99012	MD	Oyen	575	8	0	0%		371±33
74148	MD	Lloydminster	726	9	0	0%		417±34
95083	MD	Lloydminster	575	8	0	0%		>500

*Wisc-1 (wt/wt) first passage hamster transmission results from Chapter 2. Samples where lack of transmission was likely due to low titre are shaded in grey. Low transmitting samples are shaded in yellow. Samples with transmission close to 100%, similar to Wisc-1 (Chapter 2), are shaded in green.

Table 3-4. Second hamster passage of samples with different PrP^{res} migration patterns

Initial cervid isolate	First passage migration pattern	N	Incubation period	Second passage migration pattern
75020	A	4	382±10	A
	B	7	464±3	double band
Elk	A	3	526±8	double band
70023	B	4	490±25	double band
Wt/wt *	A	4	373±5	A

*Wt/wt second passage from Chapter 2 for comparison.

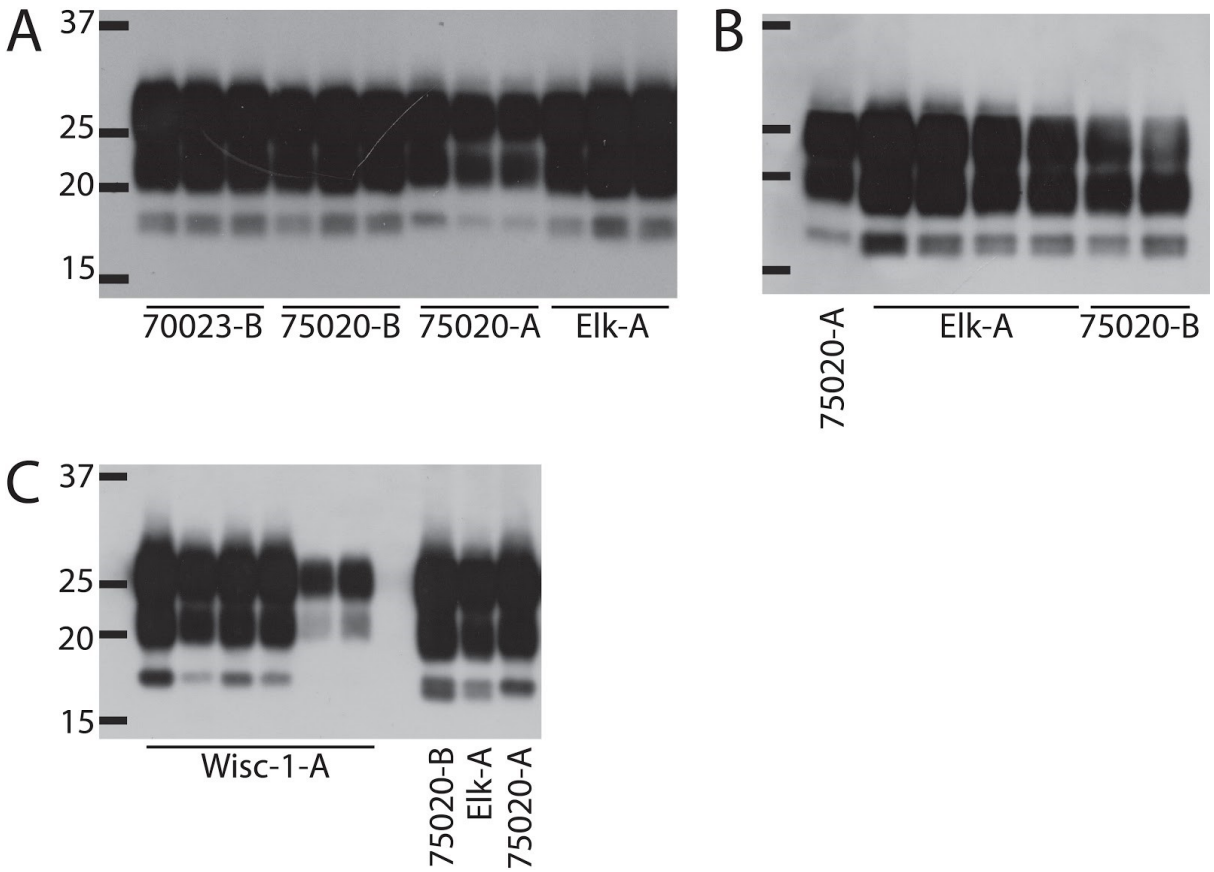

Figure 3-3. Two PrP^{res} migration patterns were evident in the brains of hamsters following the second passage. **A**. Screening of second hamster passage samples. **B**. Comparison of the PrP^{res} double-banded migration pattern, indicated by the red arrows. **C**. Comparison of PrP^{res} from second passage Wisc-1 samples and hunter-harvested isolates. Samples were digested in 50 µg/mL proteinase K for 45 minutes. The first lane contains the protein ladder demonstrating molecular weight in kilodaltons (kDa). The origin of the isolate inoculated into the hamsters is shown below the immunoblot, along with the migration pattern associated with the first passage hamster sample (i.e. samples labelled Wisc-1-A were inoculated with Wisc-1 and has migration pattern A upon first passage). Primary antibody: 3F4.

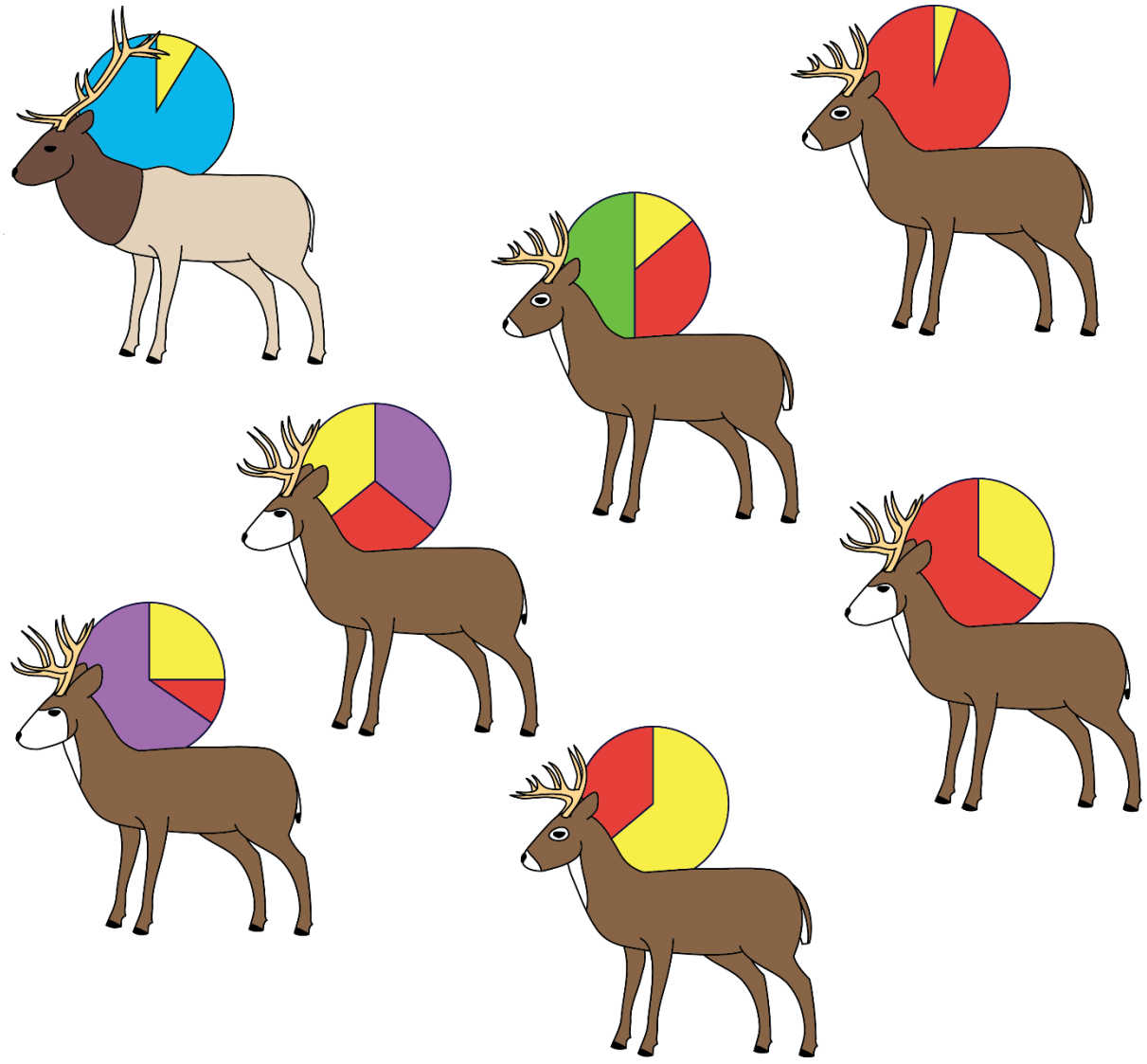

Figure 3-4. Diagram demonstrating the putative diversity of CWD. CWD positive cervids may carry multiple different CWD conformers, which is represented by the circle near each cervid that depicts all the prion in each animal. The different colours in the circle represent the different conformers, and their prominence infectious load is depicted by the proportion of the total circle.

4 Differential binding of prions to vegetation

Manuscript in preparation

Triscott E, Aiken JM, McKenzie D

4.1 Abstract

The geographic range of chronic wasting disease (CWD), a contagious prion disease of cervids, continues to expand throughout North America and northern Europe. Infectivity is shed in bodily fluids, contaminating the environment, and contributing to transmission. This may lead to the formation of reservoirs of infectivity and the contamination of agricultural products. To determine the contribution of CWD-contaminated plants to disease transmission, I developed an assay for the detection of prion agents on vegetation, specifically focusing on plants consumed by cervids and/or those common in the Canadian CWD enzootic regions. The interaction of prions with plant surfaces is governed by both species of plant and the length of time CWD interacts with the plant surface.

4.2 Introduction

Chronic wasting disease (CWD) is an infectious prion disease affecting cervids. Its geographic range continues to expand throughout North America, affecting 26 American states and three Canadian provinces, and it is also present in northern Europe and South Korea. Like all prion diseases, CWD is universally fatal and has a long asymptomatic incubation period prior to the onset of clinical signs. CWD can be transmitted through direct contact between animals, and increased deer density and interrelatedness appear to facilitate the spread of CWD [261,264,268,270,275]. However, since infectivity is shed in the urine, saliva, and faeces of infected cervids [169,170,224,279], CWD transmission also occurs indirectly through the environment [168,192,283].

Previous methods developed to detect infectivity in the environment have focused on prion-contaminated soils [287,351], however, soil characteristics, including mineralogy and organic content, depend on location, climate, and terrain. Many of these attributes alter the interaction between prions and soils and may even degrade or enhance infectivity [190,290,296–299], which complicates determining the extent of overall environmental contamination.

Infectivity, shed in the biofluids of infected animals, will first encounter other materials, such as vegetation, before interacting with soils. These materials are likely to accumulate substantial levels of contamination, especially in areas of high cervid density and CWD prevalence. This has been demonstrated in studies of scrapie-contaminated pastures, where the removal of pen furniture, like water troughs and feed buckets, considerably reduces indirect transmission to naïve sheep, indicating that these surfaces, and not soils, were responsible for the majority of indirect prion transmission [286]. Stakeholders have voiced concern over the possibility of CWD contaminated agricultural products [352–355], indicating a need to assess the risk of these materials. To this end, I developed a method of detecting PrP bound to vegetation to better monitor environmental prion contamination, especially on vegetal surfaces, and to provide insights into the horizontal transmission of CWD.

Previous studies have examined PrP associated with vegetation, or prions in faecal samples that contain a high concentration of plant matter. Pritzkow et al. (2015) studied the interaction between plants and prions via PMCA amplification of contaminated plant tissue [302]. Prion amplification of faecal samples uses RT-QuIC instead of PMCA [222,345,356]. However, the *in vitro* detection of prions by these amplification methods were inconsistent and most required a concentration step prior to amplification, using either NaPTA precipitation, which is specific for PrP^{Sc} [357], or iron-oxide beads [194,304,345,356]. As well, plants may contain a wide variety of compounds, such as flavonoids and phenolic compounds, which could interfere with prion concentration or amplification, since oxidized phenolic compounds cross-link proteins [358–360]. Developing a better method to detect PrP^{Sc} in vegetation will allow monitoring of environmental CWD, providing a better way of determining the levels of environmental contamination cervids will consume, as well as monitoring the level of contamination in hay and feed used for livestock. In this study, I examined several physical

and chemical methods to extract PrP from contaminated plants, developing a method of detecting PrP on vegetation that can be further optimized for environmental monitoring. The interaction between PrP and vegetation is then explored using this method.

4.3 Methods

4.3.1 Brain homogenate sources

For the comparison of common vegetation, I used Wisc-1 infected brain homogenate from transgenic mice expressing wild-type white tailed deer PrP [219]. PMCA was performed using elk CWD from transgenic mice expressing elk PrP. For all other CWD experiments, clarified brain homogenate from an experimentally infected wt/wt white tailed deer [158] was used. Different concentrations of brain homogenate were used to compensate for variation between tg33 and cervid PrP expression levels. For the HY experiments, we used 10% (wt/vol) HY brain homogenate derived from a pool of clinically positive hamsters.

4.3.2 Vegetation sources

Wheatgrass, (hard red wheat; *Triticum aestivum*), and yarrow (*Achillea millefolium var. occidentalis*) seeds were purchased from West Coast Seeds (SKU#SS112 and FL3825, respectively). Seeds were germinated on a moist paper towel and then planted in potting soil and grown under long day conditions (16 hours of light a day) using a benchtop system (SunBlaster T5HO Growlight Garden). Caladium leaves (*Caladium bicolor*) were sampled from a house plant grown indoors without a growth light. Environmental vegetation samples were obtained from the University of Alberta and a property 35 km east of Edmonton (Alberta, Canada) with the agreement of the landowner in July-August 2017. We focused on sampling plants that comprise deer diet or likely contribute to leaf litter. These samples included leaves from trembling aspen (*Populus tremuloides*), balsam poplar (*Populus balsamifera*), black currant (*Ribes hudsonianum*), red clover (*Trifolium pratense*), wild grass (genus *Poacae*), yarrow (*Achillea millefolium*), burr oak (*Querus macrocarpa*), smooth blue

aster (*Symphyotrichum laeve*), common plantain (*Plantago major*), wild rose (*Rosa acicularus*), red osier dogwood (*Cornus sericea*), American elm (*Ulmus americana*), common lilac (*Syringa vulgaris*), and highbush cranberry (*Viburnum edule*). Plants were used fresh unless otherwise indicated. The lichen (*Cladonia rangiferina*) was obtained by Dr. Alsu Kuznetsova from a location 40 km north of Fort McMurray (Alberta, Canada) and was kept at -20ºC prior to use.

4.3.3 Immunoblot Procedure

Immunoblotting was performed as in Appendix 4. Immunoblots were incubated in BAR224 (Cayman (SPI bio) #10009035) for the CWD immunoblots, 3F4 (a kind gift from Richard Rubenstein, SUNY-Downstate) for HY, or Sha31 (Cayman #11866) for the PMCA immunoblot. Antibodies were diluted 1:10 000. For the PMCA blot, goat anti-mouse IgG-AP conjugate (Promega #S3721) was used as a secondary antibody, the immunoblot developed using the AttoPhos AP Fluorescent Substrate System (Promega #S1000) and visualized using the ImageQuant LAS4000. Analysis of signal strength was performed using ImageJ software. Greyscale images of the immunoblots were inverted and signal intensity was measured using density histograms, from which the average signal intensity of the background was subtracted. Sample signal strength was normalized by dividing by the positive control and graphed using Prism software.

4.3.4 Coomassie staining

Coomassie staining was used to assess the amount of protein loaded on the immunoblot. The immunoblot membrane was incubated in Coomassie brilliant blue R250 (0.1% (wt/vol) Coomasie Blue R250 in 10% acetic acid, 50% methanol, 40% distilled water (w/v/v)) for 5 minutes. The membrane was then incubated in 20 mL of destain solution (50% water, 40%

methanol, and 10% acetic acid (v/v/v)) to remove excess Coomassie. The membrane was then air-dried.

4.3.5 Detecting PrP in a vegetation homogenate

To determine if vegetation interferes with the detection of PrP, a 3 cm^2 piece of balsam poplar leaf was frozen at -80ºC and then pulverized using a Pellet Pestle (Fisher #12-141-363) and dry ice. The powder was then resuspended in 1.8 mL distilled water. Brain homogenate (10 or 5 µL) was added to 200 µL of the balsam poplar homogenate. These spiked samples were centrifuged at 500 rpm for 15 minutes and the supernatant was methanol precipitated by adding 4 volume equivalents of ice-cold methanol and incubating samples at -80ºC for one hour. Samples were then centrifuged at 14000 rpm for 30 minutes and the supernatant was discarded. The pellet was then dried in a SpeedVac for 1 hour. In other samples, 200 µL of 10% sodium dodecyl sulfate (Invitrogen #15525017 in mqH_2O) was added prior to centrifugation. In the third experimental group, samples were NaPTA precipitated by incubating 300 µL of the supernatant, 500 µL 4% (wt/vol) sodium lauroylsarcosine, and 100 µL distilled water with shaking for 10 minutes at 37ºC. Then 2 µL 25U/µL Benzonase (Sigma-Aldrich #E1014-25KU) and 0.5 µL 2M $MgCl_2$ were added and the samples were incubated an additional 30 minutes with shaking at 37ºC. Samples were then incubated at 37ºC overnight with the addition of NaPTA (Sigma Aldrich #496626) (warmed to 37ºC), to a final concentration of 0.3%. The samples were then centrifuged at 13200 rpm for half an hour and the supernatant was discarded. The pellet was then resuspended in 20 µL of 0.1% sodium lauroyl sarcosine.

4.3.6 Improvement of PrP detection using plant buffer and surfactants

A 1 cm^2 caladium plant sample was frozen overnight at -80ºC, then ground using a mini-pestle on dry ice. Uninfected brain homogenate (10% (wt/vol)) from a transgenic mouse

expressing cervid PrP (tg33) was added, and 500 µL of Plant Buffer (100mM HEPES pH 7.4, 5 mM EDTA, 10 mM DTT, 10% glycerol, 0.3% DIECA, 0.75g/10 mL PVPP; ±1% Triton X-100) was added and the sample vortexed. Samples were shaken at room temperature for 5 minutes followed by centrifugation for 15 minutes at 12000 rpm at 4ºC. The supernatant was collected, centrifuged for an additional 5 minutes, and then 200 µL of the supernatant was methanol precipitated. An equivalent amount of uninfected brain homogenate was loaded as the negative control. To test the ability to detect bound PrP, brain homogenate was added to the plant samples and they were incubated overnight. The plant samples were then rinsed in water and the unbound fraction was methanol precipitated. The rinsed plant sample was ground and processed as described for the spiked samples.

4.3.7 Enzymatic digestion

Protease digestion was performed as follows. After treatment with the Plant Buffer with 1% Triton X-100 (Sigma Aldrich #X100) and methanol, samples were resuspended in 20 µL of RIPA (50mM Tris Base, 150mM NaCl, 1mM EDTA, 1% CA-360, 0.25% Na-deoxycholate) containing proteinase K to a final PK concentration of 16 µg/mL-120 µg/mL. Samples were digested for either 15 or 30 minutes at 37ºC, with shaking. 20 µL of 2.5X Laemmli sample buffer (0.75 M Tris-Cl pH6.8, 0.5% Bromophenol blue, 25% (v/v) glycerol, 5% (w/v) SDS, 12.5% (v/v) β-mercaptoethanol) was added and the samples processed by immunoblot. For the non-digested samples, samples were resuspended in 40 µL of 2.5X sample buffer and boiled.

For the cellulase digestion, a 1 cm^2 piece of leaf was ground on top of dry ice using minipestles and spiked with 10 µL of infected brain homogenate. This was resuspended in 100 µL of cellulase (Sigma Aldrich #SAE0020) (concentration between 10^{-1} and 10^{-5}) and incubated at 55ºC for 30 minutes, following established protocols [361]. This short incubation time was selected to limit the degradation of PrP^C. Plant Buffer with 1% Triton X-

100 (400 µL) was added and the samples were incubated on ice for 30 minutes prior to methanol precipitation.

4.3.8 Improved grinding of plant samples

Elm and lilac leaves were cut into 1 cm^2 squares. For the spiked samples, a vegetation homogenate was made by drying the leaf pieces for 1 hour using the SpeedVac followed by freezing at -80ºC prior to pulverization, using either a pellet pestle or the BioMasherII Closed System Disposable Tissue Homogenizer (Kimble #749625-0020) over dye ice, followed by resuspension in 500 µL Plant Buffer and spiked with brain homogenate. These homogenates were incubated for 30 minutes on ice and methanol precipitated. For the bound and unbound samples, 10 µL 5% (wt/vol) brain homogenate added to the plant samples and incubated overnight at 4ºC. These were rinsed in 200 µL water, which was precipitated as the unbound fraction. The bound samples were processed as in the spiked samples.

4.3.9 Boiling in surfactants compared to complete protein precipitation

Plant samples were incubated overnight with 10 µL of brain homogenate. Samples were rinsed, and five different bound-PrP detection methods were performed (A, B, C, D, and E). In A, samples were dried, frozen, pulverized, and resuspended in the Plant Buffer, which was then methanol precipitated, as detailed in previous sections. In B, samples were boiled in a 2.5X Laemmli sample buffer for 10 minutes. In C, D, and E, the samples were boiled in 5% SDS, 10% SDS, or 1% Triton X-100 for 10 minutes respectively prior to methanol precipitation.

4.3.10 Vegetation binding assay

Vegetation was incubated with brain homogenate overnight at 4ºC, then incubated with 200 µL water for 15 minutes at room temperature with shaking. The wash, containing unbound PrP, was TCA/acetone precipitated by adding 100% TCA to a final concentration of 13%,

incubated at 4°C overnight, then pelleted by centrifugation at 15 minutes at 14000 rpm. The pellet was then incubated in cold acetone for 15 minutes at 4°C and centrifuged at 14000 rpm for 10 minutes. This acetone wash was repeated twice. The pellet was resuspended in 20 µL of 2.5X Laemmli buffer (0.75 M Tris-HCl pH6.8, 0.5% Bromophenol blue, 25% v/v glycerol, 5% w/v SDS, 12.5% v/v β-mercaptoethanol) and boiled for 10 minutes. To analyze the bound material, the rinsed plant samples were boiled in 200 µL 1% Triton X-100 for 10 minutes and the extracted proteins TCA/acetone precipitated as above (Figure 4-7).

To detect the unbound PrP^{res}, plant samples, in duplicate, were rinsed as described above, the combined and the proteins were methanol precipitated. Pellets were resuspended in 25 µL of RIPA buffer (50 mM Tris Base, 150 mM NaCl, 1 mM EDTA, 1% CA-360, 0.25% Na-deoxycholate). For the PrP^{res} samples, 15 µL of the resuspended sample was digested with 100 µg/ml proteinase K (Roche #0.115887001) in a total volume of 35 µL for 2 hours at 37°C with shaking. Then 5X Laemmli buffer (35 µL) was added and the samples were boiled for 10 minutes (Figure 4-2). For the non-digested undigested PrP samples, 5 µL of the resuspended precipitate was added to 7 µL of water and 13 µL of 5X Laemmli buffer and boiled for 10 minutes. Experiments were repeated independently at least twice, including three technical replicates where possible.

4.3.11 Amplification of PrP signal using PMCA

To test whether the bound PrP signal could be amplified using PMCA, 0.3 g of wheatgrass was incubated with 10 µL 1% (wt/vol) elk brain homogenate overnight. Samples were rinsed as usual in 200 µL water, and then the plant sample was boiled in 200 µL 1% Triton X-100 for 10 minutes. Then 10 µL of the unbound or bound fractions were used to seed elk PMCA substrate; 10% (wt/vol) perfused TgElk brain in PMCA conversion buffer (1X PBS, 150 mM NaCl, 4 mM EDTA, 1% Triton X-100, one tablet of cOmplete™ Mini, EDTA-free Protease

Inhibitor (Roche #0469315001). PMCA sonication was performed at 60 Hz for 30 seconds every 15 minutes for 24 hours, a total of 114 sonication cycles. Samples were then PK digested using 20 µL of PMCA product and analyzed by immunoblot to detect PrP^{res}.

4.3.12 PrP Binding Experiments

To compare the plant-prion interaction of wheatgrass and yarrow, 5% (wt/vol) CWD-infected brain homogenate (3 µL, 5 µL, 7 µL, 9 µL, or 11 µL) was applied to 0.03 g of plant material and processed as in Figure 4-7. Replicates of the bound fraction samples were not combined. For the HY experiments, 5 µL of 10% (wt/vol) HY was applied to 0.03 g of wheatgrass in triplicate. Samples were either processed as in Figure 4-7, where the bound sample replicates were combined, or as in Figure 4-8.

To test the binding of prions to common vegetation, 10 µL of 1.25% (wt/vol) CWD-infected brain homogenate was applied to 1 cm^2 squares of gathered vegetation in triplicate and processed (Figure 4-7). Replicates of the bound fraction samples were combined. The effect of time on the prion-plant interaction was tested by incubating 15 µL of a 2.5% CWD-infected brain homogenate with 0.03 g of wheatgrass overnight, for 1 week, or for 4 weeks. Samples were then processed as in Figure 4-7.

4.3.13 Animal Transmission of Bound and Unbound Fractions

Animal bioassays were conducted to confirm the presence of infectivity in the unbound and bound fractions. Wheatgrass (2.7 g) was harvested and incubated with 450 µL of 10% (wt/vol) HY brain homogenate and rotated overnight at room temperature, then rinsed with 4 mL of water. The amount of vegetation and the volume of brain homogenate was determined by scaling up the amount of material used in the *in vitro* assay experiments. The rinse water was mixed with an equal volume of applesauce. The wheatgrass was then pulverized using a tissue beater as much as possible in 4 mL water then 4 mL of apple sauce was added.

Weanling Syrian Golden hamsters were orally dosed with 200 µL applesauce mixed with HY for five consecutive days. Hamsters were observed for onset of clinical prion disease and, once clinical signs were established, euthanized. The length of the incubation period and standard deviation of each experimental group was calculated using Microsoft Excel. This study was conducted in accordance with the Canadian Council on Animal Care Guidelines and Policies with approval from the Health Sciences Animal Care and Use Committee of the University of Alberta, Animal Use Protocol 914.

4.3.14 Lichen comparison to other samples

I incubated 0.0265 g of vegetation and 20 µL 2.5% CWD positive brain homogenate together overnight. Samples were vortexed 5 times for 10 seconds each in 200 µL water and MeOH precipitated. To test the Triton X-100 boiling method, I performed it on yarrow, grass, and lichen (0.0275 g) that had incubated with 10 µL brain homogenate.

4.4 Results

4.4.1 Plant material interferes with the detection of PrP and NaPTA precipitation

The addition of ground vegetation was associated with reduced PrP signal in the immunoblot, such that PrP signal was not present in the 5 µL spiked samples (Figure 4-1). In the samples spiked with 10 µL of brain homogenate the addition of 10% SDS slightly increased the PrP signal. The vegetation also appeared to interfere with the NaPTA precipitation, as no signal was detected (Figure 4-1).

4.4.2 The addition of a plant-specific buffer and non-ionic surfactant increases PrP signal

Plant extracts are highly complex and contain phenolic compounds, such as flavonoids, which form irreversible covalent linkages with proteins when oxidized, interfering with protein extraction [360]. For this reason, I tried to improve PrP detection by diluting plant samples in Plant Buffer, containing DTT, DIECA and PVPP, instead of water. These

compounds prevent flavonoids from interfering with protein extraction since they prevent the oxidation of phenols and absorb phenolic compounds [360,362]. Additionally, I also tried to improve PrP extraction by adding a surfactant, since PrP is a membrane protein that is prone to aggregation. To test if PrP detection was improved by using a buffer specifically designed for plant protein purification (Plant Buffer), different volumes of normal brain homogenate were spiked into leaf homogenates and processed using a heavily modified version of a plant protein purification protocol. While PrP detection occurred down to 5 µL spiked brain homogenate, plant material still interfered with detection of PrP (Figure 4-2A). Signal was improved by the addition of a non-ionic surfactant (Triton X-100), selected due to its use in the PMCA conversion buffer. After the addition of a surfactant, PrP^{C} was detected down to 1 µL brain homogenate (Figure 4-2B). PrP was also detected in vegetation homogenates spiked with infectious PrP, as well as bound material applied to vegetation samples before homogenizing, however, signal was not strong and equally loading samples into the immunoblot was difficult due to the high viscosity of the samples (Figure 4-2C).

4.4.3 Enzymatic digestion

The inconsistent signal and low signal intensity may be due to the presence of other plant proteins. For this reason, I added a proteinase K digestion step to degrade non-PrP^{res} proteins (Figure 4-3A, B). This increased signal intensity at the highest PK concentrations, which was most evident at the 15-minute incubation, but not as obvious at the 30-minute PK digestion (Figure 4-3A). A number of enzymes have been used to improve protein extraction, including cellulase [361], which aids in the breakdown of the plant cell wall. However, the addition of cellulase was not effective (Figure 4-3C, D).

4.4.4 Plant grinding and protein purification

Improved grinding of plant material may improve detection of bound PrP, as the fineness of plant pulverization is of great importance in plant protein extraction [359]. To this end, I compared the impact of using a better grinding apparatus, the BioMasher II. Grinding was performed on dry ice on samples that had been dehydrated in the SpeedVac for 2 hours on high heat and then froze at -80ºC overnight. While better grinding of the sample was achieved, bound PrP signal was lower in the BioMasher II ground sample than the pellet pestle samples (Figure 4-4).

4.4.5 Boiling bound samples in surfactants

Since mineral-bound PrP extraction protocols were successful by boiling SDS [297], I compared our grinding protocol to boiling contaminated plant samples in Laemmli sample buffer, 5% and 10% SDS, and boiling in 1% Triton X-100. PrP signal was observed only in the Triton X-100 treatment in yarrow (Figure 4-5).

4.4.6 PMCA amplification of surfactant-extracted PrP

PMCA is a method of amplifying PrP^{Sc} signal, increasing detection [363]. PrP^{res} was present in the bound fraction that had been subjected to PMCA. PrP signal was present in two of the three replicates (Figure 4-6).

4.4.7 PrP binding to vegetation.

Yarrow and wheatgrass have very dissimilar morphologies. The wheatgrass leaf is entire and has a relatively smooth surface decorated with small trichomes, while the yarrow has feathery leaves with a high degree of pubescence. To determine if CWD interacts differently with yarrow and wheatgrass, different volumes of brain homogenate were applied to the plant samples and processed using the binding assay described in Materials and Methods followed

by immunoblot. PrP was present in both the bound and unbound fractions of both plants (Figure 4-9A and 4-9B). More PrP was present in the unbound fractions from the grass compared with the yarrow, a pattern that was reversed with the bound samples. Binding of HY to wheatgrass was similar to the binding of CWD, with more PrP in unbound fraction compared to the bound fraction when compared by immunoblot. Both fractions contained PrP^{res} (Figure 4-3C). To confirm that infectivity was present in both the bound and unbound fractions, we performed a bioassay of bound and unbound material in hamsters. There was complete transmission of the 10% HY unbound sample into hamsters with an incubation period of 180 dpi, compared with 165 dpi for the positive control. Seven of the eight hamsters inoculated with the bound fraction became clinical with an incubation period of 174 dpi (Table 4-1).

4.4.8 Interaction of prions with common vegetation

To explore how other plant species interact with CWD, we examined a variety of plant species (burr oak, wild rose, yarrow, grass, and red clover) that contribute to deer diet or are common in CWD enzootic regions. Plant samples were processed as outlined in Figure 4-7 and the PrP was quantified by immunoblot. The amount of PrP that rinsed off each plant species varied. In some plants, such as the oak (*Q. macrocarpa*), there was considerable signal in the unbound fraction, suggesting PrP did not bind to the plant sample. For other plant samples, such as the wild rose (*R. acicularus*), there were low amounts of PrP in the unbound fraction, indicating most of the PrP remained bound to the plant samples (Figure 4-10A). PrP was detected in the bound fraction of all plants; however, the PrP signal in the bound fraction was not necessarily the inverse of the signal observed in the unbound fraction (Figure 4-10)

4.4.9 Long incubation alters plant-prion interaction

To test the effect of time on the plant-prion interaction, we incubated CWD-infected brain homogenate with wheatgrass overnight, for one week, and for four weeks. The amount of unbound PrP decreased by half at four weeks, while the amount of bound PrP appeared to increase over the same time period (Figure 4-11).

4.4.10 Differential binding of PrP to vegetation

Lichen would be ideal to use in environmental monitoring in northern Canada, given its ubiquity, ease of sampling, and longevity in the environment, as well as its importance in the winter diet of caribou [363]. As well, lichens are occasionally used in monitoring pollution levels [364,365]. We compared the ability of *Cladonia rangiferina*, which has fruticose morphology, to that of wheat and yarrow and found that much less PrP rinses off compared to the other plants. Unfortunately, this material is not detectable using our Triton X-100 boiling method (Figure 4-12).

4.5 Discussion

The ability to detect environmental CWD will improve our ability to monitor the levels of CWD contamination in the environment and improve CWD modelling. The initial goal of this project was to assess the importance of plants in CWD transmission and the danger posed to livestock by CWD-contaminated vegetation. While I did not succeed in these goals, I was able to develop a method of detecting PrP bound to plants and to determine some factors that affect the plant-prion interaction. My assay is straightforward, uses common reagents, and can easily be scaled up. Most earlier experiments detecting prions on vegetation or in faeces first homogenized the samples, followed by total protein extraction [194,304,345,356]. This is consistent with plant protein extraction methods; however, our results suggest that homogenizing the material masks a considerable amount of PrP, and components of the plant homogenate appear to interfere with NaPTA precipitation (Figure 4-1). PrP detection can be

improved through the addition of a non-ionic surfactant (Figure 4-2), but the amount of proteins and cellular components present in the sample make the plant sample difficult to load consistently (Figure 4-2A, Figure 4-4A). To reduce the amount of interfering cellular material, many plant protein extraction protocols finely grind the plant material and subject the homogenate to several rounds of centrifugation [359]. This is problematic with regards to PrP^{Sc}, since prion amyloid has a high molecular weight and may be pelleted during centrifugation, reducing PrP signal. I avoided lengthy centrifugation steps and used clarified brain homogenate in these experiments for this reason.

4.5.1 Optimization of the grinding assay

To improve PrP detection and immunoblot loading consistency, I treated the homogenized plant samples with either cellulase or proteinase K (Figure 4-3). Treatment with a low concentration of proteinase K improved PrP detection, the protease digestion reduces the PrP signal. Since plant grinding is a key step in improving the quality of plant protein purification methods [359], I tried a more efficient grinding system. Surprisingly, improved grinding reduced PrP signal (Figure 4-4), perhaps due a higher surface area of plant material for PrP^{Sc} to bind. PrP can be extracted from soil minerals boiling the mineral-bound prions in Laemmli sample buffer, which contains, among other components, a surfactant. When the plant grinding method with compared to the surfactant boiling method, boiling in the non-ionic surfactant Triton X-100 yielded the best PrP signal, without the loading issues that had been problematic in samples that had been prepared using the grinding method or boiled in SDS (Figure 4-5). I developed this boiling procedure into a method that consistently detects PrP on a wide variety of plants (Figure 4-7) using immunoblot.

4.5.2 Surfactant extraction protocol

In this extraction protocol, contaminated samples are boiled for ten minutes in Triton X-100, the supernatant was removed, and proteins precipitated. Samples are resuspended in the Laemmli sample buffer and detected by immunoblot. This surfactant-extraction procedure was also used prior to protease digestion with a concomitant reduction in signal (Figure 4-8, 4-9C). Low levels of PrP can be detected by combining samples prior to protein precipitation or by amplifying the PrP signal using PMCA (Figure 4-6). This method does not require specialized reagents and the extraction process can be performed in a few hours. Also, as grinding and homogenization of the plant sample are not required, the probability of sample contamination and prion aerosolization are reduced.

4.5.3 Prion-plant interactions

Binding of PrP to plant materials depends on a number of factors. Plant species play a role in PrP binding, as can be seen in the differential binding of PrP to wheatgrass and yarrow grown under controlled conditions (Figure 4-9B, C). Plants gathered from the environment also exhibit this diversity, where samples such as grass and oak had more PrP in the unbound fraction compared to yarrow and rose samples (Figure 4-10). The source of this diversity may lie in the heterogeneity of leaf surfaces, which can differ in composition and morphology, and in the presence and arrangement of epidermal leaf hairs, or trichomes, which would increase the surface area available for prion binding. Furthermore, the microarchitecture and composition of the cuticle, the waxy layer coating the non-woody parts of plants, is highly variable [307–311]. The outer surface of cuticles can have a variety of surface structures which can give some plants self-cleaning properties, reducing surface contamination [315]. These factors may explain why the recoverability of the bound fractions varied between plant species (Figure 4-10), as the interactions between PrP and the plant cuticle may differ in sensitivity to disruption by surfactants. The amount of PrP bound to vegetation also increases

with longer incubation times (Figure 4-11), similar to the interaction of prions with surgical equipment [306].

It is important to note that detection of PrP is based on relative signal strength and as the detection of bound PrP is inefficient, weare likely underestimating the amount of PrP bound to the plant surface. In addition, there is variability between samples, even using controlled lab-grown plant samples (Figure 4-11). The plant epidermis is highly variable and responsive to a number of external factors. Leaf surface properties vary by cultivar and developmental stage [307–310], as well as in response to stress [311] and pathogen colonization [317]. For this reason, caution should be taken in attempting to generalize these results.

4.5.4 Conclusion

Prion infectivity deposited on vegetation will either adhere to the plant surface or be washed off into the top layers of soil. The amount of infectivity remaining bound depends on plant species and the length of the interaction. Infectivity that washes off plant surfaces may interact with plant material in the litterfall layer of soil or percolate into deeper layers of soil, interacting with a vast number of minerals, saprotrophs, and fermentation products. Further research is required to understand where infectivity will accumulate in the environment, and the impact different plant varieties and environmental conditions will have on the indirect transmission of CWD. Further optimization of this method is required for environmental monitoring, since although it works well with plants, prions bound to lichen were not detected by immunoblot (Figure 4-12). Other surfactants may be more useful for detecting prions in these samples, and further work is necessary to determine the best time of year and plants to use for this purpose.

4.6 Tables and Figures

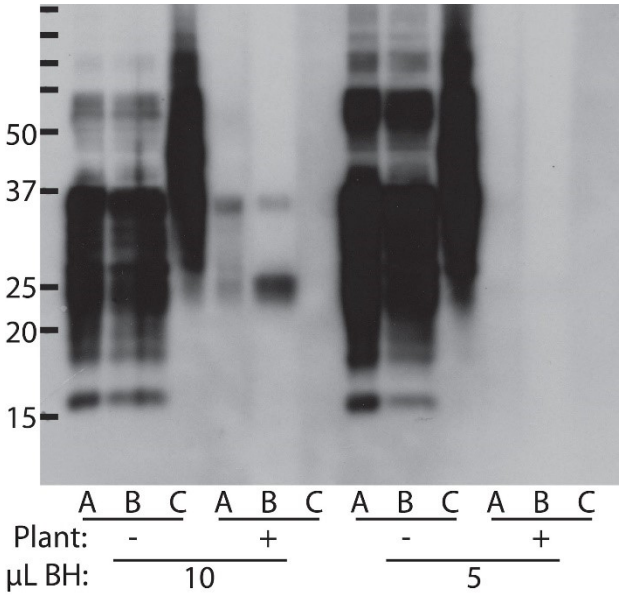

Figure 4-1. Vegetation interferes with PrP detection. A. Leaf samples were frozen and ground in water, and then the vegetation homogenate spiked with either 10 µL or 5 µL of brain homogenate. A: Samples were centrifuged and the supernatant was methanol precipitated. B: 10X SDS was added to the supernatant prior to methanol precipitation. C: Supernatant was precipitated with NaPTA. The first lane contains the protein ladder demonstrating molecular weight in kilodaltons (kDa). Primary antibody: Bar224.

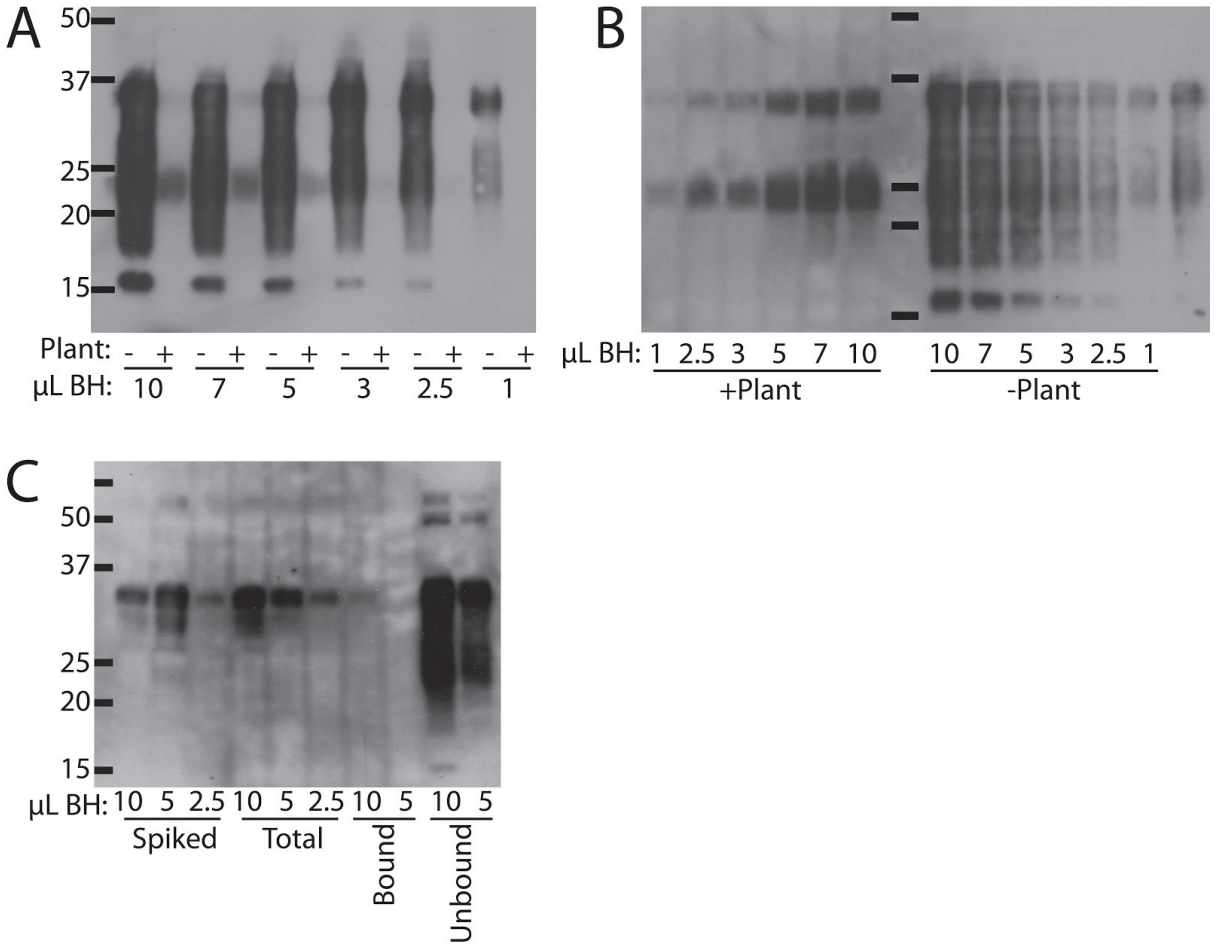

Figure 4-2. The addition of detergent to the Plant Buffer increases PrP signal. Leaf samples were frozen and ground, and then spiked with brain homogenate. **A**. Samples were incubated for 5 minutes in Plant Buffer, and then centrifuged. The supernatant was then methanol precipitated. **B.** Samples were incubated on ice for 25 minutes in Plant Buffer with 1% Triton X-100, and then centrifuged, methanol precipitating the supernatant. **C.** Samples were prepared as in B. Brain homogenate was either added after the addition of Plant Buffer (spiked), prior to grinding (total), or was incubated on the fresh leaf sample overnight and rinsed off prior to grinding, leaving the water sample containing the rinsed off brain homogenate (unbound) or the brain homogenate that remained bound (bound). The lane with the black bars contains the protein ladder demonstrating molecular weight in kilodaltons (kDa). Primary antibody: Bar224.

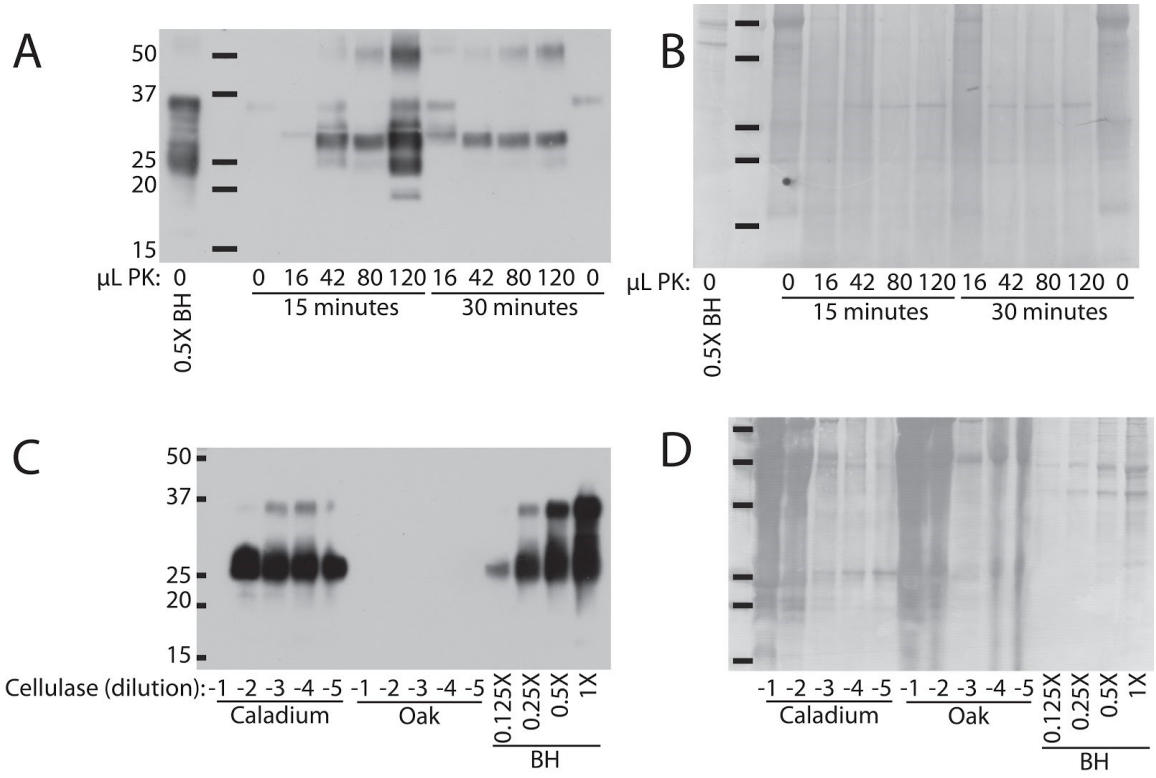

Figure 4-3. The addition of an enzymatic digestion step alters PrP signal detection. **A**. Leaf pieces were frozen and ground. Brain homogenate was applied and the samples were incubated in Plant Buffer with 1% Triton X-100 overnight. Samples were centrifuged and the supernatant was methanol precipitated. The precipitated proteins were PK-digested using 16-120 µg/mL PK for 15 or 30 minutes. The lane with the black bars contains the protein ladder demonstrating molecular weight in kilodaltons (kDa). Primary antibody: Bar224. **B**. Coomassie stained membrane of A. **C.** Ground leaf sample was incubated in cellulase (concentration between 10^{-1} and 10^{-5}) prior to incubation in Plant Buffer. **D.** Coomassie stained membrane of C.

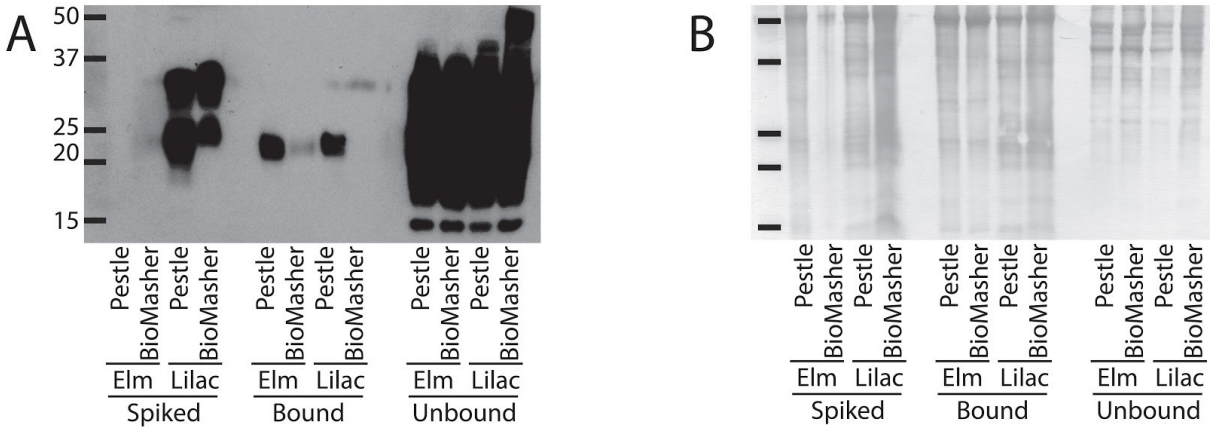

Figure 4-4. Improved grinding of the plant sample decreases PrP signal. **A.** Elm and lilac leaves were frozen and ground using either a normal pestle or the BioMasherII. In 'spiked' samples the brain homogenate was added prior to the incubation in Plant Buffer. Samples were centrifuged and the supernatant was methanol precipitated. In the 'unbound' and 'bound' samples the leaves were incubated with brain homogenate and then rinsed in water ('unbound') prior to grinding of the sample. The vegetation sample was then dried and ground as in the 'spiked' samples. The first lane contains the protein ladder demonstrating molecular weight in kilodaltons (kDa). Primary antibody: Bar224. **B**. Coomassie stained membrane of A.

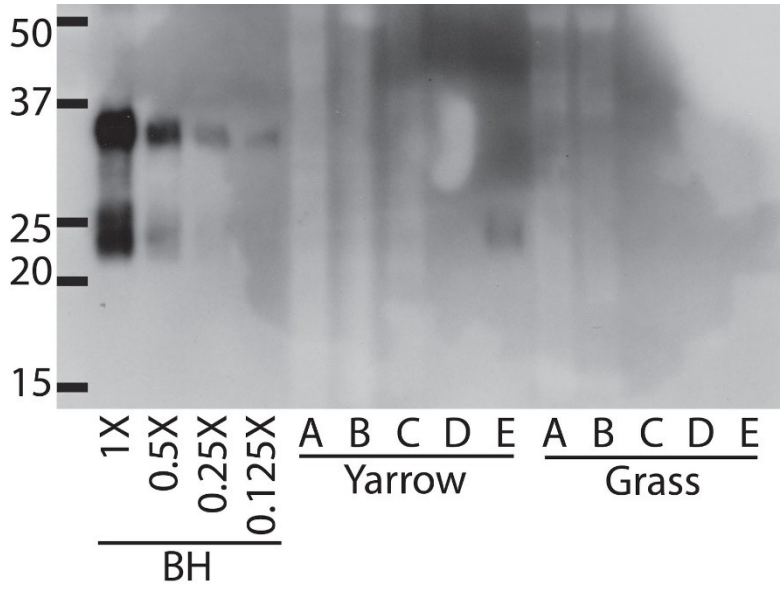

Figure 4-5. Bound PrP can be extracted by boiling samples in Triton X-100. Plant samples were incubated with brain homogenate and then rinsed in water. A: Plant samples were dried and ground as usual, then incubated in Plant Buffer and centrifuged. Supernatant was then TCA precipitated. B: Plant samples were boiled in Laemmli buffer. C: Plant sample was boiled in 5% SDS. D: Plant sample was boiled in 10% SDS. E: Plant samples were boiled in 1% Triton X-100 and TCA precipitate. The first lane contains the protein ladder demonstrating molecular weight in kilodaltons (kDa). Primary antibody: Bar224.

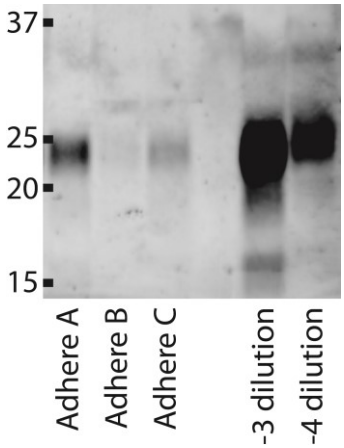

Figure 4-6. PMCA reaction of the bound fraction. 10 µL of the bound fraction was used to seed a single round of PMCA. The reaction was subjected to 30 seconds of 60 Hz sonication every 15 minutes for 24 hours. The first lane contains the protein ladder demonstrating molecular weight in kilodaltons (kDa). Primary antibody: Sha31.

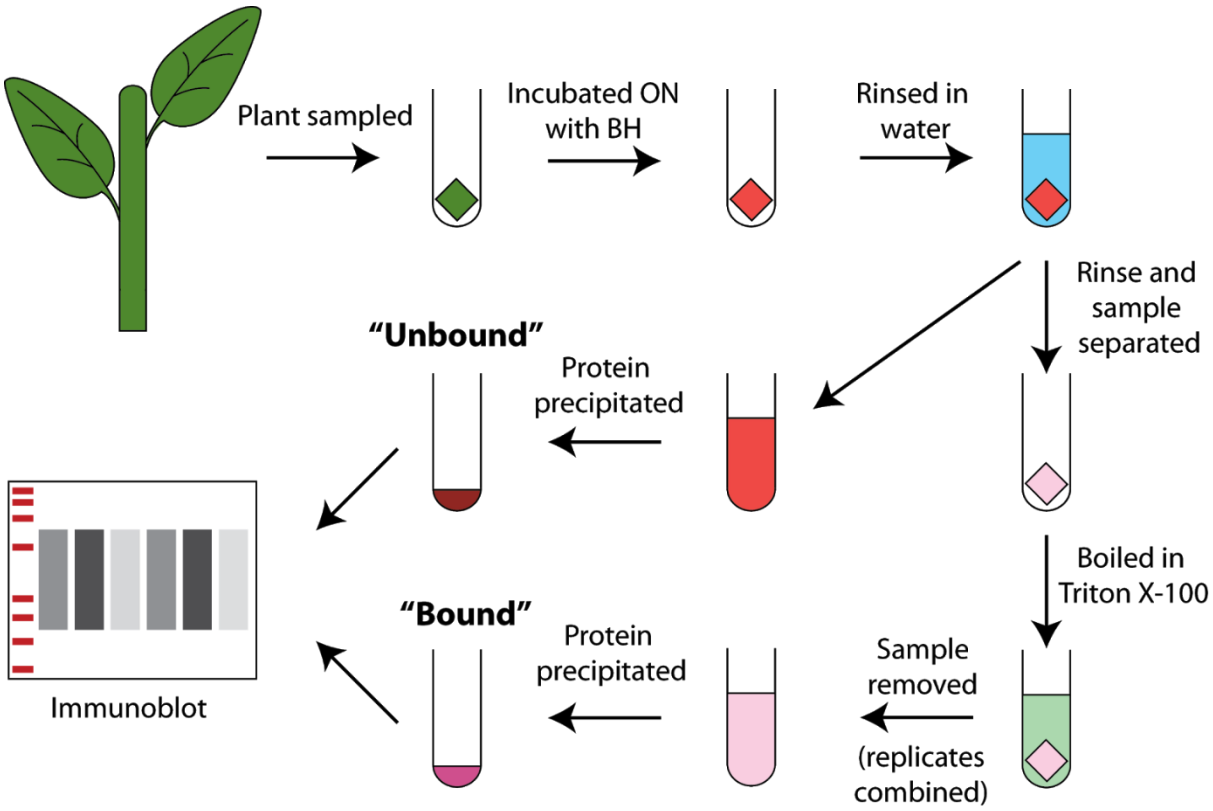

Figure 4-7. Schema of total PrP binding assay.

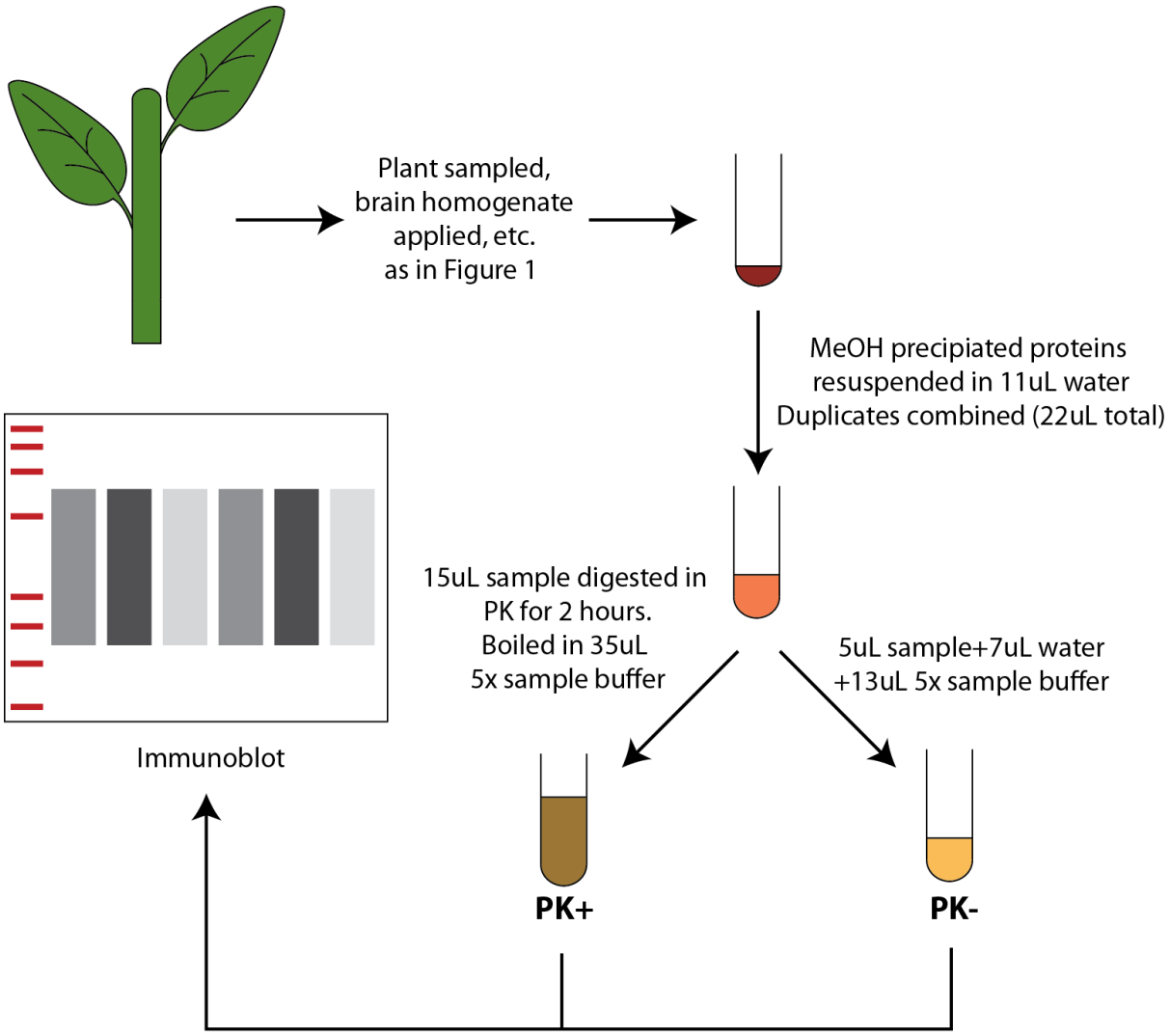

Figure 4-8. Schema of PrP^{Sc} binding assay.

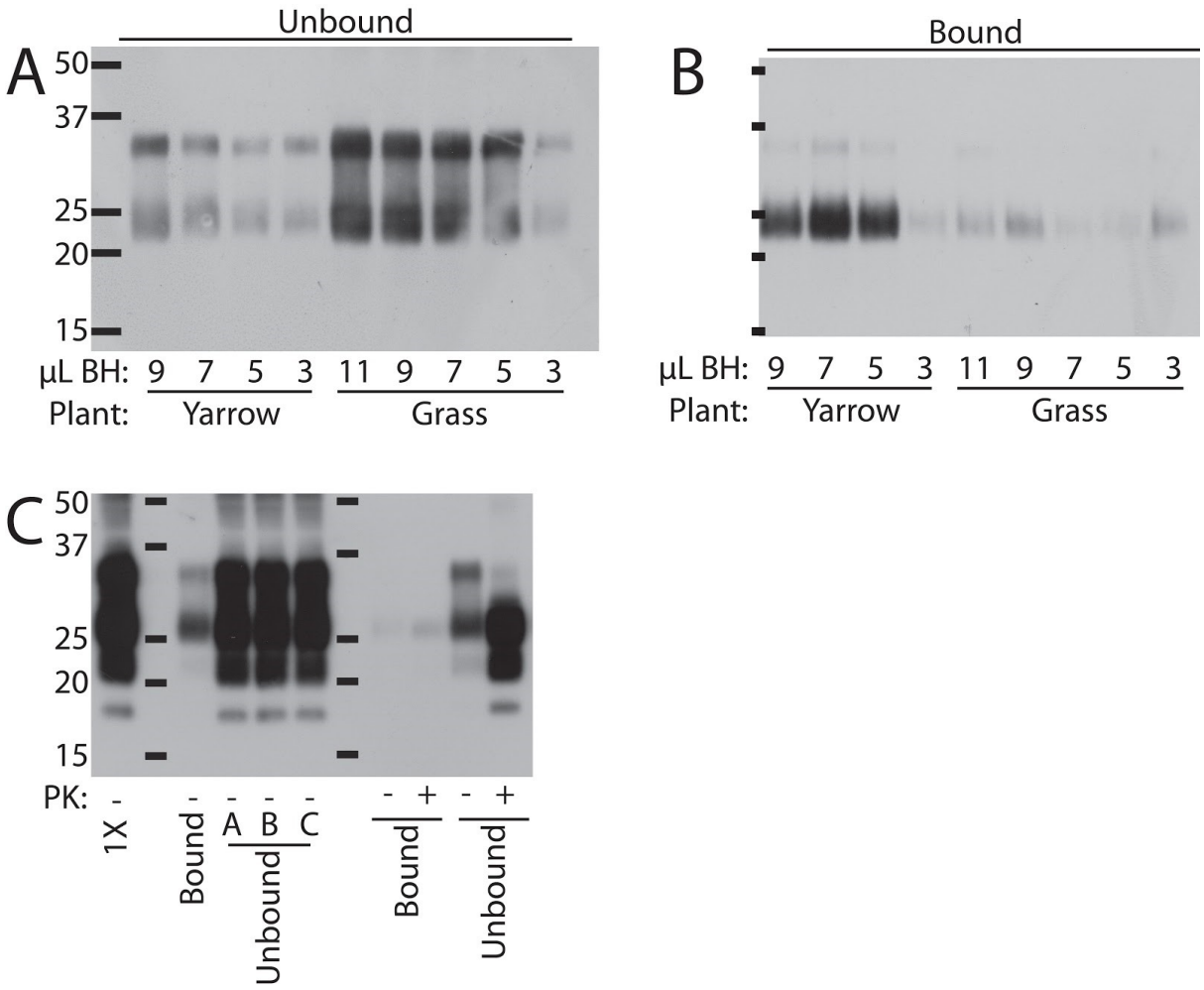

Figure 4-9. Differential binding of prions to vegetation. **A.** Different volumes of brain homogenate were incubated with yarrow or grass overnight. Proteins were precipitated from the unbound fraction and analyzed by immunoblot. **B**. Bound proteins were extracted from the rinsed plant samples by boiling in Triton X-100. **C**. PrP^{res} material was present in both the bound and unbound fraction. HY brain homogenate was applied to fresh grass and incubated at 4°C overnight. Grass was rinsed in water and the proteins were extracted from the unbound fraction and either resuspended in Laemmli sample buffer (PK-) or digested in proteinase K (PK +). The lane with the black bars contains the protein ladder demonstrating molecular weight in kilodaltons (kDa). Primary antibody: Bar224 (A and B), or 3F4 (C).

Table 4-1. Hamsters were orally inoculated with unbound and bound fractions of wheatgrass incubated with HY.

Material	n	Clinical	Incubation period (days)	% clinical
Unbound	8	8	180 ±16	100
Bound	8	7	174 ±8	87.5
HY alone	4	4	165 ±0.50	100

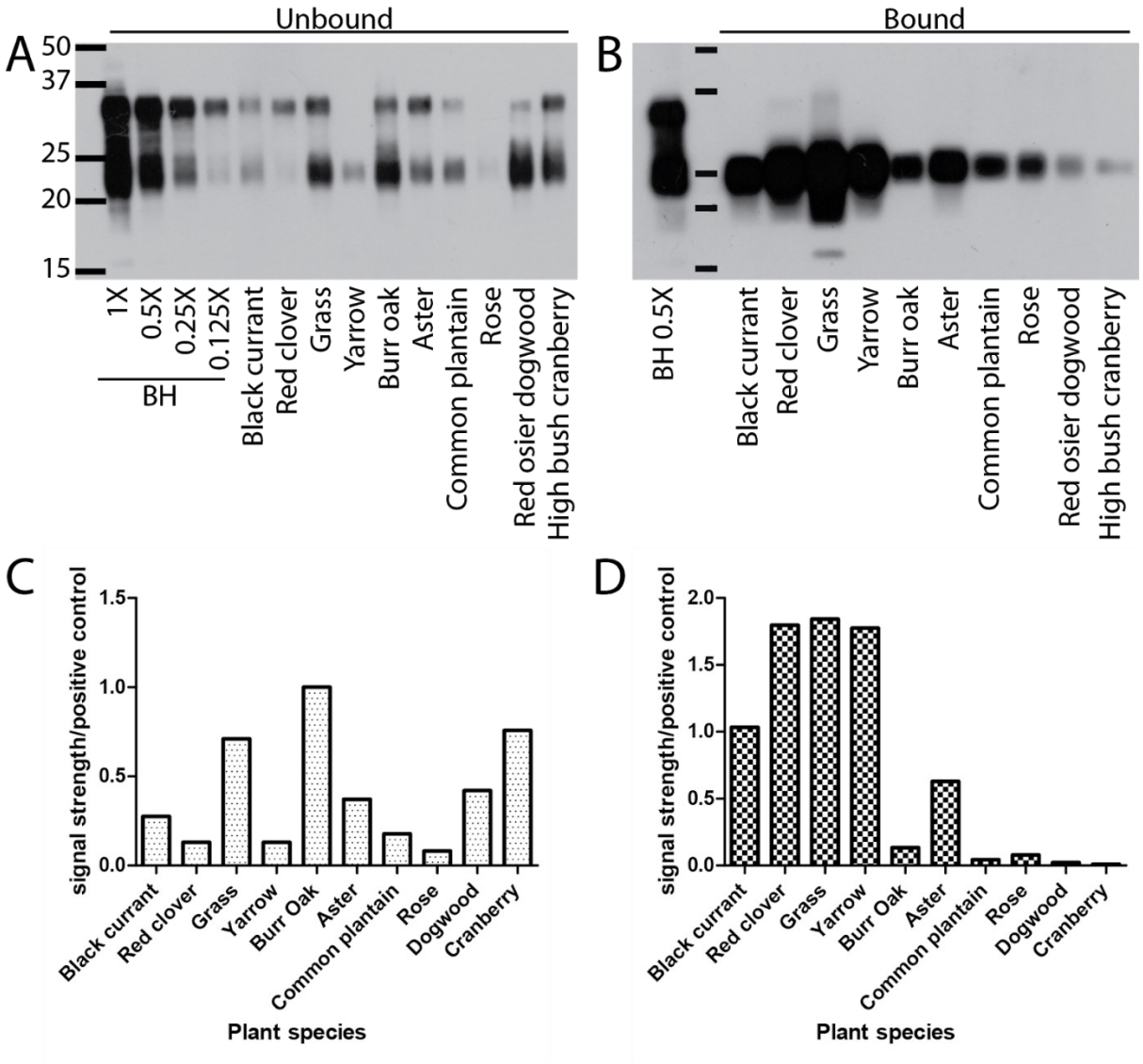

Figure 4-10. Prion binding depends on plant species. **A.** Brain homogenate was applied to the plant samples and incubated overnight at 4°C. The vegetation was subsequently rinsed with water. Proteins were TCA precipitated from the unbound fraction and analyzed by immunoblot. The first four lanes are a dilution series of the total brain homogenate. **B.** Bound proteins were extracted from the rinsed vegetation by boiling in Triton X-100. Replicates were combined and proteins were extracted from the rinse and analyzed by immunoblot. The lane with the black bars contains the protein ladder demonstrating molecular weight in kilodaltons (kDa). Primary antibody: Bar224. **C and D**. Semi-quantitative signal strength analysis of blots A and B. (

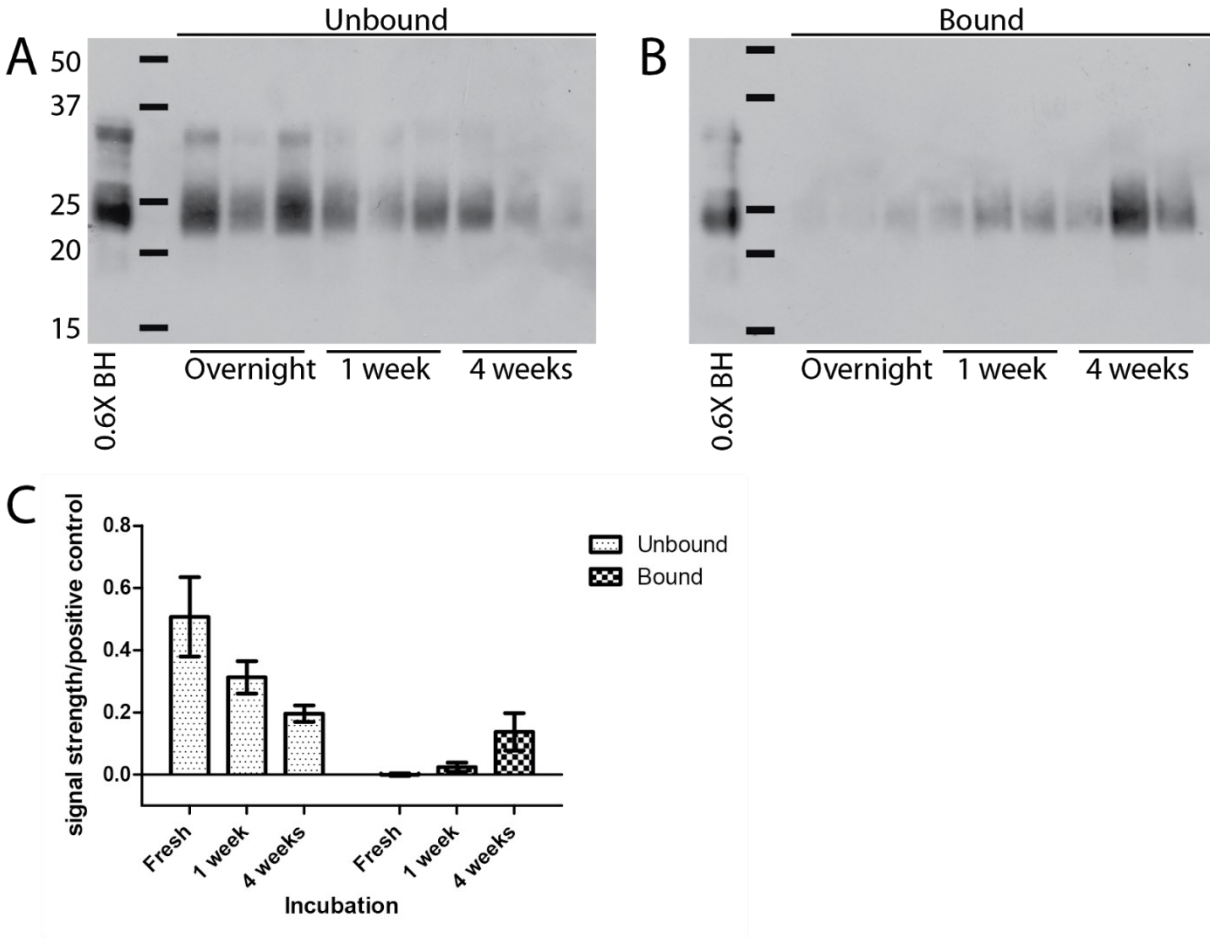

Figure 4-11. Longer incubation results in more PrP bound to plant material. Brain homogenate was incubated with fresh grass overnight or for either one week or four weeks. **A.** Proteins were precipitated from the unbound fraction and analyzed by immunoblot. Primary antibody: Bar224. **B.** Bound proteins were extracted by boiling in Triton X-100. The lane with the black bars contains the protein ladder demonstrating molecular weight in kilodaltons (kDa). Primary antibody: Bar224. **C.** Semi-quantitative signal strength analysis of blot A and B.

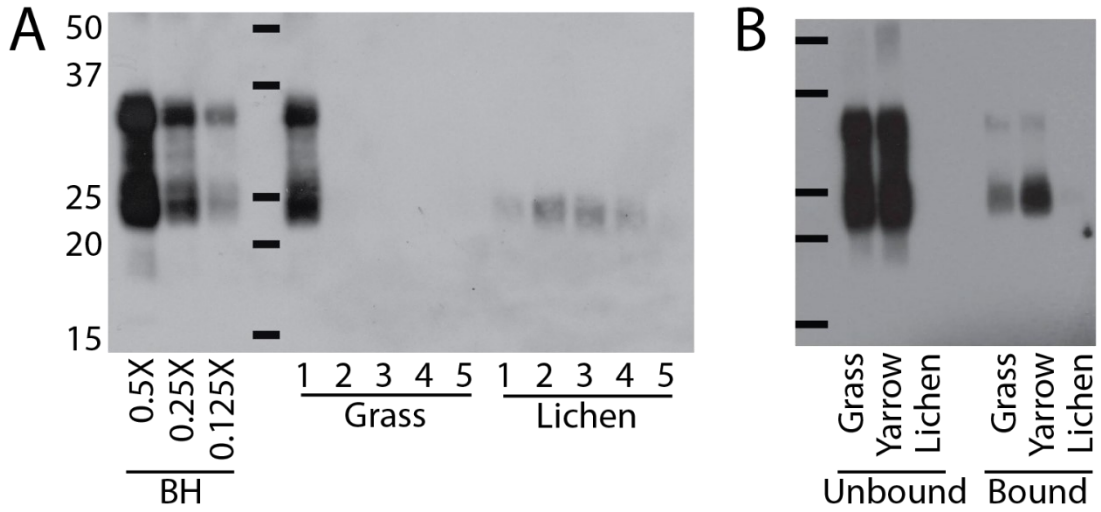

Figure 4-12. PrP binds to lichen and cannot be detected using my method. **A**. Brain homogenate was incubated with lichen or grass overnight. Samples were vortexed 5 times for 10 seconds each in water and each rinse was methanol precipitated. Primary antibody: Bar224. **B**. Vegetation samples were incubated with brain homogenate overnight. Samples were rinsed in water ('unbound'), then boiled in 1% Triton ('bound'). Samples were then precipitated. The lane with the black bars contains the protein ladder demonstrating molecular weight in kilodaltons (kDa). Primary antibody: Bar224.

5 Importance of CWD strains and environmental contamination for surveillance and prion ecology

5.1 The importance of understanding CWD transmission

In this thesis, I investigated the complexity of CWD transmission by examining strain diversity and prion adherence to plants. The variability I found in both CWD host range and plant adherence is concerning and demonstrates the difficulty in monitoring and controlling this disease. This is further exacerbated by variability in adherence of prions to plants (Chapter 4). Environmental contamination increases the likelihood of interspecies transmission of CWD since direct contact does not need to occur between animals, raising concerns for the expansion of CWD range, as contaminated feed and bedding can be transported to areas where CWD is not endemic. This concern has led to Norway regulating hay and straw imports from CWD-affected areas [352], and has given rise to food safety concerns within CWD endemic regions [353–355]. For this reason, it is of utmost importance to develop methods of monitoring environmental CWD. As well, accurate disease models, which must fully encompass the variability of CWD transmission, are important to predict the impact of CWD and assess mitigation methods.

5.2 Variability of CWD transmission properties

In Chapters 2 and 3, I examined the host range of CWD by studying the transmissibility of a number of isolates to hamsters. The transmission properties of isolates from cervids with PrP polymorphisms differed from the previously characterized Wisc-1 isolate (Table 2-1). This is in keeping with previous studies that demonstrated different CWD strains in cervids expressing non-wildtype PrP [219,222,344]. However, I also observed transmission differences in isolates from wildtype deer, which express identical PrP sequences (Table 3-3). The CWD isolates in these studies fell into three distinct categories based on their transmissibility to hamsters. These categories were correlated with cervid species (most white-tailed deer had high transmissibility to hamsters) and location (isolates from a similar location had low transmissibility to hamsters). Differences in CWD host range, correlated to both cervid species [247–249,251,255] and location [254], have been previously observed,

however, we studied a variety of isolates from individual cervids while other studies tested pooled CWD samples consisting of a variety of PrP polymorphisms or examined only a handful of isolates [239,247–249,251,254]. By examining a range of CWD isolates, instead of pooled samples, and controlling for titer, we can better understand the true diversity of the CWD host range (Figure 5-1).

In these studies, I used host range as a proxy for prion strain, without characterizing the strain characteristics of the original isolates. Given concerns of interspecies transmission, host range is an environmentally relevant strain characteristic with obvious real-world implications. Similar studies have also used host range to compare the diversity of other prion isolates, demonstrating both the strain uniformity of BSE and the diversity of classical scrapie [209–211]. However, isolates with a similar hamster transmission pattern will not necessarily contain the same strain, and transmission differences in hamsters does not necessarily imply differences in more ecologically relevant species.

Further characterization of these CWD isolates, using other rodent models and biochemical techniques, is ongoing. By transmitting isolates that looked different in hamsters to other rodent models, including transgenic mice expressing PrP from humans, livestock, and wildlife from the CWD endemic region, we can better understand the potential impact of the CWD variants identified in these studies. It would also be important to characterize biochemical differences in the original cervid isolates, both to confirm the existence of strain mixtures in these samples and to develop methods of differentiating CWD strains. Assays like the conformation stability assay, which differentiates prions by their stability in guanidine [366], may be used to confirm the existence of different CWD variants in the hunter-harvested CWD isolates, however, it is important to find a higher throughput screening method for the purposes of disease monitoring.

5.3 Comparison to Scrapie

Similar transmission studies have been conducted using scrapie isolates [209–211]. These studies also demonstrated a great degree of variability in the host ranges of scrapie isolates, even isolates from sheep or goats of an identical genotype from the same herd harvested at the same time [209]. Some of these scrapie isolates also resulted in multiple banding patterns after interspecies transmission [210,211], which was taken as additional evidence of strain variation in these samples. The two PrP^{res} migration patterns I observed, patterns A and B, may also be due to the coexistence of multiple PrP^{Sc} conformers in the cervid isolates or, alternatively, have emerged during the interspecies transmission to hamsters. Given that the two patterns are not evenly distributed between isolates, as I would expect if they emerged during hamster passage, and the similarity to the results of the previously mentioned scrapie transmission studies, the former appears more likely. However, more research should be performed to determine if multiple PrP^{Sc} conformers, or indeed strains, correlating to these two migration patterns in hamsters are present in the original cervid isolates.

Scrapie and CWD share several characteristics that may foster the existence and perpetuation of prion mixtures. Both diseases cycle through animals of diverse PrP polymorphisms, breed, and species, which may allow for the emergence of novel prion strains [134,136,137,182,219,222,223,367]. As well, peripheral replication and shedding are important in the transmission of both diseases [56,169,170,224,279,346,347], which could further increase the conformer variability of these diseases [109,211]. The existence of CWD conformer mixtures poses some problems in understanding the potential ecological impact of CWD, since the host range of CWD may depend on the specific area and cervid species of interest. For this reason, finding biochemical differences between strains to be able to properly study the zoonotic properties should be of utmost importance.

5.4 Development of the Vegetation Binding Assay

The original objective of this project was to assess the risk of prion transmission through contaminated vegetation. This data could be incorporated into epidemiological models of CWD transmission and would allow governments to make evidence-based decisions on contentious CWD-related issues, such as the import of hay from CWD-endemic areas [352] and develop and evaluate CWD mitigation efforts. While I did not fulfil this objective, I was able to develop an assay to detect PrP adhered to vegetation. In this assay, the entire plant sample is boiled in a surfactant, which releases PrP that can be detected by immunoblot (Figure 4-9). This method minimizes the impact that plant proteins and other compounds will have on PrP detection (Figure 4-1). As well, this assay can be linked to amplification methods such as PMCA (Figure 4-6) to improve detection. This simple assay can be used to assess the impact climatic and temporal factors can have on the prion-plant interaction (Figure 4-11).

The interaction between prions and vegetation, both aerial vegetation and leaflitter, would also play a central role in the levels of infectivity in soils (Figure 5-1). Low adherence of CWD to plants mean that infectivity will be washed into the soil by precipitation. Depending on soil type, this may allow these constant, low levels of infectivity to percolate into deeper layers of soil and possibly be degraded by saprotrophs, especially during the warm season. On the other hand, if infectivity remains adhered to plant material until autumn, large amounts of CWD will enter the soil simultaneously, and, at least in northern areas, will remain bioavailable throughout the winter when the soil is frozen. The amount and type of precipitation would also impact this process since the frequency of precipitation may impact the binding of PrP to plants. This demonstrates how climatic and geographic factors must also be considered in environmental transmission and the development of a protocol for monitoring environmental contamination.

5.5 Future Applications of the Vegetation Binding Assay

Implementation of my PrP vegetation binding assay for monitoring environmental CWD contamination will require further optimization to increase detection limits. Different surfactants may increase the amount of PrP that can be extracted from plant surfaces. As well, scaling up this procedure and optimizing the amplification of PrP^{Sc} using RT-QuIC or PMCA will facilitate biomonitoring. To assess the levels of CWD contamination in a particular area, a number of different individual plants of the same species would be processed using the assay and the incidence of prion contamination would be calculated by dividing the number of contaminated plant samples by the total number of samples processed.

$$Contamination\ incidence = \frac{Number\ of\ contaminated\ samples}{Total\ number\ of\ samples}$$

This procedure would be repeated using several common plant species with different prion adherence capacities to calculate the contamination index of the location. This index could be used to compare the CWD infectious load of different areas, controlling for climatic and seasonal variation.

$$Contamination\ index = \frac{High\ capacity\ contamination\ incidence}{Low\ capacity\ contamination\ incidence}$$

As well, the use of different plant varieties with different residence times in the environment would let us appreciate not only the total amount of deposited infectivity, which would be calculated using incidence from long-residence time plants, but also how much infectivity has been deposited recently, which would be important to understand disease dynamics, especially in areas where cervids are migratory.

The vegetation binding assay can also be used to assess the prion adherence capacity of agricultural products, especially of grasses that are used as feed and bedding, which are not heavily processed and thus at a greater risk of transmitting CWD. In addition, the effect of

foliar fertilizers and insecticides, which often contain wetting agents that may modify prion-plant interactions, should be explored. Additionally, this assay could be used to discover which cuticle characteristics most impact CWD adherence, perhaps by utilizing the extensive Arabidopsis mutant library. Using data gathered from such experiments, we could limit CWD contamination on agricultural products by specifically cultivating crop cultivars that share features associated with low prion adherence capacity, or alternatively bioengineer crops with these properties. This would reduce the risk of interspecies transmission to livestock and humans.

5.6 Concluding remarks

Given the complexity of this fatal neurological disease, CWD management approaches must be multifaceted and must consider the diversity of CWD and its transmission properties. Models of CWD, which are central to assessing and evaluating mitigation efforts, must consider many of the factors discussed in this thesis. The choices made now in CWD management and mitigation will determine not only the future of our cervid populations, but also will have ramifications on human and livestock health for decades to come.

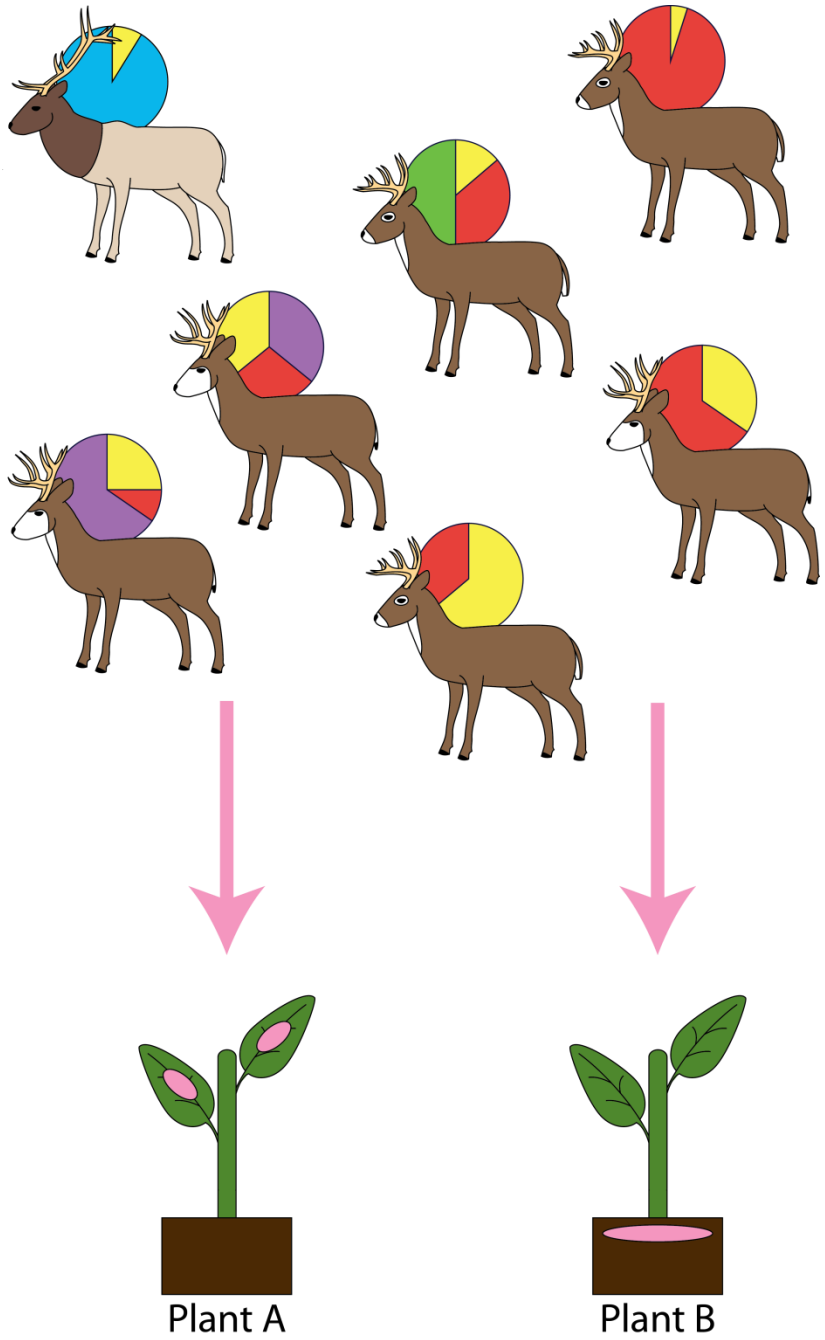

Figure 5-1. CWD-infected cervids carry a range of conformers, varying by the type of cervid and cervid PrP alleles. This material will be shed onto plants and other vegetation, whose prion adherence capacity will determine how much infectivity will percolate into the soil. CWD positive cervids may carry multiple different CWD conformers, which is represented by the circle near each cervid that depicts all the PrP^{Sc} conformers in each animal. The different colours in the circle represent the different conformers, and their prominence infectious load is depicted by their proportion of the total circle.

Works Cited

1. Hornshaw MP, McDermott JR, Candy JM. Copper binding to the N-terminal tandem repeat regions of mammalian and avian prion protein. Biochem Biophys Res Commun. 1995;207: 621–629. doi:10.1006/bbrc.1995.1233
2. Brown DR, Qin K, Herms JW, Madlung A, Manson J, Strome R, et al. The cellular prion protein binds copperin vivo. Nature. 1997;390: 684–687. doi:10.1038/37783
3. Safar J, Wille H, Itri V, Groth D, Serban H, Torchia M, et al. Eight prion strains have PrP(Sc) molecules with different conformations. Nat Med. 1998;4: 1157–1165. doi:10.1038/2654
4. Kaneko K, Zulianello L, Scott M, Cooper CM, Wallace a C, James TL, et al. Evidence for protein X binding to a discontinuous epitope on the cellular prion protein during scrapie prion propagation. Proc Natl Acad Sci U S A. 1997;94: 10069–10074. doi:10.1073/pnas.94.19.10069
5. Riek R, Hornemann S, Wider G, Billeter M, Glockshuber R, Wuthrich K. NMR structure of the mouse prion protein domain PrP(121-231). Nature. 1996;382: 180–182. doi:10.1038/382180a0
6. Zahn R, Liu A, Lührs T, Riek R, Von Schroetter C, Garcia FL, et al. NMR solution structure of the human prion protein. Proc Natl Acad Sci U S A. 2000;97: 145–150. doi:10.1073/pnas.97.1.145
7. Riesner D. Riesner D Biochemistry and structure of PrP^{C} and PrP^{Sc}. Br Med Bull. 2003;66: 1–13. doi:10.1093/bmb/dg66.021
8. Turk E, Teplow DB, Hood LE, Prusiner SB. Purification and properties of the cellular and scrapie hamster prion proteins. Eur J Biochem. 1988;176: 21–30. doi:10.1111/j.1432-1033.1988.tb14246.x
9. Premzl M, Gready JE, Jermiin LS, Simonic T, Marshall Graves JA. Evolution of vertebrate genes related to prion and shadoo proteins - Clues from comparative genomic analysis. Mol Biol Evol. 2004;21: 2210–2231. doi:10.1093/molbev/msh245
10. Benestad SL, Austbø L, Tranulis MA, Espenes A, Olsaker I. Healthy goats naturally devoid of prion protein. Vet Res. 2012;43: 87. doi:10.1186/1297-9716-43-87
11. Richt JA, Kasinathan P, Hamir AN, Castilla J, Sathiyaseelan T, Vargas F, et al. Production of cattle lacking prion protein. Nat Biotechnol. 2007;25: 132–138. doi:10.1038/nbt1271
12. Skedsmo FS, Malachin G, Våge DI, Hammervold MM, Salvesen Ø, Ersdal C, et al. Demyelinating polyneuropathy in goats lacking prion protein. FASEB J. 2020;34: 2359–2375. doi:10.1096/fj.201902588R
13. Weissmann C, Aguzzi A. PrP's Double Causes Trouble. Science (80-). 1999;286: 914–915.
14. Striebel JF, Race B, Pathmajeyan M, Rangel A, Chesebro B. Lack of influence of prion protein gene expression on kainate-induced seizures in mice: studies using congenic, coisogenic and transgenic strains. Neuroscience. 2013;238: 11–18. doi:10.1016/j.neuroscience.2013.02.004
15. Steele AD, Lindquist S, Aguzzi A. The prion protein knockout mouse: a phenotype under challenge. Prion. 2007;1: 83–93. doi:10.4161/pri.1.2.4346
16. Rutishauser D, Mertz KD, Moos R, Brunner E, Rülicke T, Calella AM, et al. The comprehensive native interactome of a fully functional tagged prion protein. PLoS One. 2009;4. doi:10.1371/journal.pone.0004446
17. Collinge J, Whittington MA, Sidle KCL, Smith CJ, Palmer MS, Clarke AR, et al. Prion protein is necessary for normal synaptic function. Nature. 1994;370: 295–297.

doi:10.1038/370295a0
18. Carleton A, Tremblay P, Vincent JD, Lledo PM. Dose-dependent, prion protein (PrP)-mediated facilitation of excitatory synaptic transmission in the mouse hippocampus. Pflugers Arch Eur J Physiol. 2001;442: 223–229. doi:10.1007/s004240100523
19. Huber R, Deboer T, Tobler I. Prion protein: A role in sleep regulation? J Sleep Res. 1999;8: 30–36. doi:10.1046/j.1365-2869.1999.00006.x
20. Sánchez-Alavez M, Conti B, Moroncini G, Criado JR. Contributions of neuronal prion protein on sleep recovery and stress response following sleep deprivation. Brain Res. 2007;1158: 71–80. doi:10.1016/j.brainres.2007.05.010
21. Wulf M-A, Senatore A, Aguzzi A. The biological function of the cellular prion protein: an update. BMC Biol. 2017;15: 34. doi:10.1186/s12915-017-0375-5
22. Carulla P, Llorens F, Matamoros-Angles A, Aguilar-Calvo P, Espinosa JC, Gavín R, et al. Involvement of PrP C in kainate-induced excitotoxicity in several mouse strains. Sci Rep. 2015;5. doi:10.1038/srep11971
23. Khosravani H, Zhang Y, Tsutsui S, Hameed S, Altier C, Hamid J, et al. Prion protein attenuates excitotoxicity by inhibiting NMDA receptors. J Cell Biol. 2008;181: 551–555. doi:10.1083/jcb.200711002
24. Herms JW, Korte S, Gall S, Schneider I, Dunker S, Kretzschmar HA. Altered intracellular calcium homeostasis in cerebellar granule cells of prion protein-deficient mice. J Neurochem. 2000;75: 1487–1492. doi:10.1046/j.1471-4159.2000.0751487.x
25. Mitteregger G, Vosko M, Krebs B, Xiang W, Kohlmannsperger V, Nölting S, et al. The role of the octarepeat region in neuroprotective function of the cellular prion protein. Brain Pathol. 2007;17: 174–183. doi:10.1111/j.1750-3639.2007.00061.x
26. Fluharty BR, Biasini E, Stravalaci M, Sclip A, Diomede L, Balducci C, et al. An N-terminal fragment of the prion protein binds to amyloid-β oligomers and inhibits their neurotoxicity in vivo. J Biol Chem. 2013;288: 7857–7866. doi:10.1074/jbc.M112.423954
27. Klamt F, Dal-Pizzol F, Conte Da Frota ML, Walz R, Andrades ME, Da Silva EG, et al. Imbalance of antioxidant defense in mice lacking cellular prion protein. Free Radic Biol Med. 2001;30: 1137–1144. doi:10.1016/S0891-5849(01)00512-3
28. White AR, Collins SJ, Maher F, Jobling MF, Stewart LR, Thyer JM, et al. Prion protein-deficient neurons reveal lower glutathione reductase activity and increased susceptibility to hydrogen peroxide toxicity. Am J Pathol. 1999;155: 1723–1730. doi:10.1016/S0002-9440(10)65487-9
29. Gasperini L, Meneghetti E, Legname G, Benetti F. In absence of the cellular prion protein, alterations in copper metabolism and copper-dependent oxidase activity affect iron distribution. Front Neurosci. 2016;10. doi:10.3389/fnins.2016.00437
30. Prusiner SB. Molecular biology of prion diseases. Science (80-). 1991;252: 1515–1521. doi:10.2222/jsv.49.193
31. Rambaran RN, Serpell LC. Amyloid fibrils: abnormal protein assembly. Prion. Taylor & Francis; 2008. pp. 112–117. doi:10.4161/pri.2.3.7488
32. Jarrett JT, Lansbury PT. Seeding “one-dimensional crystallization” of amyloid: A pathogenic mechanism in Alzheimer’s disease and scrapie? Cell. 1993. pp. 1055–1058. doi:10.1016/0092-8674(93)90635-4
33. Safar J, Roller PP, Gajdusek DC, Gibbs CJ. Thermal stability and conformational transitions of scrapie amyloid (prion) protein correlate with infectivity. Protein Sci. 1993;2: 2206–2216. doi:10.1002/pro.5560021220
34. Pan KM, Baldwin M, Nguyen J, Gasset M, Serban A, Groth D, et al. Conversion of alpha-helices into beta-sheets features in the formation of the scrapie prion proteins. Proc Natl Acad Sci U S A. 1993;90: 10962–10966. doi:VL - 90

35. McKinley MP, Bolton DC, Prusiner SB. A protease-resistant protein is a structural component of the Scrapie prion. Cell. 1983;35: 57–62. doi:10.1016/0092-8674(83)90207-6
36. Brown P, Rohwer RG, Gajdusek DC. Newer Data on the Inactivation of Scrapie Virus or Creutzfeldt-Jakob Disease Virus in Brain Tissue. J Infect Dis. 1986;153: 1145–1148. doi:10.1016/S0399-077X(71)80055-0
37. Taylor D. M, Fernie K, Mcconnell I, Steele P. J. Observations on thermostable subpopulations of the unconventional agents that cause transmissible degenerative encephalopathies. Vet Microbiol. 1998 Nov. doi:10.1016/S0378-1135(98)00257-0
38. Vázquez-Fernández E, Vos MR, Afanasyev P, Cebey L, Sevillano AM, Vidal E, et al. The Structural Architecture of an Infectious Mammalian Prion Using Electron Cryomicroscopy. PLoS Pathog. 2016;12: 1–21. doi:10.1371/journal.ppat.1005835
39. Wille H, Michelitsch MD, Guénebaut V, Supattapone S, Serban A, Cohen FE, et al. Structural studies of the scrapie prion protein by electron crystallography. Proc Natl Acad Sci U S A. 2002;99: 3563–3568. doi:10.1073/pnas.052703499
40. Wille H, Requena J. The Structure of PrP^{Sc} Prions. Pathogens. 2018;7: 20. doi:10.3390/pathogens7010020
41. Sawaya MR, Sambashivan S, Nelson R, Ivanova MI, Sievers SA, Apostol MI, et al. Atomic structures of amyloid cross-β spines reveal varied steric zippers. Nature. 2007;447: 453–457. doi:10.1038/nature05695
42. Groveman BR, Dolan MA, Taubner LM, Kraus A, Wickner RB, Caughey B. Parallel in-register intermolecular β-sheet architectures for prion-seeded prion protein (PrP) amyloids. J Biol Chem. 2014;289: 24129–24142. doi:10.1074/jbc.M114.578344
43. McKinnon C, Goold R, Andre R, Devoy A, Ortega Z, Moonga J, et al. Prion-mediated neurodegeneration is associated with early impairment of the ubiquitin–proteasome system. Acta Neuropathol. 2016;131: 411–425. doi:10.1007/s00401-015-1508-y
44. Andre R, Tabrizi SJ. Misfolded PrP and a novel mechanism of proteasome inhibition. Prion. Taylor & Francis; 2012. pp. 32–36. doi:10.4161/pri.6.1.18272
45. Deriziotis P, André R, Smith DM, Goold R, Kinghorn KJ, Kristiansen M, et al. Misfolded PrP impairs the UPS by interaction with the 20S proteasome and inhibition of substrate entry. EMBO J. 2011;30: 3065–3077. doi:10.1038/emboj.2011.224
46. Kristiansen M, Deriziotis P, Dimcheff DE, Jackson GS, Ovaa H, Naumann H, et al. Disease-Associated Prion Protein Oligomers Inhibit the 26S Proteasome. Mol Cell. 2007;26: 175–188. doi:10.1016/j.molcel.2007.04.001
47. Lin Z, Zhao D, Yang L. Interaction between misfolded PrP and the ubiquitin-proteasome system in prion-mediated neurodegeneration. Acta Biochimica et Biophysica Sinica. Oxford Academic; 2013. pp. 477–484. doi:10.1093/abbs/gmt020
48. Choi S Il, Ju WK, Choi EK, Kim J, Lea HZ, Carp RI, et al. Mitochondrial dysfunction induced by oxidative stress in the brains of hamsters infected with the 263 K scrapie agent. Acta Neuropathol. 1998;96: 279–286. doi:10.1007/s004010050895
49. Lee DW, Sohn HO, Lim HB, Lee YG, Kim YS, Carp RI, et al. Alteration of free radical metabolism in the brain of mice infected with scrapie agent. Free Radic Res. 1999;30: 499–507. doi:10.1080/10715769900300541
50. Clinton J, Forsyth C, Royston MC, Roberts GW. Synaptic degeneration is the primary neuropathological feature in prion disease: A preliminary study. Neuroreport. 1993;4: 65–68. doi:10.1097/00001756-199301000-00017
51. Lashuel HA, Hartley D, Petre BM, Walz T, Lansbury PT. Neurodegenerative disease: Amyloid pores from pathogenic mutations. Nature. 2002;418: 291. doi:10.1038/418291a
52. Hughes D, Halliday M. What Is Our Current Understanding of PrP^{Sc}-Associated

Neurotoxicity and Its Molecular Underpinnings? Pathogens. 2017;6: 63. doi:10.3390/pathogens6040063
53. Saá P, Harris DA, Cervenakova L. Mechanisms of prion-induced neurodegeneration. Expert Rev Mol Med. 2016;18. doi:10.1017/erm.2016.8
54. Collinge J, Whitfield J, McKintosh E, Beck J, Mead S, Thomas DJ, et al. Kuru in the 21st century-an acquired human prion disease with very long incubation periods. Lancet. 2006;367: 2068–2074. doi:10.1016/S0140-6736(06)68930-7
55. Bruce ME, Will RG, Ironside JW, McConnell I, Drummond D, Suttie A, et al. Transmissions to mice indicate that "new variant" CJD is caused by the BSE agent. Nature. 1997;389: 498–501. doi:10.1038/39057
56. Terry LA, Howells L, Bishop K, Baker CA, Everest S, Thorne L, et al. Detection of prions in the faeces of sheep naturally infected with classical scrapie. Vet Res. 2011;42: 65. doi:10.1186/1297-9716-42-65
57. Gonzalez-Romero D, Barria MA, Leon P, Morales R, Soto C. Detection of infectious prions in urine. FEBS Lett. 2008;582: 3161–3166. doi:10.1016/j.febslet.2008.08.003
58. Tamgüney G, Richt J a., Hamir AN, Greenlee JJ, Miller MW, Wolfe LL, et al. Salivary prions in sheep and deer. Prion. 2012;6: 52–61. doi:10.4161/pri.6.1.16984
59. Brown P, Brandel JP, Sato T, Nakamura Y, MacKenzie J, Will RG, et al. Iatrogenic creutzfeldt-Jakob disease, final assessment. Emerg Infect Dis. 2012;18: 901–907. doi:10.3201/eid1806.120116
60. Yamada S, Aiba T, Endo Y, Hara M, Kitamoto T, Tateishi J. Creutzfeldt-Jakob Disease Transmitted by a Cadaveric Dura Mater Graft. Neurosurgery. 1994;34: 740–744. doi:10.1097/00006123-199404000-00027
61. Ae R, Hamaguchi T, Nakamura Y, Yamada M, Tsukamoto T, Mizusawa H, et al. Update: Dura Mater Graft-Associated Creutzfeldt-Jakob Disease-Japan, 1975-2017. Morb Mortal Wkly Rep. 2018;67: 274–278.
62. Gajdusek DC, Zigas V. Kuru. Clinical, pathological and epidemiological study of an acute progressive degenerative disease of the central nervous system among natives of the Eastern Highlands of New Guinea. The American Journal of Medicine. Elsevier; 1959. pp. 442–469. doi:10.1016/0002-9343(59)90251-7
63. Alpers MP. Review. The epidemiology of kuru: Monitoring the epidemic from its peak to its end. Philosophical Transactions of the Royal Society B: Biological Sciences. Royal Society; 2008. pp. 3707–3713. doi:10.1098/rstb.2008.0071
64. Collinge J, Whitfield J, Mckintosh E, Frosh A, Mead S, Hill AF, et al. A clinical study of kuru patients with long incubation periods at the end of the epidemic in Papua New Guinea. Philos Trans R Soc Lond B Biol Sci. 2008;363: 3725–3739. doi:10.1098/rstb.2008.0068
65. Wilesmith JW, Ryan JB, Atkinson MJ. Bovine spongiform encephalopathy: epidemiological studies on the origin. Vet Rec. 1991;128: 199–203. doi:10.1136/vr.128.9.199
66. Huor A, Espinosa JC, Vidal E, Cassard H, Douet JY, Lugan S, et al. The emergence of classical BSE from atypical/Nor98 scrapie. Proc Natl Acad Sci U S A. 2019;116: 26853–26862. doi:10.1073/pnas.1915737116
67. Capobianco R, Casalone C, Suardi S, Mangieri M, Miccolo C, Limido L, et al. Conversion of the BASE prion strain into the BSE strain: The origin of BSE? PLoS Pathog. 2007;3. doi:10.1371/journal.ppat.0030031
68. Torres JM, Andréoletti O, Lacroux C, Prieto I, Lorenzo P, Larska M, et al. Classical bovine spongiform encephalopathy by transmission of H-type prion in homologous prion protein context. Emerg Infect Dis. 2011;17: 1636–1644. doi:10.3201/eid1709.101403

69. Hill AF, Desbruslais M, Joiner S, Sidle KCL, Gowland I, Collinge J, et al. The same prion strain causes vCJD and BSE [10]. Nature. 1997. pp. 448–450. doi:10.1038/38925
70. Scott MR, Will R, Ironside J, Nguyen HO, Tremblay P, DeArmond SJ, et al. Compelling transgenetic evidence for transmission of bovine spongiform encephalopathy prions to humans. Proc Natl Acad Sci USA. 1999;96: 15137–15142. doi:10.1073/pnas.96.26.15137
71. Brandel J-PP, Heath CA, Head MW, Levavasseur E, Knight R, Laplanche J-LL, et al. Variant creutzfeldt-jakob disease in france and the united kingdom: evidence for the same agent strain. Ann Neurol. 2009;65: 249–256. doi:10.1002/ana.21583
72. Will RG, Zeidler M, Stewart GE, Macleod MA, Ironside JW, Cousens SN, et al. Diagnosis of new variant Creutzfeldt-Jakob disease. Ann Neurol. 2000;47: 575–582. doi:10.1002/1531-8249(200005)47:5<575::AID-ANA4>3.0.CO;2-W
73. Zeidler M, Stewart GE, Barraclough CR, Bateman DE, Bates D, Burn DJ, et al. New variant Creutzfeldt-Jakob disease: Neurological features and diagnostic tests. Lancet. 1997;350: 903–907. doi:10.1016/S0140-6736(97)07472-2
74. Heath CA, Cooper SA, Murray K, Lowman A, Henry C, MacLeod MA, et al. Validation of diagnostic criteria for variant Creutzfeldt-Jakob disease. Ann Neurol. 2010;67: 761–770. doi:10.1002/ana.21987
75. Mok T, Jaunmuktane Z, Joiner S, Campbell T, Morgan C, Wakerley B, et al. Variant Creutzfeldt-Jakob disease in a patient with heterozygosity at PRNP codon 129. N Engl J Med. 2017;376: 292–294. doi:10.1056/NEJMc1610003
76. Sigurdson CJ, Williams ES, Miller MW, Spraker TR, O'rourke KI, Hoover EA. Oral transmission and early lymphoid tropism of chronic wasting disease PrP(res) in mule deer fawns (*Odocoileus hemionus*). J Gen Virol. 1999;80: 2757–2764. doi:10.1099/0022-1317-80-10-2757
77. Hoffmann C, Ziegler U, Buschmann A, Weber A, Kupfer L, Oelschlegel A, et al. Prions spread via the autonomic nervous system from the gut to the central nervous system in cattle incubating bovine spongiform encephalopathy. J Gen Virol. 2007;88: 1048–1055. doi:10.1099/vir.0.82186-0
78. Beekes M, Mcbride PA. Early accumulation of pathological PrP in the enteric nervous system and gut-associated lymphoid tissue of hamsters orally infected with scrapie. Neurosci Lett. 2000;278: 181–184. doi:10.1016/S0304-3940(99)00934-9
79. Donaldson DS, Kobayashi a, Ohno H, Yagita H, Williams IR, Mabbott N a. M cell-depletion blocks oral prion disease pathogenesis. Mucosal Immunol. 2012;5: 216–225. doi:10.1038/mi.2011.68
80. Prinz M, Huber G, Macpherson AJS, Heppner FL, Glatzel M, Eugster H-P, et al. Oral prion infection requires normal numbers of Peyer's patches but not of enteric lymphocytes. Am J Pathol. 2003;162: 1103–11. doi:10.1016/S0002-9440(10)63907-7
81. Donaldson DS, Sehgal A, Rios D, Williams IR, Mabbott NA. Increased Abundance of M Cells in the Gut Epithelium Dramatically Enhances Oral Prion Disease Susceptibility. PLoS Pathog. 2016;12: 1–36. doi:10.1371/journal.ppat.1006075
82. Jeffrey M, González L, Espenes A, Press CM, Martin S, Chaplin M, et al. Transportation of prion protein across the intestinal mucosa of scrapie-susceptible and scrapie-resistant sheep. J Pathol. 2006;209: 4–14. doi:10.1002/path.1962
83. Race R, Oldstone M, Chesebro B. Entry versus Blockade of Brain Infection following Oral or Intraperitoneal Scrapie Administration: Role of Prion Protein Expression in Peripheral Nerves and Spleen. J Virol. 2000;74: 828–833. doi:10.1128/jvi.74.2.828-833.2000
84. McBride PA, Schulz-Schaeffer WJ, Donaldson M, Bruce M, Diringer H, Kretzschmar

HA, et al. Early Spread of Scrapie from the Gastrointestinal Tract to the Central Nervous System Involves Autonomic Fibers of the Splanchnic and Vagus Nerves. J Virol. 2001;75: 9320–9327. doi:10.1128/jvi.75.19.9320-9327.2001
85. Mabbott NA, MacPherson GG. Prions and their lethal journey to the brain. NatRevMicrobiol. 2006;4: 201–211. doi:10.1038/nrmicro1346
86. Beekes M, McBride PA. The spread of prions through the body in naturally acquired transmissible spongiform encephalopathies. FEBS J. 2007;274: 588–605. doi:10.1111/j.1742-4658.2007.05631.x
87. Brown P. Bovine spongiform encephalopathy and variant Creutzfeldt-Jakob disease. BMJ. 2001;322: 841–4. doi:10.3201/eid0701.700006
88. Douet J, Lacroux C, Litaise C, Lugan S, Corbière F, Arnold M, et al. Mono-nucleated blood cell populations display different abilities to transmit prion disease by the transfusion route. J Virol. 2016;90: JVI.02783-15. doi:10.1128/JVI.02783-15
89. Andréoletti O, Litaise C, Simmons H, Corbière F, Lugan S, Costes P, et al. Highly efficient prion transmission by blood transfusion. Bartz J, editor. PLoS Pathog. 2012;8: e1002782. doi:10.1371/journal.ppat.1002782
90. Bruce ME, Dickinson AG. Biological evidence that scrapie agent has an independent genome. J Gen Virol. 1987;68: 79–89. doi:10.1099/0022-1317-68-1-79
91. Fraser H, Dickinson AG. Scrapie in mice. Agent-strain differences in the distribution and intensity of grey matter vacuolation. J Comp Pathol. 1973;83: 29–40. doi:10.1016/0021-9975(73)90024-8
92. Dickinson AG, Meikle VMH. Host-genotype and agent effects in scrapie incubation: Change in allelic interaction with different strains of agent. MGG Mol Gen Genet. 1971;112: 73–79. doi:10.1007/BF00266934
93. Dickinson AG, Meikle VM, Fraser H. Identification of a gene which controls the incubation period of some strains of scrapie agent in mice. J Comp Pathol. 1968;78: 293–299. doi:10.1016/0021-9975(68)90005-4
94. Kimberlin RH, Cole S, Walker CA. Temporary and permanent modifications to a single strain of mouse scrapie on transmission to rats and hamsters. J Gen Virol. 1987;68: 1875–1881. doi:10.1099/0022-1317-68-7-1875
95. Bessen RA, Marsh RF. Identification of two biologically distinct strains of transmissible mink encephalopathy in hamsters. J Gen Virol. 1992;73: 329–334. doi:10.1099/0022-1317-73-2-329
96. Parchi P, Capellari S, Chen S, Petersen R, Gambetti P, Kopp N, et al. Typing prion isoforms. Nature. 1997;386: 232–233. doi:10.1111/mms.12203
97. Somerville RA, Chong A, Mulqueen OU, Birkett CR, Wood SCER, Hope J, et al. Biochemical typing of scrapie strains. Nature. 1997. p. 564. doi:10.1038/386564a0
98. Safar J, Wille H, Itri V, Groth D, Serban H, Torchia M, et al. Eight prion strains have PrP(Sc) molecules with different conformations. Nat Med. 1998;4: 1157–65. doi:10.1038/2654
99. Bessen RA, Marsh RF. Biochemical and physical properties of the prion protein from two strains of the transmissible mink encephalopathy agent. J Virol. 1992;66: 2096–2101. Available: http://www.ncbi.nlm.nih.gov/pubmed/1347795%5Cnhttp://www.ncbi.nlm.nih.gov/pmc/articles/PMC289000/pdf/jvirol00166-0282.pdf
100. Bessen RA, Marsh RF. Distinct PrP properties suggest the molecular basis of strain variation in transmissible mink encephalopathy. J Virol. 1994;68: 7859–7868. doi:10.1128/jvi.68.12.7859-7868.1994
101. Bessen RA, Kocisko DA, Raymond GJ, Nandan S, Lansbury PT, Caughey B, et al. Non-genetic propagation of strain-specific properties of scrapie prion protein. Nature.

1995;375: 698–700. doi:10.1038/375698a0
102. Pirisinu L, Tran L, Chiappini B, Vanni I, Di Bari MA, Vaccari G, et al. Novel Type of Chronic Wasting Disease Detected in Moose (Alces alces), Norway. Emerg Infect Dis. 2018;24: 2210–2218. doi:10.3201/eid2412.180702
103. Saijo E, Hughson AG, Raymond GJ, Suzuki A, Horiuchi M, Caughey B. PrP Sc - Specific Antibody Reveals C-Terminal Conformational Differences between Prion Strains. J Virol. 2016;90: 4905–4913. doi:10.1128/jvi.00088-16
104. Stack MJ, Chaplin MJ, Clark J. Differentiation of prion protein glycoforms from naturally occurring sheep scrapie, sheep-passaged scrapie strains (CH1641 and SSBP1), bovine spongiform encephalopathy (BSE) cases and Romney and Cheviot breed sheep experimentally inoculated with BSE using. Acta Neuropathol. 2002;104: 279–286. doi:10.1007/s00401-002-0556-2
105. Bartz JC, Aiken JM, Bessen RA. Delay in onset of prion disease for th HY strain of transmissible mink encephalopathy as a result of prior peripheral inoculation with the replication-deficient DY strain. J Gen Virol. 2004;85: 265–273. doi:10.1099/vir.0.19394-0
106. Bessen RA, Martinka S, Kelly J, Gonzalez D. Role of the Lymphoreticular System in Prion Neuroinvasion from the Oral and Nasal Mucosa. J Virol. 2009;83: 6435–6445. doi:10.1128/jvi.00018-09
107. Kimberlin RH, Walker CA. Pathogenesis of Scrapie (Strain 263K) in Hamsters Infected Intracerebrally, Intraperitoneally or Intraocularly. J Gen Virol. 1986;67: 255–263.
108. Collis SC, Kimberlin RH. Long-term persistence of scrapie infection in mouse spleens in the absence of clinical disease. FEMS Microbiol Lett. 1985;29: 111–114. doi:10.1111/j.1574-6968.1985.tb00844.x
109. Le Dur A, Laï TL, Stinnakre M-G, Laisné A, Chenais N, Rakotobe S, et al. Divergent prion strain evolution driven by PrP^{C} expression level in transgenic mice. Nat Commun. 2017;8: 14170. doi:10.1038/ncomms14170
110. Bruce ME, McConnell I, Fraser H, Dickinson AG. The disease characteristics of different strains of scrapie in Sinc congenic mouse lines: Implications for the nature of the agent and host control of pathogenesis. J Gen Virol. 1991;72: 595–603. doi:10.1099/0022-1317-72-3-595
111. Puchtler H, Sweat F, Levine M. On the Binding of Congo Red by amyloid. J Histochem Cytochem. 1962;10: 355–364. doi:10.1002/anie.201916630
112. Van Keulen LJM, Schreuder BEC, Meloen RH, Mooij-Harkes G, Vromans MEW, Langeveld JPM. Immunohistochemical detection of prion protein in lymphoid tissues of sheep with natural scrapie. J Clin Microbiol. 1996;34: 1228–1231. doi:10.1128/jcm.34.5.1228-1231.1996
113. Miller JM, Jenny AL, Taylor WD, Marsh RF, Rubenstein R, Race RE. Immunohistochemical detection of prion protein in sheep with scrapie. J Vet Diagnostic Investig. 1993;5: 309–316. doi:10.1128/jcm.34.5.1228-1231.1996
114. Fraser H, Dickinson AGG. The sequential development of the brain lesions of scrapie in three strains of mice. J Comp Pathol. 1968;78: 301–311. doi:10.1016/0021-9975(68)90006-6
115. Di Bari MA, Nonno R, Agrimi U. The mouse model for scrapie: Inoculation, clinical scoring, and histopathological techniques. Methods Mol Biol. 2012;849: 453–471. doi:10.1007/978-1-61779-551-0_31
116. Amor S, Puentes F, Baker D, Van Der Valk P. Inflammation in neurodegenerative diseases. Immunology. 2010. pp. 154–169. doi:10.1111/j.1365-2567.2009.03225.x
117. Prusiner SB, Bolton DC, Groth DF, Bowman KA, Patricia Cochran S, McKinley MP.

Further Purification and Characterization of Scrapie Prions. Biochemistry. 1982;21: 6942–6950. doi:10.1021/bi00269a050
118. Demart S, Fournier JG, Creminon C, Frobert Y, Lamoury F, Marce D, et al. New insight into abnormal prion protein using monoclonal antibodies. Biochem Biophys Res Commun. 1999;265: 652–657. doi:10.1006/bbrc.1999.1730
119. McCutcheon S, Langeveld JPM, Tan BC, Gill AC, De Wolf C, Martin S, et al. Prion protein-specific antibodies that detect multiple TSE agents with high sensitivity. PLoS One. 2014;9: 91143. doi:10.1371/journal.pone.0091143
120. Xiao X, Yuan J, Haïk S, Cali I, Zhan Y, Moudjou M, et al. Glycoform-Selective Prion Formation in Sporadic and Familial Forms of Prion Disease. PLoS One. 2013;8. doi:10.1371/journal.pone.0058786
121. Tagliavini F, Lievens PMJ, Tranchant C, Warter JM, Mohr M, Giaccone G, et al. A 7-kDa Prion Protein (PrP) Fragment, an Integral Component of the PrP Region Required for Infectivity, Is the Major Amyloid Protein in Gerstmann-Sträussler-Scheinker Disease A117V. J Biol Chem. 2001;276: 6009–6015. doi:10.1074/jbc.M007062200
122. Thackray AM, Hopkins L, Klein MA, Bujdoso R. Mouse-Adapted Ovine Scrapie Prion Strains Are Characterized by Different Conformers of PrP^{Sc}. J Virol. 2007;81: 12119–12127. doi:10.1128/jvi.01434-07
123. Saborio GP, Permanne B, Soto C. Sensitive detection of pathological prion protein by cyclic amplification of protein misfolding. Nature. 2001;411: 810–813. doi:10.1038/35081095
124. Barria MA, Gonzalez-Romero D, Soto C. Cyclic amplification of prion protein misfolding. Methods Mol Biol. 2012;849: 199–212. doi:10.1007/978-1-61779-551-0_14
125. Makarava N, Savtchenko R, Baskakov I V. Methods of Protein Misfolding Cyclic Amplification. Methods in Molecular Biology Humana Press Inc.; 2017 pp. 169–183. doi:10.1007/978-1-4939-7244-9_13
126. Atarashi R, Sano K, Satoh K, Nishida N. Real-time quaking-induced conversion: a highly sensitive assay for prion detection. Prion. 2011;53: 150–153. doi:10.4161/pri.5.3.16893
127. Davenport KA, Henderson DM, Bian J, Telling GC, Mathiason CK, Hoover EA. Insights into Chronic Wasting Disease and Bovine Spongiform Encephalopathy Species Barriers by Use of Real-Time Conversion. J Virol. 2015;89: 9524–31. doi:10.1128/JVI.01439-15
128. Green KM, Castilla J, Seward TS, Napier DL, Jewell JE, Soto C, et al. Accelerated high fidelity prion amplification within and across prion species barriers. PLoS Pathog. 2008;4. doi:10.1371/journal.ppat.1000139
129. Jones M, Wight D, Barron R, Jeffrey M, Manson J, Prowse C, et al. Molecular model of prion transmission to humans. Emerg Infect Dis. 2009;15: 2013–2016. doi:10.3201/eid1512.090194
130. McGowan JP. Scrapie in sheep. Scottish J Agric. 1922;5: 365–375.
131. Detwiler L a, Baylis M. The epidemiology of scrapie. Rev Sci Tech. 2003;22: 121–43. Available: http://www.ncbi.nlm.nih.gov/pubmed/12793776
132. Konold T, Phelan L. Clinical examination protocol to detect atypical and classical scrapie in sheep. J Vis Exp. 2014 [cited 4 Aug 2020]. doi:10.3791/51101
133. O'Rourke KI, Melco RP, Mickelson JR. Allelic frequencies of an ovine scrapie susceptibility gene. Anim Biotechnol. 1996;7: 155–162. doi:10.1080/10495399609525856
134. Hunter N, Foster JD, Goldmann W, Stear MJ, Hope J, Bostock C. Natural scrapie in a closed flock of Cheviot sheep occurs only in specific PrP genotypes. Arch Virol.

1996;141: 809–824. doi:10.1007/BF01718157
135. Hunter N, Goldmann W, Foster JD, Cairns D, Smith G. Natural scrapie and PrP genotype: Case-control studies in British sheep. Vet Rec. 1997;141: 137–140. doi:10.1136/vr.141.6.137
136. Gubbins S, Roden JA. Breeding programmes for TSE resistance in British sheep: II. Assessing the impact on the prevalence and incidence of scrapie. Prev Vet Med. 2006;73: 17–31. doi:10.1016/j.prevetmed.2005.08.002
137. Truscott JE, Ferguson NM. Control of scrapie in the UK sheep population. Epidemiol Infect. 2009;137: 775–786. doi:10.1017/S0950268808001064
138. Benestad SL, Sarradin P, Thu B, Schönheit J, Tranulis MA, Bratberg B. Cases of scrapie with unusual features in Norway and designation of a new type, Nor98. Vet Rec. 2003;153: 202–208. doi:10.1136/vr.153.7.202
139. Brotherston JG, Renwick CC, Stamp JT, Zlotnik I, Pattison IH. Spread of scrapie by contact to goats and sheep. J Comp Pathol. 1968;78: 9–17. doi:10.1016/0021-9975(68)90107-2
140. Dickinson AG, Stamp JT, Renwick CC. Maternal and lateral transmission of scrapie in sheep. J Comp Pathol. 1974;84: 19–25. doi:10.1016/0021-9975(74)90023-1
141. Race R, Jenny A, Sutton D. Scrapie infectivity and proteinase K-resistant prion protein in sheep placenta, brain, spleen, and lymph node: Implications for transmission and antemortem diagnosis. J Infect Dis. 1998;178: 949–953. doi:10.1086/515669
142. Andréoletti O, Orge L, Benestad SL, Beringue V, Litaise C, Simon S, et al. Atypical/Nor98 scrapie infectivity in sheep peripheral tissues. PLoS Pathog. 2011;7. doi:10.1371/journal.ppat.1001285
143. Marsh RF, Burger D, Eckroade R, Zu GM, Hanson RP. A preliminary report on the experimental host range of the transmissible mink encephalopathy agent. J Infect Dis. 1969;120: 713–719. doi:10.1093/infdis/120.6.713
144. Marsh RF, Kimberlin RH. Comparison of scrapie and transmissible mink encephalopathy in hamsters. II. Clinical signs, pathology, and pathogenesis. J Infect Dis. 1975;131: 104–110. doi:10.1093/infdis/131.2.104
145. Bartz JC, Bessen RA, McKenzie D, Marsh RF, Aiken JM. Adaptation and selection of prion protein strain conformations following interspecies transmission of transmissible mink encephalopathy. J Virol. 2000;74: 5542–5547. doi:10.1128/JVI.74.12.5542-5547.2000
146. Schutt CR, Bartz JC. Prion interference with multiple prion isolates. Prion. 2008;2: 61–63. doi:10.4161/pri.2.2.6806
147. Dickinson AG, Fraser H, Meikle VMH, Outram GW. Competition between different scrapie agents in mice. Nat New Biol. 1972;237: 244–245.
148. Dickinson AG, Fraser H, Mcconnell I, Outram GW, Sales DI, Taylor DM. Extraneural competition between different scrapie agents leading to loss of infectivity. Nature. 1975;253: 556. doi:10.1038/253556a0
149. Shikiya RA, Ayers JI, Schutt CR, Kincaid AE, Bartz JC. Coinfecting Prion Strains Compete for a Limiting Cellular Resource. J Virol. 2010;84: 5706–5714. doi:10.1128/jvi.00243-10
150. Williams ES, Young S. Chronic wasting disease of captive mule deer: a spongiform encephalopathy. J Wildl Dis. 1980;16: 89–98. doi:10.7589/0090-3558-16.1.89
151. Guiroy DC, Williams ES, Yanagihara R, Gajdusek DC. Immunolocalization of scrapie amyloid (PrP27-30) in chronic wasting disease of Rocky Mountain elk and hybrids of captive mule deer and white-tailed deer. Neurosci Lett. 1991;126: 195–198. doi:10.1016/0304-3940(91)90552-5
152. Sohn HJ, Kim JH, Choi KS, Nah JJ, Joo YS, Jean YH, et al. A case of chronic wasting

disease in an elk imported to Korea from Canada. J Vet Med Sci. 2002;64: 855–858. doi:10.1292/jvms.64.855
153. Lee Y-H, Sohn H-J, Kim M-J, Kim H-J, Lee W-Y, Yun E-I, et al. Strain characterization of the Korean CWD cases in 2001 and 2004. J Vet Med Sci. 2013;75: 95–98. doi:10.1292/jvms.12-0077
154. Benestad SL, Mitchell G, Simmons M, Ytrehus B, Vikøren T. First case of chronic wasting disease in Europe in a Norwegian free-ranging reindeer. Vet Res. 2016;47: 88. doi:10.1186/s13567-016-0375-4
155. Argue CK, Ribble C, Lees VW, McLane J, Balachandran A. Epidemiology of an outbreak of chronic wasting disease on elk farms in Saskatchewan. Can Vet J. 2007;48: 1241–1248.
156. USGS National Wildlife Health Center. Expanding distribution of chronic wasting disease. In: usgs.gov [Internet]. 2020 [cited 4 Oct 2020]. Available: https://www.usgs.gov/centers/nwhc/science/expanding-distribution-chronic-wasting-disease?qt-science_center_objects=0#qt-science_center_objects
157. Dubé C, Mehren KG, Barker IK, Peart BL, Balachandran A. Retrospective investigation of chronic wasting disease of cervids at the Toronto Zoo, 1973-2003. Can Vet J. 2006;47: 1185–1193.
158. Johnson C, Johnson J, Vanderloo JP, Keane D, Aiken JM, McKenzie D. Prion protein polymorphisms in white-tailed deer influence susceptibility to chronic wasting disease. J Gen Virol. 2006;87: 2109–2114. doi:10.1099/vir.0.81615-0
159. Devivo MT, Edmunds DR, Kauffman MJ, Schumaker BA, Binfet J, Kreeger TJ, et al. Endemic chronic wasting disease causes mule deer population decline in Wyoming. PLoS One. 2017;12: e0186512. doi:10.1371/journal.pone.0186512
160. Edmunds DR, Kauffman MJ, Schumaker BA, Lindzey FG, Cook WE, Kreeger TJ, et al. Chronic Wasting Disease Drives Population Decline of White-Tailed Deer. PLoS One. 2016;11: e0161127. doi:10.1371/journal.pone.0161127
161. Wild MA, Hobbs NT, Graham MS, Miller MW. the Role of Predation in Disease Control: a Comparison of Selective and Nonselective Removal on Prion Disease Dynamics in Deer. J Wildl Dis. 2011;47: 78–93. doi:10.7589/0090-3558-47.1.78
162. Schuler KL, Jenks JA, Klaver RW, Jennelle CS, Bowyer RT. Chronic wasting Dsease detection and mortality sources in semi-protected deer population. Wildlife Biol. 2018;2018. doi:10.2981/wlb.00437
163. Race BL, Meade-White KD, Ward A, Jewell J, Miller MW, Williams ES, et al. Levels of abnormal prion protein in deer and elk with chronic wasting disease. Emerg Infect Dis. 2007;13: 824–830. doi:10.3201/eid1306.070186
164. Otero A, Duque Velásquez C, Johnson C, Herbst A, Bolea R, Badiola JJ, et al. Prion protein polymorphisms associated with reduced CWD susceptibility limit peripheral PrP CWD deposition in orally infected white-tailed deer. BMC Vet Res. 2019;15. doi:10.1186/s12917-019-1794-z
165. Keane DP, Barr DJ, Bochsler PN, Hall SM, Gidlewski T, O'Rourke KI, et al. Chronic wasting disease in a Wisconsin white- tailed deer farm. J Vet Diagnostic Investig. 2008;20: 698–703.
166. Fox KA, Jewell JE, Williams ES, Miller MW. Patterns of PrP^{CWD} accumulation during the course of chronic wasting disease infection in orally inoculated mule deer (*Odocoileus hemionus*). J Gen Virol. 2006;87: 3451–3461. doi:10.1099/vir.0.81999-0
167. Mathiason CK, Powers JG, Dahmes SJ, Osborn DA, Miller K V., Warren RJ, et al. Infectious prions in the saliva and blood of deer with chronic wasting disease. Science (80-). 2006;314: 133–136. doi:10.1126/science.1132661
168. Mathiason CK, Hays SA, Powers J, Hayes-Klug J, Langenberg J, Dahmes SJ, et al.

Infectious prions in pre-clinical deer and transmission of chronic wasting disease solely by environmental exposure. PLoS One. 2009;4. doi:10.1371/journal.pone.0005916
169. Henderson DM, Denkers ND, Hoover CE, Garbino N, Mathiason CK, Hoover EA. Longitudinal Detection of Prion Shedding in Saliva and Urine by Chronic Wasting Disease-Infected Deer by Real-Time Quaking-Induced Conversion. J Virol. 2015;89: 9338–9347. doi:10.3945/jn.115.211250\r10.1128/jvi.01118-15
170. Tamgüney G, Miller MW, Wolfe LL, Sirochman TM, Glidden D V, Palmer C, et al. Asymptomatic deer excrete infectious prions in faeces. Nature. 2009;461: 529–532. doi:10.1038/nature09031
171. Tennant JM, Li M, Henderson DM, Tyer ML, Denkers ND, Haley NJ, et al. Shedding and stability of CWD prion seeding activity in cervid feces. Caughey B, editor. PLoS One. 2020;15: e0227094. doi:10.1371/journal.pone.0227094
172. Plummer IH, Wright SD, Johnson CJ, Pedersen JA, Samuel MD. Temporal patterns of chronic wasting disease prion excretion in three cervid species. J Gen Virol. 2017;98: 1932–1942. doi:10.1099/jgv.0.000845
173. Kimberlin RH, Walker CA. Characteristics of a short incubation model of scrapie in the golden hamster. J Gen Virol. 1977;34: 295–304. doi:10.1099/0022-1317-34-2-295
174. Kimberlin RH, Walker CA. Evidence that the transmission of one source of scrapie agent to hamsters involves separation of agent strains from a mixture. J Gen Virol. 1978;39: 487–496. doi:10.1099/0022-1317-39-3-487
175. Kurt TD, Sigurdson CJ. Cross-species transmission of CWD prions. Prion. 2016;10: 83–91. doi:10.1080/19336896.2015.1118603
176. Kurt TD, Telling GC, Zabel MD, Hoover EA. Trans-species amplification of PrP^{CWD} and correlation with rigid loop 170N. Virology. 2009;387: 235–243. doi:10.1016/j.virol.2009.02.025
177. Kurt TD, Aguilar-Calvo P, Jiang L, Rodriguez JA, Alderson N, Eisenberg DS, et al. Asparagine and glutamine ladders promote cross-species prion conversion. J Biol Chem. 2017;292: 19076–19086. doi:10.1074/jbc.M117.794107
178. Wadsworth JDF, Asante EA, Desbruslais M, Linehan JM, Joiner S, Gowland I, et al. Human prion protein with valine 129 prevents expression of variant CJD phenotype. Science (80-). 2004;306: 1793–1796. doi:10.1126/science.1103932
179. Mead S, Stumpf MPH, Whitfield J, Beck J a, Poulter M, Campbell T, et al. Balancing selection at the prion protein gene consistent with prehistoric kurulike epidemics. Science (80-). 2003;300: 640–643. doi:10.1126/science.1083320
180. Cervenáková L, Goldfarb LG, Garruto R, Lee HS, Gajdusek DC, Brown P. Phenotype-genotype studies in kuru: implications for new variant Creutzfeldt-Jakob disease. Proc Natl Acad Sci U S A. 1998;95: 13239–41. doi:10.1073/pnas.95.22.13239
181. Asante EA, Smidak M, Grimshaw A, Houghton R, Tomlinson A, Jeelani A, et al. A naturally occurring variant of the human prion protein completely prevents prion disease. Nature. 2015;522: 478–81. doi:10.1038/nature14510
182. O'Rourke KI, Besser TE, Miller MW, Cline TF, Spraker TR, Jenny AL, et al. PrP genotypes of captive and free-ranging Rocky Mountain elk (*Cervus elaphus nelsoni*) with chronic wasting disease. J Gen Virol. 1999;80: 2765–2769. doi:10.1099/0022-1317-80-10-2765
183. Johnson C, Johnson J, Clayton M, McKenzie D, Aiken J. Prion protein gene heterogeneity in free-ranging white-tailed deer within the chronic wasting disease affected region of Wisconsin. J Wildl Dis. 2003;39: 576–581. doi:10.7589/0090-3558-39.3.576
184. Wilson GA, Nakada SM, Bollinger TK, Pybus MJ, Merrill EH, Coltman DW.

Polymorphisms at the PRNP gene influence susceptibility to chronic wasting disease in two species of deer (*Odocoileus Spp*.) in western Canada. J Toxicol Environ Health A. 2009;72: 1025–9. doi:10.1080/15287390903084264
185. Kelly AC, Mateus-Pinilla NE, Diffendorfer J, Jewell E, Ruiz MO, Killefer J, et al. Prion sequence polymorphisms and chronic wasting disease resistance in Illinois white-tailed deer (*Odocoileus virginianus*). Prion. 2008;2: 28–36. doi:10.4161/pri.2.1.6321
186. Vázquez-Miranda H, Zink RM. Geographic Distribution of Chronic Wasting Disease Resistant Alleles in Nebraska, with Comments on the Evolution of Resistance. J Fish Wildl Manag. 2020;11: 46–55. doi:10.3996/012019-jfwm-002
187. Jewell JE, Conner MM, Wolfe LL, Miller MW, Williams ES. Low frequency of PrP genotype 225SF among free-ranging mule deer (*Odocoileus hemionus*) with chronic wasting disease. J Gen Virol. 2005;86: 2127–2134. doi:10.1099/vir.0.81077-0
188. Brandt AL, Green ML, Ishida Y, Roca AL, Mateus-Pinilla NE, Brandt AL, et al. Influence of the geographic distribution of prion protein gene sequence variation on patterns of chronic wasting disease spread in white-tailed deer (*Odocoileus virginianus*). Prion. 2018;00: 1–12. doi:10.1080/19336896.2018.1474671
189. Haley NJ, Merrett K, Stein AB, Simpson D, Carlson A, Mitchell G, et al. Estimating relative CWD susceptibility and disease progression in farmed white-tailed deer with rare PRNP alleles. Caughey B, editor. PLoS One. 2019;14: e0224342. doi:10.1371/journal.pone.0224342
190. Johnson CJ, Pedersen JA, Chappell RJ, McKenzie D, Aiken JM. Oral transmissibility of prion disease is enhanced by binding to soil particles. PLoS Pathog. 2007;3: 0874–0881. doi:10.1371/journal.ppat.0030093
191. Rourke KIO, Spraker TR, Zhuang D, Greenlee JJ, Gidlewski TE, Hamir AN. Elk with a long incubation prion disease phenotype have a unique PrP d profile. Neuroreport. 2007;18: 5–8.
192. Moore J, Kunkle R, West Greenlee MH, Nicholson E, Richt J, Hamir A, et al. Horizontal transmission of chronic wasting disease in Reindeer. Emerg Infect Dis. 2016;22: 2142–2145. doi:10.3201/eid2212.160635
193. Moore SJ, Vrentas CE, Hwang S, West Greenlee MH, Nicholson EM, Greenlee JJ. Pathologic and biochemical characterization of PrP^{Sc} from elk with PRNP polymorphisms at codon 132 after experimental infection with the chronic wasting disease agent. BMC Vet Res. 2018;14. doi:10.1186/s12917-018-1400-9
194. Cheng YC, Hannaoui S, John TR, Dudas S, Czub S, Gilch S. Early and Non-Invasive Detection of Chronic Wasting Disease Prions in Elk Feces by Real- Time Quaking Induced Conversion. PLoS One. 2016;11: e0166187. doi:10.1371/journal.pone.0166187
195. Monello RJ, Galloway NL, Powers JG, Madsen-Bouterse SA, Edwards WH, Wood ME, et al. Pathogen-mediated selection in free-ranging elk populations infected by chronic wasting disease. Proc Natl Acad Sci. 2017;114: 12208–12212. doi:10.1073/pnas.1707807114
196. Almberg ES, Cross PC, Johnson CJ, Heisey DM, Richards BJ. Modeling routes of chronic wasting disease transmission: environmental prion persistence promotes deer population decline and extinction. PLoS One. 2011;6: e19896. doi:10.1371/journal.pone.0019896
197. Miller MW, Williams ES, McCarty CW, Spraker TR, Kreeger TJ, Larsen CT, et al. Epizootiology of chronic wasting disease in free-ranging cervids in Colorado and Wyoming. J Wildl Dis. 2000;36: 676–690. doi:10.7589/0090-3558-36.4.676
198. Gross JE, Miller MW. Chronic Wasting Disease in Mule Deer: Disease Dynamics and

Control. J Wildl Manage. 2001;65: 205. doi:10.2307/3802899
199. Wasserberg G, Osnas EE, Rolley RE, Samuel MD. Host culling as an adaptive management tool for chronic wasting disease in white-tailed deer: A modelling study. J Appl Ecol. 2009;46: 457–466. doi:10.1111/j.1365-2664.2008.01576.x
200. Jennelle CS, Henaux V, Wasserberg G, Thiagarajan B, Rolley RE, Samuel MD. Transmission of chronic wasting disease in Wisconsin white-tailed deer: Implications for disease spread and management. PLoS One. 2014;9. doi:10.1371/journal.pone.0091043
201. Oraby T, Vasilyeva O, Krewski D, Lutscher F. Modeling seasonal behavior changes and disease transmission with application to chronic wasting disease. J Theor Biol. 2014;340: 50–59. doi:10.1016/j.jtbi.2013.09.003
202. Mateus-Pinilla N, Weng HY, Ruiz MO, Shelton P, Novakofski J. Evaluation of a wild white-tailed deer population management program for controlling chronic wasting disease in Illinois, 2003-2008. Prev Vet Med. 2013;110: 541–548. doi:10.1016/j.prevetmed.2013.03.002
203. Manjerovic MB, Green ML, Mateus-Pinilla N, Novakofski J. The importance of localized culling in stabilizing chronic wasting disease prevalence in white-tailed deer populations. Prev Vet Med. 2014;113: 139–145. doi:10.1016/j.prevetmed.2013.09.011
204. Uehlinger FD, Johnston AC, Bollinger TK, Waldner CL, Johnson AC, Bollinger TK, et al. Systemic review of management strategies to control chronic wasting disease in wild deer populations in North America. Dobson AP, editor. BMC Vet Res. 2016;12: 173. doi:10.1371/journal.pbio.1001970
205. Potapov A, Merrill E, Pybus M, Lewis MA. Chronic Wasting Disease: Transmission Mechanisms and the Possibility of Harvest Management. PLoS One. 2016;11: e0151039. doi:10.1371/journal.pone.0151039
206. Puoti G, Giaccone G, Rossi G, Canciani B, Bugiani O, Tagliavini F. Sporadic Creutzfeldt-Jakob disease: Co-occurrence of different types of PrP(Sc) in the same brain. Neurology. 1999;53: 2173–2176. doi:10.1212/wnl.53.9.2173
207. Haldiman T, Kim C, Cohen Y, Chen W, Blevins J, Qing L, et al. Co-existance of distinct prion types enables confirmational evolution of human. J Biol Chem. 2013;288: 29846–29861. doi:10.1074/jbc.M113.500108
208. Kobayashi A, Iwasaki Y, Takao M, Saito Y, Iwaki T, Qi Z, et al. A Novel Combination of Prion Strain Co-Occurrence in Patients with Sporadic Creutzfeldt-Jakob Disease. Am J Pathol. 2019;189: 1276–1283. doi:10.1016/j.ajpath.2019.02.012
209. Bruce ME, Boyle A, Cousens S, McConnell I, Foster J, Goldman W, et al. Strain characterization of natural sheep scrapie and comparison with BSE. J Gen Virol. 2002;83: 695–704. doi:10.1099/0022-1317-83-3-695
210. Nonno R, Marin-Moreno A, Carlos Espinosa J, Fast C, Van Keulen L, Spiropoulos J, et al. Characterization of goat prions demonstrates geographical variation of scrapie strains in Europe and reveals the composite nature of prion strains. Sci Rep. 2020;10. doi:10.1038/s41598-019-57005-6
211. Barrio T, Filali H, Otero A, Sheleby-Elías J, Marín B, Vidal E, et al. Mixtures of prion substrains in natural scrapie cases revealed by ovinised murine models. Sci Rep. 2020;10: 1–15. doi:10.1038/s41598-020-61977-1
212. Kimberlin RH, Walker CA. Pathogenesis of Scrapie (Strain 263K) in Hamsters Infected lntracerebrally, lntraperitoneally or Intraocularly. J Gen Virol. 1986;67: 255–263.
213. Collinge J. Prion strain mutation and selection. Science (80-). 2010;328: 1111–1112. doi:10.1126/science.1190815
214. Weissmann C, Li J, Mahal SP, Browning S. Prions on the move. EMBO Reports. John

Wiley & Sons, Ltd; 2011. pp. 1109–1117. doi:10.1038/embor.2011.192
215. Collinge J, Clarke AR. A general model of prion strains and their pathogenicity. Science. 2007;318: 930–936. doi:10.1126/science.1138718
216. Baskakov I V. The many shades of prion strain adaptation. Prion. 2014;8: 169–172. doi:10.4161/pri.27836
217. Angers RC, Kang HE, Napier D, Browning S, Seward T, Mathiason C, et al. Prion strain mutation determined by prion protein conformational compatibility and primary structure. Science (80). 2010;328: 1154–1158. doi:10.1126/science.1187107
218. Johnson CJ, Herbst A, Duque-Velasquez C, Vanderloo JP, Bochsler P, Chappell R, et al. Prion protein polymorphisms affect chronic wasting disease progression. PLoS One. 2011;6. doi:10.1371/journal.pone.0017450
219. Duque Velásquez C, Kim C, Herbst A, Daude N, Garza MC, Wille H, et al. Deer Prion Proteins Modulate the Emergence and Adaptation of Chronic Wasting Disease Strains. J Virol. 2015;89: 12362–73. doi:10.1128/JVI.02010-15
220. Meade-White K, Race B, Trifilo M, Bossers A, Favara C, Lacasse R, et al. Resistance to Chronic Wasting Disease in Transgenic Mice Expressing a Naturally Occurring Allelic Variant of Deer Prion Protein. J Virol. 2007;81: 4533–4539. doi:10.1128/JVI.02762-06
221. Herbst A, Velásquez CDCD, Triscott E, Aiken JMJM, McKenzie D. Chronic Wasting Disease Prion Strain Emergence and Host Range Expansion. Emerg Infect Dis. 2017;23: 1598–1600. doi:10.3201/eid2309.161474
222. Hannaoui S, Amidian S, Cheng YC, Duque Velásquez C, Dorosh L, Law S, et al. Destabilizing polymorphism in cervid prion protein hydrophobic core determines prion conformation and conversion efficiency. PLoS Pathog. 2017;13: 1–24. doi:10.1371/journal.ppat.1006553
223. Moore J, Tatum T, Hwang S, Vrentas C, West Greenlee MH, Kong Q, et al. Novel Strain of the Chronic Wasting Disease Agent Isolated From Experimentally Inoculated Elk With LL132 Prion Protein. Sci Rep. 2020;10: 3148. doi:10.1038/s41598-020-59819-1
224. Haley NJ, Mathiason CK, Carver S, Zabel M, Telling GC, Hoover EA. Detection of Chronic Wasting Disease Prions in Salivary, Urinary, and Intestinal Tissues of Deer: Potential Mechanisms of Prion Shedding and Transmission. J Virol. 2011;85: 6309–6318. doi:10.1128/JVI.00425-11
225. Vikøren T, Våge J, Madslien KI, Røed KH, Rolandsen CM, Tran L, et al. First detection of chronic wasting disease in a wild red deer (*Cervus elaphus*) in Europe. J Wildl Dis. 2019;55: 970–972. doi:10.7589/2018-10-262
226. Miller MW, Wild MA, Williams ES. Epidemiology of Chronic Wasting Disease in Captive Rocky Mountain Elk. J Wildl Dis. 1998;34: 532–538. doi:10.7589/0090-3558-34.3.532
227. Kreeger TJ, Montgomery DL, Jewell JE, Schultz W, Williams ES. Oral transmission of chronic wasting disease in captive Shira's moose. J Wildl Dis. 2006;42: 640–645. doi:10.7589/0090-3558-42.3.640
228. Nalls A V., McNulty E, Powers J, Seelig DM, Hoover C, Haley NJ, et al. Mother to Offspring Transmission of Chronic Wasting Disease in Reeves' Muntjac Deer. PLoS One. 2013;8. doi:10.1371/journal.pone.0071844
229. Hamir AN, Greenlee JJ, Nicholson EM, Kunkle RA, Richt JA, Miller JM, et al. Experimental transmission of chronic wasting disease (CWD) from elk andwhite-tailed deer to fallow deer by intracerebral route: Final report. Can J Vet Res. 2011;75: 152–156.
230. Wilson R, Plinston C, Hunter N, Casalone C, Corona C, Tagliavini F, et al. Chronic

wasting disease and atypical forms of bovine spongiform encephalopathy and scrapie are not transmissible to mice expressing wild-type levels of human prion protein. J Gen Virol. 2012;93: 1624–1629. doi:10.1099/vir.0.042507-0
231. Kong Q, Huang S, Zou W, Vanegas D, Wang M, Wu D, et al. Chronic Wasting Disease of Elk: Transmissibility to Humans Examined by Transgenic Mouse Models. J Neurosci. 2005;25: 7944–7949. doi:10.1523/JNEUROSCI.2467-05.2005
232. Sandberg MK, Al-Doujaily H, Sigurdson CJ, Glatzel M, O'Malley C, Powell C, et al. Chronic wasting disease prions are not transmissible to transgenic mice overexpressing human prion protein. J Gen Virol. 2010;91: 2651–2657. doi:10.1099/vir.0.024380-0
233. Tamguney G, Giles K, Bouzamondo-Bernstein E, Bosque PJ, Miller MW, Safar J, et al. Transmission of Elk and Deer Prions to Transgenic Mice. J Virol. 2006;80: 9104–9114. doi:10.1128/JVI.00098-06
234. Kurt TD, Jiang L, Fernández-borges N, Bett C, Liu J, Yang T, et al. Human prion protein sequence elements impede cross-species chronic wasting disease transmission. J Clin Invest. 2015;125: 1485–1496. doi:10.1172/JCI79408.sus
235. Marsh RF, Kincaid AE, Bessen RA, Bartz JC. Interspecies Transmission of Chronic Wasting Disease Prions to Squirrel Monkeys (Saimiri sciureus). J Virol. 2005;79: 13794–13796. doi:10.1128/JVI.79.21.13794
236. Race B, Williams K, Orrú CD, Hughson AG, Lubke L, Chesebro B. Lack of Transmission of Chronic Wasting Disease to Cynomolgus Macaques. Journal of virology. 2018. doi:10.1128/JVI.00550-18
237. Comoy EE, Mikol J, Luccantoni-Freire S, Correia E, Lescoutra-Etchegaray N, Durand V, et al. Transmission of scrapie prions to primate after an extended silent incubation period. Sci Rep. 2015;5: 1–11. doi:10.1038/srep11573
238. Czub S, Schulz-Schaeffer WJ, Stahl-Hennig C, Beekes M, Schaetzl H, Motzkus D. First Evidence of intracranial and peroral transmission of chronic wasting disease (CWD) into Cynomolgus macaques: A work in progress. PRION 2017 CONFERENCE EDINBURGH, SCOTLAND. 2017. p. 23.
239. Raymond GJJ, Bossers A, Raymond LD, O'Rourke KI, McHolland LE, Bryant PK, et al. Evidence of a molecular barrier limiting susceptibility of humans, cattle and sheep to chronic wasting disease. EMBO J. 2000;19: 4425–4430. doi:10.1093/emboj/19.17.4425
240. Barria MA, Telling GC, Gambetti P, Mastrianni JA, Soto C. Generation of a new form of human PrP^{Sc} in vitro by interspecies transmission from cervid prions. J Biol Chem. 2011;286: 7490–7495. doi:10.1074/jbc.M110.198465
241. Barria MA, Libori A, Mitchell G, Head MW. Susceptibility of Human Prion Protein to Conversion by Chronic Wasting Disease Prions. Emerg Infect Dis. 2018;24: 1482–1489. doi:10.3201/eid2408.161888
242. Luers L, Bannach O, Stöhr J, Wördehoff MM, Wolff M, Nagel-Steger L, et al. Seeded Fibrillation as Molecular Basis of the Species Barrier in Human Prion Diseases. PLoS One. 2013;8. doi:10.1371/journal.pone.0072623
243. Barria MA, Balachandran A, Morita M, Kitamoto T, Barron R, Manson J, et al. Molecular barriers to zoonotic transmission of prions. Emerg Infect Dis. 2014;20: 88–97. doi:10.3201/eid2001.130858
244. Bartz JC, Marsh RF, McKenzie DI, Aiken JM. The host range of chronic wasting disease is altered on passage in ferrets. Virology. 1998;251: 297–301. doi:10.1006/viro.1998.9427
245. Moore SJ, West Greenlee MH, Kondru N, Manne S, Smith JD, Kunkle RA, et al. Experimental Transmission of the Chronic Wasting Disease Agent to Swine after Oral or Intracranial Inoculation. J Virol. 2017;91: e00926-17. doi:10.1128/jvi.00926-17

246. Hamir AN, Kunkle R a, Cutlip RC, Miller JM, Williams ES, Richt J a. Transmission of chronic wasting disease of mule deer to Suffolk sheep following intracerebral inoculation. J Vet Diagn Invest. 2006;18: 558–565. doi:10.1177/104063870601800606
247. Hamir AN, Kunkle RA, Cutlip RC, Miller JM, O'Rourke KI, Williams ES, et al. Experimental Transmission of Chronic Wasting Disease Agent from Mule Deer to Cattle by the Intracerebral Route. J Vet Diagnostic Investig. 2005;17: 276–281. doi:10.1177/104063870501700313
248. Hamir AN, Miller JM, Kunkle RA, Hall SM, Richt JA. Susceptibility of Cattle to First-passage Intracerebral Inoculation with Chronic Wasting Disease Agent from White-tailed Deer. Vet Pathol. 2007;44: 487–493. doi:10.1354/vp.44-4-487
249. Greenlee JJ, Nicholson EM, Smith JD, Kunkle RA, Hamir AN. Susceptibility of cattle to the agent of chronic wasting disease from elk after intracranial inoculation. J Vet Diagnostic Investig. 2012;24: 1087–1093. doi:10.1177/1040638712461249
250. Harrington RD, Baszler T V., O'Rourke KI, Schneider DA, Spraker TR, Liggitt HD, et al. A species barrier limits transmission of chronic wasting disease to mink (Mustela vison). J Gen Virol. 2008;89: 1086–1096. doi:10.1099/vir.0.83422-0
251. Moore SJ, Smith JD, Richt JA, Greenlee JJ. Raccoons accumulate PrP Sc after intracranial inoculation of the agents of chronic wasting disease or transmissible mink encephalopathy but not atypical scrapie. J Vet Diagnostic Investig. 2019;31: 200–209. doi:10.1177/1040638718825290
252. Mathiason CK, Nalls A V., Seelig DM, Kraft SL, Carnes K, Anderson KR, et al. Susceptibility of Domestic Cats to Chronic Wasting Disease. J Virol. 2013;87: 1947–1956. doi:10.1128/JVI.02592-12
253. Heisey DM, Mickelsen N a, Schneider JR, Johnson CJ, Johnson CJ, Langenberg J a, et al. Chronic wasting disease (CWD) susceptibility of several North American rodents that are sympatric with cervid CWD epidemics. J Virol. 2010;84: 210–5. doi:10.1128/JVI.00560-09
254. Perrott MR, Sigurdson CJ, Mason GL, Hoover EA. Evidence for distinct chronic wasting disease (CWD) strains in experimental CWD in ferrets. J Gen Virol. 2012;93: 212–221. doi:10.1099/vir.0.035006-0
255. Raymond GJ, Raymond LD, Meade-White KD, Hughson AG, Favara C, Gardner D, et al. Transmission and adaptation of chronic wasting disease to hamsters and transgenic mice: evidence for strains. J Virol. 2007;81: 4305–14. doi:10.1128/JVI.02474-06
256. Selariu A, Powers JG, Nalls A, Brandhuber M, Mayfield A, Fullaway S, et al. In utero transmission and tissue distribution of chronic wasting disease-associated prions in free-ranging Rocky Mountain elk. J Gen Virol. 2015;96: 3444–3455. doi:10.1099/jgv.0.000281
257. Joly DO, Samuel MD, Langenberg JA, Blanchong JA, Batha CA, Rolley RE, et al. Spatial epidemiology of chronic wasting disease in Wisconsin white-tailed deer. J Wildl Dis. 2006;42: 578–588. doi:10.7589/0090-3558-42.3.578
258. Garlick MJ, Powell JA, Hooten MB, MacFarlane LR. Homogenization, sex, and differential motility predict spread of chronic wasting disease in mule deer in southern Utah. J Math Biol. 2014;69: 369–399. doi:10.1007/s00285-013-0709-z
259. Walter WD, Baasch DM, Hygnstrom SE, Trindle BD, Tyre AJ, Millspaugh JJ, et al. Space use of sympatric deer in a riparian ecosystem in an area where chronic wasting disease is endemic. Wildlife Biol. 2011;17: 191–209. doi:10.2981/10-055
260. Evans TS, Kirchgessner MS, Eyler B, Ryan CW, Walter WD. Habitat influences distribution of chronic wasting disease in white-tailed deer. J Wildl Manage. 2015;80: 284–291. doi:10.1002/jwmg.1004
261. Nobert BR, Merrill EH, Pybus MJ, Bollinger TK, Hwang Y Ten. Landscape

connectivity predicts chronic wasting disease risk in Canada. J Appl Ecol. 2016 [cited 16 Apr 2016]. doi:10.1111/1365-2664.12677
262. Kelly AC, Mateus-Pinilla NE, Douglas M, Douglas M, Brown W, Ruiz MO, et al. Utilizing disease surveillance to examine gene flow and dispersal in white-tailed deer. J Appl Ecol. 2010;47: 1189–1198. doi:10.1111/j.1365-2664.2010.01868.x
263. Robinson SJ, Samuel MD, Rolley RE, Shelton P. Using landscape epidemiological models to understand the distribution of chronic wasting disease in the Midwestern USA. Landsc Ecol. 2013;28: 1923–1935. doi:10.1007/s10980-013-9919-4
264. Farnsworth ML, Wolfe LL, Hobbs NT, Burnham KP, Williams ES, Theobald DM, et al. Human Land Use Influences Chronic Wasting Disease Prevalence in Mule Deer. Ecol Appl. 2005;15: 119–126. doi:10.1890/04-0194
265. Storm DJ, Samuel MMD, Rolley RE, Shelton P, Keuler NS, Richards BJ, et al. Deer density and disease prevalence influence transmission of chronic wasting disease in white-tailed deer. Ecosphere. 2013;4. doi:10.1890/ES-12-00141.1
266. Rees EE, Merrill EH, Bollinger TK, Hwang Y Ten, Pybus MJ, Coltman DW. Targeting the detection of chronic wasting disease using the hunter harvest during early phases of an outbreak in Saskatchewan, Canada. Prev Vet Med. 2012;104: 149–159. doi:10.1016/j.prevetmed.2011.10.016
267. Osnas EE, Heisey DM, Rolley RE, Samuel MD. Spatial and temporal patterns of chronic wasting disease: Fine-scale mapping of a wildlife epidemic in Wisconsin. Ecol Appl. 2009;19: 1311–1322. doi:10.1890/08-0578.1
268. Habib TJ, Merrill EH, Pybus MJ, Coltman DW. Modelling landscape effects on density-contact rate relationships of deer in eastern Alberta: Implications for chronic wasting disease. Ecol Modell. 2011;222: 2722–2732. doi:10.1016/j.ecolmodel.2011.05.007
269. OYER AM, MATHEWS NE, SKULDT LH. Long-Distance Movement of a White-Tailed Deer Away From a Chronic Wasting Disease Area. J Wildl Manage. 2007;71: 1635–1638. doi:10.2193/2006-381
270. Grear DA, Samuel MD, Scribner KT, Weckworth B V., Langenberg JA. Influence of genetic relatedness and spatial proximity on chronic wasting disease infection among female white-tailed deer. J Appl Ecol. 2010;47: 532–540. doi:10.1111/j.1365-2664.2010.01813.x
271. Cullingham CI, Nakada SM, Merrill EH, Bollinger TK, Pybus MJ, Coltman DW. Multiscale population genetic analysis of mule deer (*Odocoileus hemionus hemionus*) in western Canada sheds new light on the spread of chronic wasting disease. Can J Zool. 2011;89: 134–147. doi:10.1139/Z10-104
272. Cullingham CI, Merrill EH, Pybus MJ, Bollinger TK, Wilson GA, Coltman DW. Broad and fine-scale genetic analysis of white-tailed deer populations: Estimating the relative risk of chronic wasting disease spread. Evol Appl. 2011;4: 116–131. doi:10.1111/j.1752-4571.2010.00142.x
273. Grear D a, Samuel MD, Langenberg J a, Keane DP. Demographic patterns and harvest vulnerability of chronic wasting disease infected white-tailed deer in Wisconsin. J Wildl Manage. 2006;70: 546–553. doi:http://dx.doi.org/10.2193/0022-541X(2006)70[546:DPAHVO]2.0.CO;2
274. Lang KR, Blanchong JA. Population genetic structure of white-tailed deer: Understanding risk of chronic wasting disease spread. J Wildl Manage. 2012;76: 832–840. doi:10.1002/jwmg.292
275. Blanchong J a, Samuel MD, Scribner KT, Weckworth B V, Langenberg J a, Filcek KB. Landscape genetics and the spatial distribution of chronic wasting disease. Biol Lett. 2008;4: 130–133. doi:10.1098/rsbl.2007.0523

276. Miller MW, Conner MM. Epidemiology of chronic wasting disease in free-ranging mule deer: spatial, temporal, and demographic influences on observed prevalence patterns. J Wildl Dis. 2005;41: 275–290. doi:10.7589/0090-3558-41.2.275
277. Samuel MD, Storm DJ. Chronic wasting disease in white-tailed deer: Infection, mortality, and implications for heterogeneous transmission. Ecology. 2016;97: 3195–3205. doi:10.1002/ecy.1538
278. Henderson DM, Davenport KA, Haley NJ, Denkers ND, Mathiason CK, Hoover EA. Quantitative assessment of prion infectivity in tissues and body fluids by real-time quaking-induced conversion. J Gen Virol. 2015;96: 210–219. doi:10.1099/vir.0.069906-0
279. John TR, Schätzl HM, Gilch S. Early detection of chronic wasting disease prions in urine of pre-symptomatic deer by real-time quaking-induced conversion assay. Prion. 2013;7: 253–8. doi:10.4161/pri.24430
280. Davenport KA, Mosher BA, Brost BM, Henderson DM, Denkers ND, Nalls A V., et al. Assessment of chronic wasting disease prion shedding in deer saliva with occupancy modeling. J Clin Microbiol. 2018;56: 1–14. doi:10.1128/JCM.01243-17
281. Denkers ND, Hoover CE, Davenport KA, Henderson DM, McNulty EE, Nalls A V., et al. Very low oral exposure to prions of brain or saliva origin can transmit chronic wasting disease. Caughey B, editor. PLoS One. 2020;15: e0237410. doi:10.1371/journal.pone.0237410
282. Angers RC, Seward TS, Napier D, Green M, Hoover E, Spraker T, et al. Chronic Wasting Disease Prions in Elk Antler Velvet. Emerg Infect Dis. 2009;15: 696–703. doi:10.3201/eid1505.081458
283. Miller MW, Williams ES, Hobbs NT, Wolfe LL. Environmental sources of prion transmission in mule deer. Emerg Infect Dis. 2004;10: 1003–1006. doi:10.3201/eid1006.040010
284. Georgsson G, Sigurdarson S, Brown P. Infectious agent of sheep scrapie may persist in the environment for at least 16 years. J Gen Virol. 2006;87: 3737–3740. doi:10.1099/vir.0.82011-0
285. Brown P, Gajdusek DC. Survival of scrapie virus after three years interment Brown 1991. Lancet. 1991;337: 269–270.
286. Konold T, Hawkins SAC, Thurston LC, Maddison BC, Gough KC, Duarte A, et al. Objects in Contact with Classical Scrapie Sheep Act as a Reservoir for Scrapie Transmission. Front Vet Sci. 2015;2: 1–7. doi:10.3389/fvets.2015.00032
287. Plummer IH, Johnson CJ, Chesney AR, Pedersen JA, Samuel D. Mineral licks as environmental reservoirs of chronic wasting disease prions. PLoS One. 2018;13: e0196745. doi:10.1371/journal.pone.0196745
288. Hugh-Jones M, Blackburn J. The ecology of Bacillus anthracis. Mol Aspects Med. 2009;30: 356–367. doi:10.1016/j.mam.2009.08.003
289. Turner WC, Kausrud KL, Beyer W, Easterday WR, Barandongo ZR, Blaschke E, et al. Lethal exposure: An integrated approach to pathogen transmission via environmental reservoirs. Sci Rep. 2016;6: 27311. doi:10.1038/srep27311
290. Johnson CJ, Phillips KE, Schramm PT, McKenzie D, Aiken JM, Pedersen JA. Prions adhere to soil minerals and remain infectious. PLoS Pathog. 2006;2: 296–302. doi:10.1111/j.1745-5871.2006.00403.x
291. Maddison BC, Owen JP, Bishop K, Shaw G, Rees HC, Gough KC. The interaction of ruminant PrP^{Sc} with soils is influenced by prion source and soil type. Environ Sci Technol. 2010;44: 8503–8508. doi:10.1021/es101591a
292. Saunders SE, Bartz JC, Bartelt-Hunt SL. Soil-mediated prion transmission: Is local soil-type a key determinant of prion disease incidence? Chemosphere. 2012;87: 661–

667. doi:10.1016/j.chemosphere.2011.12.076
293. Dorak SJ, Green ML, Wander MM, Ruiz MO, Buhnerkempe MG, Tian T, et al. Clay content and pH: Soil characteristic associations with the persistent presence of chronic wasting disease in northern Illinois. Sci Rep. 2017;7. doi:10.1038/s41598-017-18321-x
294. O'Hara Ruiz M, Kelly AC, Brown WM, Novakofski JE, Mateus-Pinilla NE. Influence of landscape factors and management decisions on spatial and temporal patterns of the transmission of chronic wasting disease transmission in white-tailed deer. Geospat Heal. 2013;8: 215–227. doi:10.4081/gh.2013.68
295. Green ML, Manjerovic MB, Mateus-Pinilla N, Novakofski J. Genetic assignment tests reveal dispersal of white-tailed deer: implications for chronic wasting disease. J Mammal. 2014;95: 646–654. doi:10.1644/13-MAMM-A-167
296. Russo F, Johnson CJ, Johnson CJ, McKenzie D, Aiken JM, Pedersen JA. Pathogenic prion protein is degraded by a manganese oxide mineral found in soils. J Gen Virol. 2009;90: 275–280. doi:10.1099/vir.0.003251-0
297. Kuznetsova A, Cullingham C, McKenzie D, Aiken JJM. Soil humic acids degrade CWD prions and reduce infectivity. Bartz JC, editor. PLOS Pathog. 2018;14: e1007414. doi:10.1371/journal.ppat.1007414
298. Smith CB, Booth CJ, Wadzinski TJ, Legname G, Chappell R, Johnson CJ, et al. Humic substances interfere with detection of pathogenic prion protein. Soil Biol Biochem. 2014;68: 309–316. doi:10.1016/j.soilbio.2013.10.005
299. Giachin G, Narkiewicz J, Scaini D, Ngoc AT, Margon A, Sequi P, et al. Prion protein interaction with soil humic substances: Environmental implications. Johnson CJ, editor. PLoS One. 2014;9: e100016. doi:10.1371/journal.pone.0100016
300. Yuan Q, Telling G, Bartelt-Hunt SL, Bartz JC. Dehydration of prions on environmentally relevant surfaces protects them from inactivation by freezing and thawing. J Virol. 2018;92: JVI.02191-17. doi:10.1128/JVI.02191-17
301. Johnson CJ, Bennett JP, Biro SM, Duque-Velasquez JC, Rodriguez CM, Bessen RA, et al. Degradation of the disease-associated prion protein by a serine protease from lichens. PLoS One. 2011;6. doi:10.1371/journal.pone.0019836
302. Pritzkow S, Morales R, Moda F, Khan U, Telling GC, Hoover E, et al. Grass Plants Bind, Retain, Uptake, and Transport Infectious Prions. Cell Rep. 2015;11: 1168–1175. doi:10.1016/j.celrep.2015.04.036
303. Hirneisen KA, Sharma M, Kniel KE. Human Enteric Pathogen Internalization by Root Uptake into Food Crops. Foodborne Pathog Dis. 2012;9: 396–405. doi:10.1089/fpd.2011.1044
304. Rasmussen J, Gilroyed BH, Reuter T, Dudas S, Neumann NF, Balachandran A, et al. Can plants serve as a vector for prions causing chronic wasting disease? Prion. 2014;8: 136–142. doi:10.4161/pri.27963
305. Pritzkow S, Morales R, Lyon A, Concha-Marambio L, Urayama A, Soto C. Efficient prion disease transmission through common environmental materials. J Biol Chem. 2018;293: 3363–3373. doi:10.1074/jbc.M117.810747
306. Secker TJ, Hervé R, Keevil CW, Dancer SJ. Adsorption of prion and tissue proteins to surgical stainless steel surfaces and the efficacy of decontamination following dry and wet storage conditions. J Hosp Infect. 2011;78: 251–255. doi:10.1016/j.jhin.2011.03.021
307. Jetter R, Schäffer S. Chemical composition of the Prunus laurocerasus leaf surface. Dynamic changes of the epicuticular wax film during leaf development. Plant Physiol. 2001;126: 1725–1737. doi:10.1104/pp.126.4.1725
308. España L, Heredia-Guerrero JA, Segado P, Benítez JJ, Heredia A, Domínguez E. Biomechanical properties of the tomato (Solanum lycopersicum) fruit cuticle during

development are modulated by changes in the relative amounts of its components. New Phytol. 2014;202: 790–802. doi:10.1111/nph.12727
309. Tranquada GC, Victor JJ, Erb U. Early Season Development of Micro/Nano-Morphology and Superhydrophobic Wetting Properties on Aspen Leaf Surfaces. Am J Plant Sci. 2015;06: 2197–2208. doi:10.4236/ajps.2015.613222
310. Wang H, Shi H, Li Y, Yu Y, Zhang J. Seasonal variations in leaf capturing of particulate matter, surface wettability and micromorphology in urban tree species. Front Environ Sci Technol. 2013;7: 1–10. doi:10.1007/s11783-013-0524-1
311. Kosma DK, Bourdenx B, Bernard A, Parsons EP, Lu S, Joubes J, et al. The Impact of Water Deficiency on Leaf Cuticle Lipids of Arabidopsis. Plant Physiol. 2009;151: 1918–1929. doi:10.1104/pp.109.141911
312. Silva Fernandes. Studies on plant cuticle: VIII. Surface waxes in relation to water-repellency. Ann Appl Biol. 1965;56: 297–304. doi:10.1111/j.1744-7348.1965.tb01239.x
313. Boize L, Budin C, Purdue G. The influence of leaf surface roughness on the spreading of oil spray drops. Ann Appl Biol. 1976;84: 205–211. doi:10.1111/j.1744-7348.1976.tb01749.x
314. Wagner P, Fürstner R, Barthlott W, Neinhuis C. Quantitative assessment to the structural basis of water repellency in natural and technical surfaces. J Exp Bot. 2003;54: 1295–1303. doi:10.1093/jxb/erg127
315. Barthlott W, Neinhuis C. Purity of the sacred lotus, or escape from contamination in biological surfaces. Planta. 1997;202: 1–8. doi:10.1007/s004250050096
316. Neinhuis C, Barthlott W. Seasonal changes of leaf surface contamination in beech , oak , and ginkgo in relation to leaf micromorphology and wvettabiity. New Phytol. 1998;138: 91–98.
317. Knoll D, Schreiber L. Plant-microbe interactions: Wetting of ivy (Hedera helix L.) leaf surfaces in relation to colonization by epiphytic microorganisms. Microb Ecol. 2000;40: 33–42. doi:10.1007/s002480000012
318. Velásquez CD, Kim C, Haldiman T, Kim C, Herbst A, Aiken J, et al. Chronic wasting disease (CWD) prion strains evolve via adaptive diversification of conformers in hosts expressing prion protein polymorphisms. J Biol Chem. 2020;295: 4985–5001. doi:10.1074/jbc.RA120.012546
319. Pirisinu L, Tran L, Chiappini B, Vanni I, Di Bari MA, Vaccari G, et al. Novel type of chronic wasting disease detected in moose (Alces alces), Norway. Emerg Infect Dis. 2018;24: 2210–2218. doi:10.3201/eid2412.180702
320. Prusiner SB, Lipton HL. Molecular biology and transgenetics of prion diseases. Crit Rev Biochem Mol Biol. 1991;26: 397–438. doi:10.3109/10409239109086789
321. Kurt TD, Jiang L, Bett C, Eisenberg D, Sigurdson CJ. A proposed mechanism for the promotion of prion conversion involving a strictly conserved tyrosine residue in the α2- β2 loop of PrP^{C}. J Biol Chem. 2014;289: 10660–10667. doi:10.1074/jbc.M114.549030
322. Moore RC, Hope J, McBride PA, McConnell I, Selfridge J, Melton DW, et al. Mice with gene targetted prion protein alterations show that Prnp, Sinc and Prni are congruent. Nat Genet. 1998;18: 118–125. doi:10.1038/ng0298-118
323. Supattapone S, Muramoto T, Legname G, Mehlhorn I, Cohen FE, DeArmond SJ, et al. Identification of Two Prion Protein Regions That Modify Scrapie Incubation Time. J Virol. 2001;75: 1408–1413. doi:10.1128/jvi.75.3.1408-1413.2001
324. Hsiao K, Baker HF, Crow TJ, Poulter M, Owen F, Terwilliger JD, et al. Linkage of a prion protein missense variant to Gerstmann-Sträussler syndrome. Nature. 1989;338: 342–345. doi:10.1038/338342a0

325. Kitamoto T, Amano N, Terao Y, Nakazato Y, Isshiki T, Mizutani T, et al. A new inherited prion disease (PrP-P105L mutation) showing spastic paraparesis. Ann Neurol. 1993;34: 808–813. doi:10.1002/ana.410340609
326. Apostol MI, Sawaya MR, Cascio D, Eisenberg D. Crystallographic studies of prion protein (PrP) segments suggest how structural changes encoded by polymorphism at residue 129 modulate susceptibility to human prion disease. J Biol Chem. 2010;285: 29671–29675. doi:10.1074/jbc.C110.158303
327. Hosszu LLP, Jackson GS, Trevitt CR, Jones S, Batchelor M, Bhelt D, et al. The residue 129 polymorphism in human prion protein does not confer susceptibility to Creutzfeldt-Jakob disease by altering the structure or global stability of PrP^{C}. J Biol Chem. 2004;279: 28515–28521. doi:10.1074/jbc.M313762200
328. Hosszu LLP, Conners R, Sangar D, Batchelor M, Sawyer EB, Fisher S, et al. Structural effects of the highly protective V127 polymorphism on human prion protein. Commun Biol. 2020;3. doi:10.1038/s42003-020-01126-6
329. Cortez LM, Kumar J, Renault L, Young HS, Sim VL. Mouse prion protein polymorphism Phe-108/Val-189 affects the kinetics of fibril formation and the response to seeding: Evidence for a Two-Step Nucleation polymerization mechanism. J Biol Chem. 2013;288: 4772–4781. doi:10.1074/jbc.M112.414581
330. Kraus A, Anson KJ, Raymond LD, Martens C, Groveman BR, Dorward DW, et al. Prion protein prolines 102 and 105 and the surrounding lysine cluster impede amyloid formation. J Biol Chem. 2015;290: 21510–21522. doi:10.1074/jbc.M115.665844
331. Morin LP, Wood RI. A Stereotaxic Atlas of the Golden Hamster. 2001.
332. Bessen RA, Robinson CJ, Seelig DM, Watschke CP, Lowe D, Shearin H, et al. Transmission of chronic wasting disease identifies a prion strain causing cachexia and heart infection in hamsters. PLoS One. 2011;6. doi:10.1371/journal.pone.0028026
333. Eckland TE, Shikiya RA, Bartz JC. Independent amplification of co-infected long incubation period low conversion efficiency prion strains. PLoS Pathog. 2018;14: e1007323. doi:10.1371/journal.ppat.1007323
334. Gerhauser I, Wohlsein P, Ernst H, Germann PG, Baumgärtner W. Vacuolation and mineralisation as dominant age-related findings in hamster brains. Exp Toxicol Pathol. 2013;65: 375–381. doi:10.1016/j.etp.2011.12.001
335. Cavanagh JB. Lesion localisation: Implications for the study of functional effects and mechanisms of action. Toxicology. 1988;49: 131–136. doi:10.1016/0300-483X(88)90184-9
336. Wohlsein P, Deschl U, Baumgärtner W. Nonlesions, Unusual Cell Types, and Postmortem Artifacts in the Central Nervous System of Domestic Animals. Vet Pathol. 2013;50: 122–143. doi:10.1177/0300985812450719
337. Ligios C, Jeffrey M, Ryder SJ, Bellworthy SJ, Simmons MM. Distinction of scrapie phenotypes in sheep by lesion profiling. J Comp Pathol. 2002;127: 45–57. doi:10.1053/jcpa.2002.0589
338. Crowell J, Hughson A, Caughey B, Bessen RA. Host Determinants of Prion Strain Diversity Independent of Prion Protein Genotype. J Virol. 2015;89: 10427–10441. doi:10.1128/JVI.01586-15
339. Hannaoui S, Schatzl HM, Gilch S. Chronic wasting disease: Emerging prions and their potential risk. PLoS Pathogens. 2017. p. e1006619. doi:10.1371/journal.ppat.1006619
340. Kimberlin RH, Walker CA, Fraser H. The genomic identity of different strains of mouse scrapie is expressed in hamsters and preserved on reisolation in mice. J Gen Virol. 1989;70: 2017–2025. doi:10.1099/0022-1317-70-8-2017
341. Bruce ME, Fraser H. Effect of route of infection on the frequency and distribution of cerebral amyloid plaques in scrapie mice. Neuropathol Appl Neurobiol. 1981;7: 289–

298. doi:10.1111/j.1365-2990.1981.tb00100.x
342. Bruce M, Chree A, McConnell I, Foster J, Pearson G, Fraser H, et al. Transmission of bovine spongiform encephalopathy and scrapie to mice: strain variation and the species barrier. Philos Trans R Soc Lond B Biol Sci. 1994;343: 405–411. doi:10.1098/rstb.1994.0036
343. Fraser H, Bruce M, Chree A, McConnell I, Wells GAH. Transmission of bovine spongiform encephalopathy and scrapie to mice. J Gen Virol. 1992;73: 1891–1897. doi:10.1098/rstb.1994.0036
344. Moore SJ, Vrentas CE, Hwang S, West Greenlee MH, Nicholson EM, Greenlee JJ, et al. Pathologic and biochemical characterization of PrP Sc from elk with PRNP polymorphisms at codon 132 after experimental infection with the chronic wasting disease agent. BMC Vet Res. 2018;14. doi:10.1186/s12917-018-1400-9
345. Cheng YC, Hannaoui S, John TR, Dudas S, Czub S, Gilch S. Real-time quaking-induced conversion assay for detection of cwd prions in fecal material. J Vis Exp. 2017;2017: 56373. doi:10.3791/56373
346. Maddison BC, Raes HC, Baker CA, Taema M, Bellworthy SJ, Thorne L, et al. Prions are secreted into the oral cavity in sheep with preclinical scrapie. J Infect Dis. 2010;201: 1672–1676. doi:10.1086/652457
347. Pattison IH, Hoare MN, Jebbett JN, Watson WA. Spread of scrapie to sheep and goats by oral dosing with foetal membranes from scrapie-affected sheep. Vet Rec. 1972;90: 465–468. doi:10.1136/vr.90.17.465
348. Béringue V, Herzog L, Jaumain E, Reine F, Sibille P, Le Dur A, et al. Facilitated cross-species transmission of prions in extraneural tissue. Science (80-). 2012;335: 472–475. doi:10.1126/science.1215659
349. Mitchell GB, Sigurdson CJ, O'Rourke KI, Algire J, Harrington NP, Walther I, et al. Experimental oral transmission of chronic wasting disease to reindeer (*Rangifer tarandus tarandus*). Kincaid AE, editor. PLoS One. 2012;7: e39055. doi:10.1371/journal.pone.0039055
350. Waddell L, Greig J, Mascarenhas M, Otten A, Corrin T, Hierlihy K. Current evidence on the transmissibility of chronic wasting disease prions to humans-A systematic review. Transbound Emerg Dis. 2017; 1–13. doi:10.1111/tbed.12612
351. Sohn HJ, Park KJ, Roh IS, Kim HJ, Park HC, Kang HE. Sodium hydroxide treatment effectively inhibits PrP^{CWD} replication in farm soil. Prion. 2019;13: 137–140. doi:10.1080/19336896.2019.1617623
352. CWD Update 121. 2018. Available: www.agfc.com/cwd
353. Rieger S. Critics warn of "totally unacceptable" risk to humans after meat from 21 tainted elk herds enters food supply | CBC News. In: CBC News [Internet]. 2019 [cited 1 Oct 2020]. Available: https://www.cbc.ca/news/canada/calgary/ elk-contaminated-chronic-wasting-disease-cwd-1.5247570
354. Bittel J. A deadly deer disease is spreading. Could it strike people, too? - The Washington Post. In: The Washington Post [Internet]. 2019 [cited 1 Oct 2020]. Available: https://www.washingtonpost.com/science/2019/06/14/deadly-deer-disease-is-spreading-could-it-strike-people-too/
355. Lowrie M. Health experts warn public over deer meat from diseased herd in Quebec allowed into food system. In: The Globe and Mail [Internet]. 2019 [cited 1 Oct 2020]. Available: https://www.theglobeandmail.com/canada/article-health-experts-sound-the-alarm-after-deer-meat-from-diseased-herd-in/
356. Henderson DM, Tennant JM, Haley NJ, Denkers ND, Mathiason CK, Hoover EA. Detection of chronic wasting disease prion seeding activity in deer and elk feces by real-time quaking-induced conversion. J Gen Virol. 2017;98: 1953–1962.

doi:10.1099/jgv.0.000844
357. Lee IS, Long JR, Prusiner SB, Safar JG. Selective precipitation of prions by polyoxometalate complexes. J Am Chem Soc. 2005;127: 13802–13803. doi:10.1021/ja055219y
358. Davenport KA, Hoover CE, Denkers ND, Mathiason CK, Hoover EA. Modified protein misfolding cyclic amplification overcomes real-time quaking-induced conversion assay inhibitors in deer saliva to detect chronic wasting disease prions. J Clin Microbiol. 2018;56. doi:10.1128/JCM.00947-18
359. Wang W, Tai F, Chen S. Optimizing protein extraction from plant tissues for enhanced proteomics analysis. J Sep Sci. 2008;31: 2032–2039. doi:10.1002/jssc.200800087
360. Pierpoint WS. The extraction of enzymes from plant tissues rich in phenolic compounds. Methods Mol Biol. 2004;244: 65–74. doi:10.1385/1-59259-655-x:65
361. Vergara-Barberán M, Lerma-García MJ, Herrero-Martínez JM, Simó-Alfonso EF. Analytical Methods Use of an enzyme-assisted method to improve protein extraction from olive leaves. 2014 [cited 22 Nov 2020]. doi:10.1016/j.foodchem.2014.07.116
362. Isaacson T, Damasceno CM, Saravanan RS, He Y, Catalá C, Saladié M, et al. Sample extraction techniques for enhanced proteomic analysis of plant tissues. 2006 [cited 22 Nov 2020]. doi:10.1038/nprot.2006.102
363. Thomas DC, Edmonds EJ, Brown WK. The diet of woodland caribou populations in west-central Alberta. Rangifer. 1996;Special is: 337–342. doi:10.7557/2.16.4.1275
364. Fenton F. Lichens as indicators of atmospheric pollution. Irish Nat J. 1960;13: 153–159. doi:10.1163/22244662-bja10016
365. Conti ME, Cecchetti G. Biological monitoring: lichens as bioindicators of air pollution assessment - A review. Environmental Pollution. 2001. pp. 471–492. doi:10.1016/S0269-7491(00)00224-4
366. Pirisinu L, di Bari M, Marcon S, Vaccari G, D'Agostino C, Fazzi P, et al. A new method for the characterization of strain-specific conformational stability of protease-sensitive and protease-resistant PrP^{Sc}. PLoS One. 2010;5: 1–13. doi:10.1371/journal.pone.0012723
367. Baeten LA, Powers BE, Jewell JE, Spraker TR, Miller MW. A natural case of chronic wasting disease in a free-ranging moose (Alces alces shirasi). J Wildl Dis. 2007;43: 309–314. doi:10.7589/0090-3558-43.2.309

Appendices

Appendix 1. Lab grown Yarrow and Wheatgrass

Use Sunblaster growth system on a capillary mat. Lights set to long day conditions (18hr on, 6hr off). Seeds obtained from West Coast Seeds (SKU#SS112 and FL3825)

1. Germinate seeds (see below).

2. Gently remove seedlings from the paper towel and place on top of moist potted soil. Cover with cling wrap and tape closed. Leave under grow lights and keep well watered.

3. Place seedlings on top of moist potting soil and cover with cling wrap and tape closed. Leave under grow light and keep well watered.

4. Wait until plants are established and remove cling film. Remove excess seedlings.

How to germinate western yarrow (*Achillea millefolium var. occidentalis)*:

1. Place seeds (well spaced) on a moistened folded paper towel and place in a square dish. Parafilm dish closed and place it under grow lights. Proceed to step two after around 6 days, when two seed leaves clearly visible in majority of seeds

How to germinate hard red wheat (*Triticum aestivum)*:

1. Soak seeds overnight in water, then drain. Repeat. Once seed has begun to sprout (white root starts becoming visible), proceed to step two.

Appendix 2. PK digestion procedure

1. In total volume of 66.5 µL, add 10 µL brain homogenate or enough to make 100 µg protein, with the rest RIPA buffer (50mM Tris Base, 150mM NaCl, 1mM EDTA, 1% CA-360, 0.25% Na-deoxycholate).

2. Add 3.5 µL of 1mg/mL proteinase K (Roche #0.115887001).

3. Spin down, then lightly vortex. Incubate for 45 minutes at 37°C, 1350rpm.

4. End by adding 70 µL 5x Laemelli sample buffer (0.75 M Tris-Cl pH 6.8, 0.5% Bromophenol blue, 25% v/v glycerol, 5% w/v SDS, 12.5% v/v β-mercaptoethanol) and boiling for 10 minutes. Leave overnight at 4°C, spinning down condensation before use.

Appendix 3. PNGase f deglycosylation procedure

1. Performed following PK digest using deglycosylation kit (New England Biolabs #P074S).

2. Set up PK digest of 100 µg brain homogenate as in Appendix 2. Stop reaction with 2 µL PMSF.

3. 10 µL of PK reaction, 8 µL water, 2 µL of Denaturing buffer and boil for 10 minutes.

4. Spin down. Add 4 µL NP-40, 4 µL Glycobuffer 2, 8 µL mqH_2O, and 4 µL PNGase f.

5. Spin down. Incubate 3 hours at 37°C, 1350rpm.

6. Boil in 40 µL 5X Laemmli buffer to end reaction. Leave overnight at 4°C, spinning down condensation before use.

Appendix 4. Immunoblot procedure

1. Place 12 or 15 well 12% pre-pored NuPAGE 12% Bis-Tris SDS-PAGE protein gels (Invitrogen #NP0343) into the gel system. Add 800 mL of 1x MOPS (50mM MOPS, 50mM Tris base, 0.35mM SDS, 1.03mM EDTA) to the middle of the gel box, fill area between gels to the top, outside just underneath the well bottom.

2. Load samples (1:1 sample: 5X Laemmli sample buffer). For most samples, load between 6-8 µL sample.

3. Add 500 µL of 200X Antioxidant (1M Sodium bisulfite) to the area between the gels.

4. Run at 70V for 20 minutes, then 110-115V for approximately 2.5 hours, or until the blue is almost run out of the gel.

5. Assemble transfer sandwich, using 1X Transfer buffer with 10% methanol (10X transfer buffer: 190 mM Glycine, 24.5mM Tris base) using Immobilon-P PVDF membranes (Fisher Scientific #IPVH), being careful to avoid bubbles.

6. Run transfer at 35V for 1.5 hours. Make 5% skim milk by adding 50mL 1X TBS with 0.1 1% Tween-20 (10X TBS: 1.5M NaCl, 0.5M Tris, pH 7.4) and leave to mix during transfer.

7. Block membrane in milk for 45 minutes. Add antibody and leave at 4°C overnight.

8. Rinse membrane three times for four minutes in TBS-0.1% Tween 20 on the back and forth shaker, then leave in 10-15mL milk with 1:10 000 Goat Anti-mouse IgG (H+L) conjugated to HRP (Bio-Rad #170-6516) antibody for at least 1.5 hours.

9. Rinse membrane three times for four minutes. Leave last rinse in while you set up the development cassette and ECL Western Blotting substrate (Fisher Scientific #PI32106).

10. Leave membrane in a dish upside down to drain TBS-T. Mix 500 µL ECL reagent 1 to the same amount of ECL 2. Carefully cover the membrane with ECL and leave 1 minute, and then shake off additional fluid. Lay membrane between plastic sheet and close cassette. Note: make sure no ECL comes into contact with film.

11. Develop by exposing film (Super RX-N Fuji Medical X-Ray Film 100NIF; Fujifilm #47410 19291) in the dark room, then submerging in developer, rinsing, and then submerging in fixer. Wash off the fixer and hang to dry.

Appendix 5. Generalized Plant-prion interaction assay

1. Add 0.03g of plant material to 1.5mL microfuge tube in triplicate.
2. Add 10 µL of 2.5% clarified brain homogenate (varies between type of brain homogenate) directly on the plant surface. Lightly vortex to distribute.
3. Leave overnight at 4°C.
4. Incubate 10 minutes in 200 µL mqH_2O at 1350rpm.
5. Remove water to a new tube, spinning down tubes to collect as much as possible.
6. Freeze rinse and vegetation at -30°C until needed
7. TCA precipitate rinse ('unbound').
8. Add 200 µL 1% Triton X-100 in mqH_2O and boil for 10 minutes.
9. Remove detergent and add to a new tube ('bound').
10. TCA precipitate.

Note: Do not start TCA precipitation if you're not planning on doing the prep on the same day. Other detergents, such as SDS, can interfere with TCA precipitation, in this case you can perform a methanol precipitation.

Appendix 6. TCA/acetone precipitation

1. Add 30 µL 100% TCA in mqH_2O to 200 µL unbound or bound sample (13% final concentration). Incubate overnight at 4°C. Alternatively, for the same day precipitation incubate the samples for 5 minutes at -20°C, then 15 minutes at 4°C. Do not leave at -20°C until frozen, as this interferes with the precipitation.
2. Centrifuge on high for 15 minutes, carefully discard supernatant (large pellets may slip out).
3. Resuspend in 100 µL ice cold acetone and incubate on ice for 15 minutes.
4. Centrifuge on high for 10 minutes. Repeat step 2 and 3 twice.
5. Remove supernatant and let dry by leaving caps off in the chemical hood (maybe 10 minutes)
6. Resuspend in 20 µL of 2.5X Laemmli sample buffer and boil for 10 minutes. Run immunoblot immediately or leave at 4°C overnight.

Note: if the sample buffer changes to yellow, TCA was not completely washed out. Make more basic by dipping the tip in 2N NaOH, then into the sample (usually this is enough to change it back to blue).

Appendix 7. Methanol precipitation

1. To 200 µL rinse, add 800 µL ice cold methanol, mix well, and then incubate at -80C for one hour.

2. Centrifuge at maximum (14000rpm) for 30 minutes.

3. Dry in the SpeedVac for at least 30 minutes with caps loosened. (Note: it is very important to dry the samples, or else the residual methanol will interfere with the immunoblot.

4. Resuspend in 20 µL 2.5X Laemmli sample buffer and boil 10 minutes. Run immunoblot immediately or leave at 4°C overnight.

Appendix 8. Histology

Tissue fixation

1. Brains were cut sagitally and submerged into 10% Buffered Formalin Phosphate (Fisher Scientific #SF100), at least 30 mL formalin for one sagittaly-sectioned hamster brain, for at least 2 days at room temperature.

2. Samples were placed in embedding cassettes, and then incubated twice in 70% ethanol for 1 hour, then 95% ethanol for one hour, then 4 times in 100% ethanol for 1 hour.

3. Samples were then incubated in xylene for 1 hour twice, and then incubated in molten paraffin wax at 60°C for one hour, twice. Samples were then cooled and stored until needed.

4. Samples embedded in paraffin blocks were trimmed and sectioned into 5 µm thick slices using a Leica microtome (Leica # RM2255) and mounted onto Colorfrost slides (Fisher # 12-550-17) and dried overnight at 37°C.

Hematoxylin and Eosin staining

1. Deparaffinize and hydrate slides by incubating twice in xylene for 5 minutes, and then once for 3 minutes in decreasing concentrations of ethanol (100%, 95%, 80%, 70%), and then once more for 3 minutes in distilled water.

2. Incubate hydrated slides in filtered Mayer's hematoxylin (Fisher #22-110-639) for 2 minutes, then tap water for 3 minutes, then dip 10 times in 0.1% sodium bicarbonate (Sigma # S7277) followed by another incubation in tap water for 3 minutes. Incubate in Eosin Y working solution (40mL 1% Eosin Y (Sigma#E4382), 4 mL 1% phloxin B (Sigma # P4030), 1.6 mLglacial acetic acid (Fisher #351270-212), 310 mL 95% ethanol) for 30 seconds, followed by 2-3 quick rinses in distilled water.

3. Dehydrate the slides by incubating in 95% ethanol for 2 minutes, then 100% ethanol for 2 minutes, then twice in xylene for 5 minutes each time.

4. Cover the dehydrated slide with a cover slip (Fisher # 12-548-5E) and seal with cytoseal 60 (Fisher # 23-244-256). Let dry for 48 hours at room temperature.

PrP^{Sc} IHC protocol

1. Deparaffinize and hydrate slides by incubating twice in xylene for 5 minutes, and then once for 3 minutes in decreasing concentrations of ethanol (100%, 95%, 80%, 70%), and then once more for 3 minutes in distilled water.

2. Wash the hydrated slide in PBS-0.05% Tween 20 (10X PBS (Boston BioProducts # BM-220), Tween 20 (Sigma # P5927)) twice for 5 minutes and then add 10mM citrate buffer (100mM of citrate buffer stock (100mM Citric acid (Sigma#C83155), 0.5% Tween 20, pH 6.0) and heat at 121°C and 2.1 bar in a pressure cooker for 30 minutes.

3. Rinse twice in distilled water for 3 minutes and then incubate in 98% formic acid for 30 minutes, then rinse twice in distilled water for 3 minutes.

4. Incubate with 4M guanidine thiocyanate (Fisher #BP221, MW 118.16) at room temperature for 2 hours, and then rinse in PBS-0.05% Tween 20 for 5 minutes twice. Incubate in 3% H_2O_2 (Fisher # H325) and wash in PBS-0.05% Tween 20 for 5 minutes twice.

5. Antibody (3F4, 1:500) is biotinylated and diluted in 50 mM Tris-HCl pH 7.4 (Trizma base (Sigma #T1503)) with 1% BSA (OmniPur #2960) according to the manufacturer protocol (DAKO ARK™ (animal research kit), peroxidase # K3954), then applied to the slide and incubated overnight at 4°C in a humidified chamber.

6. The slide is then rinsed for 5 minutes in PBS-0.05% Tween 20 twice, then incubated with streptavidin-peroxidase (Invitrogen # 50-209Z) for 15 minutes, and then rinsed for 5 minutes in PBS-0.05% Tween 20 twice.

7. The slide is incubated in DAB (BD Pharmingen™ #550880) until it becomes brown, then washed again for 5 minutes in PBS-0.05% Tween 20 twice.

8. Incubate in Mayer's hematoxylin (Fisher # 22-110-639) for 2 minutes, rinsed in tap water for 3 minutes, then dipped 10 times in sodium bicarbonate, and then rinsed in tap water for an additional 3 minutes.

9. Dehydrate the slides by incubating in 95% ethanol for 2 minutes, then 100% ethanol for 2 minutes, then twice in xylene for 5 minutes each time.

10. Cover the dehydrated slide with a cover slip (Fisher # 12-548-5E) and seal with cytoseal 60 (Fisher # 23-244-256). Let dry for 48 hours at room temperature.

Appendix 8. Chapter 3 supplementary data

Supplemental Table 3-5. Hamsters that showed neurological signs but lacked PrP^{res}

Isolate	N	PrP^{res} negative, neurological signs	Incubation period
70045	7	1	631
74200	7	1	645
73931	9	1	727
74148	9	1	538
74448	9	3	538, 619, 711
74754	6	3	634, 699, 726

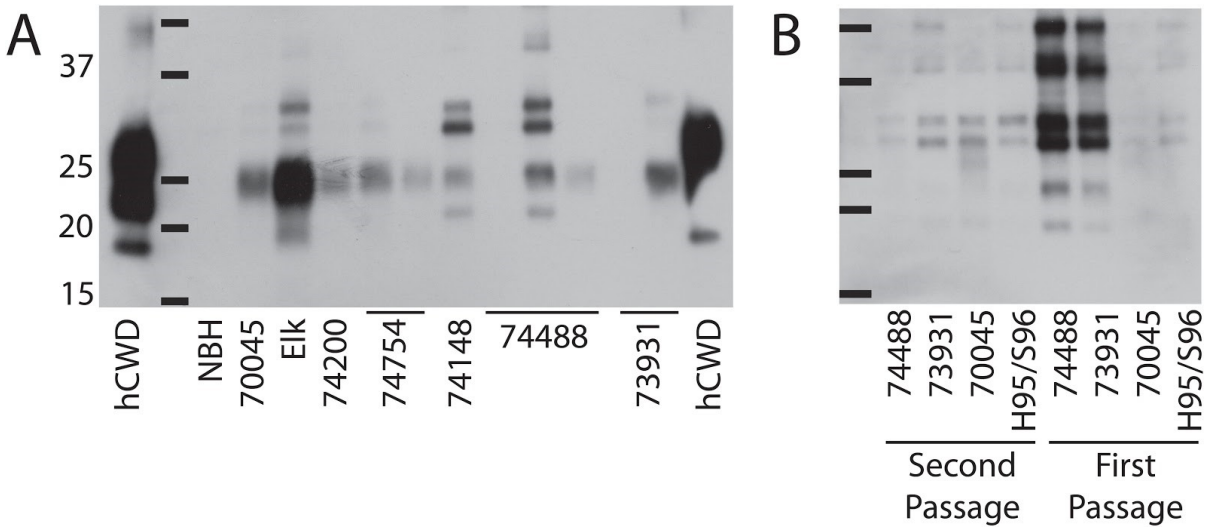

Supplemental Figure 3-4. Atypical migration patterns were present in some hamsters that displayed clinical signs, but there was no increase in signal intensity in the second passage of these hamsters. **A**. Atypical migration patterns in some first passage hamsters. PK digest performed using three times the normal amount of brain homogenate. Samples were digested in 50µg/mL proteinase K for one hour. **B**. Samples were digested in 50 µg/mL proteinase K for one hour. The lane with the black bars contains the protein ladder demonstrating molecular weight in kilodaltons (kDa). The origin of the isolate inoculated into the hamsters is shown below the immunoblot; either the deer code (e.g., 70045), uninfected hamster brain homogenate (NBH), or hamster-adapted CWD (hCWD). Primary antibody: 3F4.

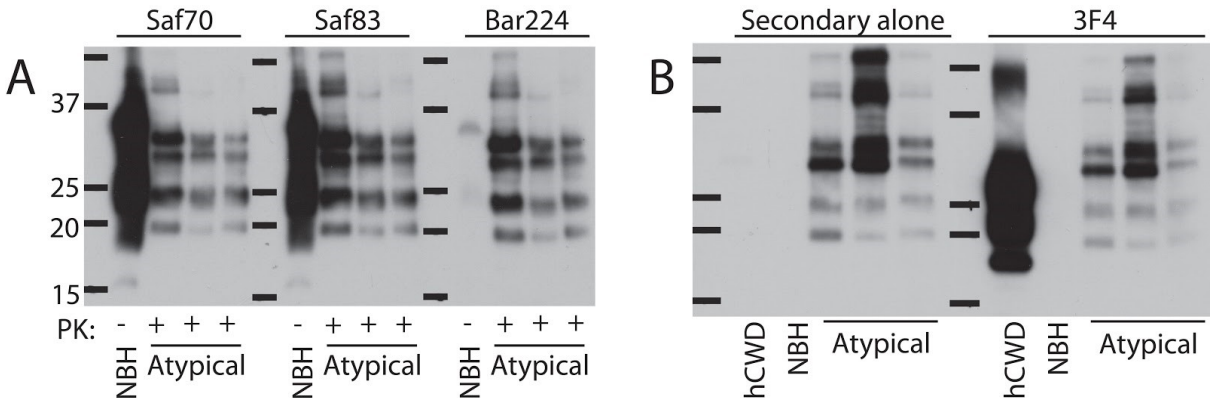

Supplemental Figure 3-5. Atypical migration pattern was due to cross reactivity with the secondary antibody. Samples were digested in 50µg/mL proteinase K for one hour. **A.** Comparison of the atypical migration pattern using three different primary antibodies, Saf70, Saf83, Bar224; secondary antibody: GαM: HRP 1:10000. **B.** Comparison of primary and secondary antibody compared to secondary alone. The lane with the black bars contains the protein ladder demonstrating molecular weight in kilodaltons (kDa). Samples were either undigested (-) or digested in PK (+). uninfected hamster brain homogenate (NBH), or hamster-adapted CWD (hCWD). Primary antibody: 3F4, Saf83, Bar224 as noted above.

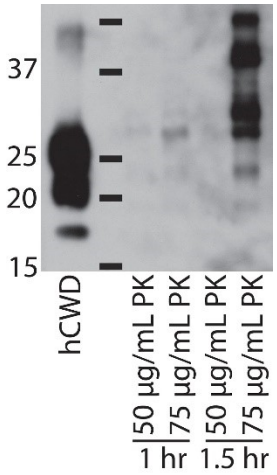

Supplemental Figure 3-6. Cross-reactivity in the secondary antibody is increased by increasing the amount of brain homogenate digested, increasing the amount of proteinase K used in the digest, and increased time of digestion (1 hour (hr) or 1.5 hours). The lane with the black bars contains the protein ladder demonstrating molecular weight in kilodaltons (kDa). Atypical samples were compared to hamster-adapted CWD (hCWD). Primary antibody: 3F4.